Die approbierte Originalversion dieser Diplom-/Masterarbeit ist in der Hauptbibliothek der Technischen Universität Wien aufgestellt und zugänglich.
http://www.ub.tuwien.ac.at

The approved original version of this diploma or master thesis is available at the main library of the Vienna University of Technology.
http://www.ub.tuwien.ac.at/eng

TECHNISCHE UNIVERSITÄT WIEN
Vienna University of Technology

Unterschrift des Betreuers

D I P L O M A R B E I T

Development of improved fluorescence probe for detecting ascorbic acid: Phthalocyaninatosilicon covalently linked to TEMPO radicals

Thema

Ausgeführt am Institut für

Angewandte Synthesechemie

der Technischen Universität Wien

und

Institut of Industrial Science

University of Tokyo

unter Anleitung von

Univ. Prof. Dr. Wolfgang **LINERT**

durch

Martin **PRIESSNER BSc.**

Görtschitztal Straße 227, 9064 Magdalensberg AUSTRIA

Wien, 26.10.2015

Datum

Unterschrift (Student)

"千里の道も一歩から。

Senri no michi mo ippo kara"

A journey of a thousand miles begins with a single step

Eine Reise von tausend Meilen beginnt mit dem ersten Schritt

Laotse (老子 4th or 5th century B.C.)

Acknowledgment

First of all I want to say a big thank you to **Univ.Prof. Dr. Wolfgang Linert**. He inspired me to do the research for my master thesis abroad which finally led to the cooperation with the prestigious University of Tokyo. He mentored and supported me throughout my six month research stay in Tokyo.

I equally want to thank **Univ.Prof. Kazuyuki Ishii** from the University of Tokyo who was so kind to accept me as a research student in his laboratory in which I worked for my master thesis. I want to thank him for his support especially when I was facing seemingly difficult insurmountable obstacles during my research progress. He always had good advice how to find a solution.

Furthermore I want to thank my tutor, supervisor, coworker, PhD student and friend **Takanori Yokoi**. I was working with him together on my research project. I enjoyed the sometimes very long hours we spent in the laboratory for obtaining good results because we shared the same passion for science. Additionally he was a very good guide who introduced me to the culinary features of Japanese food and also to the Japanese culture.

Also I want to thank my whole **coworkers and colleagues** in the laboratory of professor Ishii for the enjoyable work environment and for the enriching conversations that I was able to hold with many of them. I found myself always learning something new and interesting.

Next to all the professional acknowledgements my biggest expression of thanks is directed to **my parents Alfons and Sigrid Prießner**. They always supported me throughout my life in doing the things that I liked doing. They gave me the opportunity to study and to get a very good education. In moments where I thought I cannot find a solution for the challenges that I was facing they were the people who gave me strength to continue without doubt.

Last but not least I want to say thank my “Bro”, **brother Alfons jun. Prießner**, who always had an open ear for everything I wanted to talk about. Also for his honesty to tell me the things I needed to hear in order to make the right decisions in my life and for his mentoring throughout my career.

Vienna, October 2015

Ascorbic acid (Vitamin C) is a well-known and essential nutrient in relation to biological functions such as carnitine biosynthesis, as anti-oxidizing agents or as anti-aging agents. In particular, recently, ascorbic acid has attracted considerable attention for its uses in modern cancer therapy. Thus, it is extremely important to develop fluorescence probes to detect ascorbic acid for clarifying the biological roles.

Fluorophores linked to a nitroxide radical (FN systems) are promising candidates for detecting ascorbic acid. The nitroxide radical provides efficient fluorescence quenching and preferably reacts with ascorbic acid. Thus, the FN-based probes have been expected to be applied to the quantitative determination of ascorbic acid in aqueous solutions. However, in contrast to aqueous solutions, improvements are required to apply the FN probes to the detection of ascorbic acid in biological environments, since, in addition to ascorbic acid, the nitroxide radical easily reacts with some biological reductants such as mitochondrial NADH and superoxide. [1]

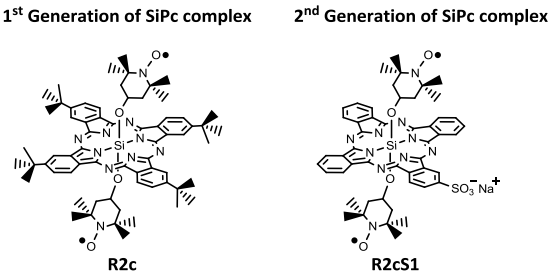

Figure 1: First and second generation of the vitamin C detecting complex

In this study, an already existing system of fluorophore with nitroxid radicals which was capable in detecting vitamin C by fluorescence was improved. One times sulfonated SiPc covalently linked to two TEMPO radicals was applied as fluorescence probe for detecting ascorbic acid in aqueous solution.

This complex was synthesized and measured by ESI-MS, absorption-spectroscopy, ESR, MCD and the fluorescence capabilities were compared with the first generation of the complex which already showed these fluorescence properties. Both complex structures can be seen in Figure 1.

Since the hydrophobic SiPc–TEMPO derivatives are insoluble in aqueous solutions, they were encapsulated in liposomes for measurement in aqueous solutions. The fluorescence of liposomal R2cS1 and R2c increased for both after ascorbic acid addition. The sensitivity, however, of the new synthesized R2cS1 complex was 10-times better than for the R2c complex.

The increased sensibility of R2cS1 over R2c is caused by the stronger polarity of the new complex due to the sulfate group. This results in a closer position to the polar regions of the liposomes which makes it easier to react with the also quite polar ascorbic acid.

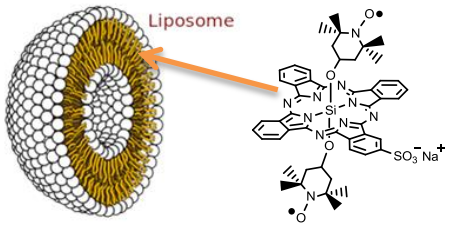

Figure 2: Positioning of the complex R2cS1 in the liposome

Furthermore a DFT calculation was carried out to explain a mysterious Q-band splitting in the absorption spectra of the R2cS1 complex. Together with the results of the MCD measurement it was discovered that the additional peak in the Q-band region is caused by a split of the orbital energies due to the asymmetry of the complex because of the sulfate group.

Wien, Oktober 2015

Ascorbinsäure (Vitamin C) ist gut bekannt als wichtiger Nährstoff in Bezug auf biologische Funktionen wie beispielsweise die Carnitin Biosynthese, als Antioxidationsmittel oder als Anti-aging Mittel.

Speziell vor kurzem hat Ascorbinsäure große Aufmerksamkeit auf sich gezogen durch seine Verwendung in der modernen Krebstherapie. Daher ist es äußerst wichtig, Fluoreszenz Proben zu entwickeln, die Ascorbinsäure in deren biologischen Rollen aufklären können. Fluorophore verbunden mit Nitroxidradikal (FN-Systeme) scheinen vielversprechende Kandidaten für die Detektion von Ascorbinsäure zu sein. Das Nitroxidradikal verursacht eine effiziente Fluoreszenz-Quenchung und reagiert vorzugsweise mit Ascorbinsäure. Daher ist zu erwarten, dass die FN-basierten fluoreszierenden Proben gut für die quantitative Bestimmung von Ascorbinsäure in wässrigen Lösungen geeignet sind.

Für den Einsatz dieses Detektionsverfahrens von Ascorbinsäure im biologischen Umfeld müssen noch Verbesserungen an den FN Systemen vorgenommen werden. Der Grund ist der, dass neben Ascorbinsäure noch einige andere Stoffe wie die mitochondriale NADH oder Superoxide mit den Radikalen reagieren können. [1]

In diesem Forschungsprojekt wurde ein bereits erforschtes System aus Fluorophor und Nitroxidradikalen, welches in der Lage ist Vitamin C durch Fluoreszenz zu detektieren, verbessert. Es wurde ein einfach sulfonierter SiPc Komplex neu synthetisiert. Dieser wurde als Fluoreszenzprobe für die Ascorbinsäuredetektion in wässriger Lösung angewendet.

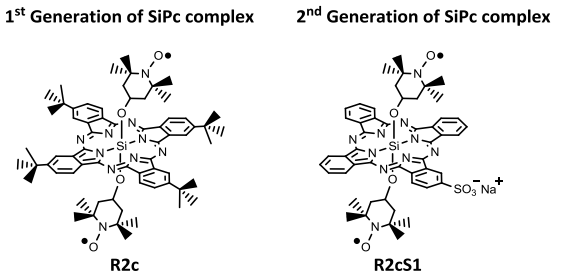

Abbildung 2: Erste und zweite Generation von Vitamin C detektierenden Komplex

Dieser Komplex wurde neu synthetisiert, und mittels ESI-MS, Absorptionsmessung, ESR und MCD gemessen. Als letzter Schritt wurde das Fluoreszenzverhalten mit dem der ersten Generation dieses Komplexes verglichen. Beide Komplexe sind in Abbildung 1 dargestellt.

Da die hydrophoben SiPc-TEMPO Derivate in Wasser unlöslich sind, wurden die Komplexe in Liposome für die Messung in wässriger Lösung eingekapselt.

Die Fluoreszenz von liposomalen R2cS1 und R2c stieg für beide Komplexe nach der Zugabe von Ascorbinsäure. Die Sensitivität des neu synthetisierten R2cS1 Komplexes war jedoch 10 Mal höher als die des alten R2c Komplexes.

Die erhöhte Sensibilität von R2cS1 gegenüber R2c wurde durch die erhöhte Polarität durch die installierte Sulfatgruppe der neuen Verbindung verursacht. Diese führt zu einem näheren Aufenthaltsortes zur polaren Außenwand im Liposom des Komplexes, welcher dadurch leichter mit dem ebenfalls polaren Vitamin C reagieren kann (siehe Abbildung 2).

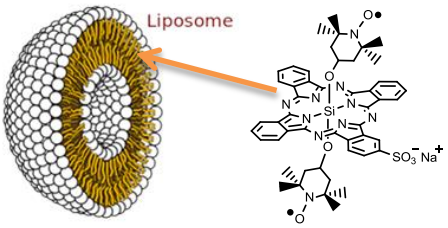

Abbildung 2: Positionierung vom R2cS1 Komplex im Liposom

Außerdem wurde noch eine DFT-Berechnung durchgeführt, welche zusammen mit der MCD Messung eine mysteriöse zweite Q-Bande im Absorptionsspektrum des R2cS1 Komplexes erklären konnte. Diese wurde durch die neuentstandene Asymmetrie des Komplexes durch die neue Sulfatgruppe verursacht, da diese die Energie der Orbitale aufspaltete.

List of Abbreviations

In addition to common abbreviations of the English language such as the chemical element symbols, additional abbreviations used in this thesis are mentioned below. Once occurring acronyms are usually explained as they occur.

AcOH	acidic acid
CT	charge transfer
DCM	dichlormethan
DMF	dimethylformamide
EPR	time-resolved electron paramagnetic resonance
ESI/MS	electrospray ionization/ mass spectrometry
ESP	electron spin resonance
EtOAc	ethyl acetate
EtOH	ethanol
H_2SO_4	sulforic acid
HF	hydrofluoric acid
IC	internal conversion
IR	infrared
ISC	intersystem crossing
MCD	magnetic circular dichroism
MeOH	methanol
Na_2CO_3	sodium carbonate
NP-TLC	normal phase thin layer chromatography
PBS	phosphate-buffered saline solution
Pc	phthalocyanine
PDD	photodynamic diagnosis
PDT	photodynamic cancer therapy
Por	porphyrin
Py	pyridine
R2cSx	x-sulfonated silicon phthalocyanine-ditetramethylpiperidinyloxyl

RP-TLC	reversed phase thin layer chromatography
SiPc	silicon phthalocyanine dihydroxide
$SiPc(TEMPO)_2$	silicon phthalocyanine ditetramethylpiperidinyloxyl
SiPcSx	x-sulfonated silicon phthalocyanine dihydroxide
SitBPc	tetra t-butyl silicon phthalocyanine dihydroxide
SM	starting material
SOC	spin-orbital coupling
S-S	singlet-singlet
TEMPO	2,2,6,6-tetramethylpiperidinyloxyl
TEMPOL	4-hydroxy-2,2,6,6-tetramethylpiperidin-1-oxyl
THF	tetrahydrofuran
Tol	toluene
TREPR	time-resolved electron paramagnetic resonance
T-T	triplet-triplet
$\Delta\varepsilon_T$	T-T extinction coefficient
ν	wavenumber of light

General Remarks

Remark to references

Citations are highlighted in the text by Arabic numerals in square brackets.

Nomenclature

The nomenclature of in the chemical literature not described compounds is carried out according to the Regulations of Chemical Abstracts. Of eviscerated or literature known compounds and reagents are partially described by simplified terms, trivial or trade name.

TLC

The TLC-arrays that were carried out in order to find a suitable separation method for the two reaction mixtures are represented in this thesis in an animated way. The reason for this is that sometimes the TLCs were very difficult to interpret because the conditions for the separation were not optimized for that separation at that point. But as the research progressed, better conditions were found and then the same TLCs that were done at the beginning were interpretable by then. For the sake of completeness some of the essential TLCs are included in the appendix

Table of Contents

A) FORMULA SCHEMES 1

A.1 SYNTHESIS OF MONO-SULFONATED SILICON(IV)PHTHALOCYANINE 2

A.2 SYNTHESIS OF MONO-SULFONATED SILICON(IV)PHTHALOCYANINE COVALENTLY LINKED TO TWO TEMPOL RADICALS 2

A.3 REACTION OF R2CS1 WITH ASCORBIC ACID 3

B) GENERAL ASPECTS 4

B.1 WHAT ARE PHTHALOCYANINES? 5

B.1.1 Historical background of phthalocyanines 6

B.1.2 Usage of phthalocyanine complexes nowadays 6

B.2 CHEMISTRY OF PHTHALOCYANINE COMPLEXES 7

B.2.1 Chemical properties of phthalocyanine complexes 7

B.2.1.1 Central atoms 7

B.2.1.2 Stability 7

B.2.1.3 Solubility 8

B.2.1.4 Color 8

B.2.1.5 Symmetry* 9

B.2.1.6 Modification possibilities 9

B.2.2 Photophysical properties of phthalocyanine complexes 11

B.2.2.1 Electronic transitions schema of the absorption sprectrum 11

B.2.2.2 Explanation of the excited-state energy diagram of Pc 12

B.2.2.3 Calculation of the different observable parameters 14

B.2.2.4 Measurement methods of the observable parameters 14

B.2.3 Comparison of Pc and Por complexes 15

B.2.3.1 Spectroscopic comparison Pc & Por 15

B.2.3.2 Permeability of radiation of biological tissue 17

B.3 APPLICATION OF PHTHALOCYANINES 20

B.3.1 Characteristic Bioimaging Applications 20

B.3.1.1 Principle of PDD 20

B.3.1.2 Previous research of SitBuPc fluorophore 21

B.3.1.3 Photophysical properties of phthalocynanines linked to nitrodixe radicals 22

B.3.1.4 Electronic absorption, MCD, and fluorescence spectra 25

B.3.1.5 Steady state EPR spectra of SiPc derivatives 26

C) SPECIFIC PART 28

C.1 INTRODUCTION TO VITAMIN C DETECTION 29

C.2 AIM OF THE THESIS 29

C.2.1 Synthesis of the Pc complex 30

C.2.1.1 First reaction step 30
C.2.1.2 Second reaction step 31
C.2.1.3 Reduction of the Pc complex 32
C.2.2 What is the difference between the 1st and 2nd generation of the Pc complex? *32*

D) EXPERIMENTAL PART 34

D.1 GENERAL REMARKS 35
D.1.1 Chromatographic methods *35*
D.1.1.1 Thin layer chromatography 35
D.1.1.2 Column chromatography 35
D.1.2 Analysis methods *35*
D.1.2.1 Spectrophotometric assay 35
D.1.2.2 ESI-MS 35
D.1.2.3 ESR measurement 36
D.1.2.4 Fluorescence measurement 36
D.1.2.5 MCD measurement 36
D.1.2.6 Elemental analysis 37
D.2 EXPERIMENTAL PROCEDURES 37
D.2.1 Experiments carried out for the discovery of the synthesis of mono-sulfonated silicon-phthalocyanine *37*
D.2.1.1 Reaction A01 37
D.2.1.2 Reaction A02 43
D.2.1.3 Reaction A03 46
D.2.1.4 Reaction A04 50
D.2.1.5 Reaction A05 51
D.2.1.6 Reaction A06 52
D.2.1.7 Reaction A07 53
D.2.1.8 The search for better TLC separation method 54
D.2.1.9 TLC experiments: 56
D.2.1.10 Reaction A08 60
D.2.1.11 Reaction A09 62
D.2.1.12 Reaction A10 64
D.2.2 Second reaction step *69*
D.2.2.1 Reaction B01 69
D.2.2.2 Reaction B02 72
D.2.2.3 Reaction B02 73
D.2.2.4 Reaction B04 and B05 74
D.2.2.5 TLC experiments 77
D.2.2.6 Purification of the product mixture B05-B09 83
D.2.3 Measurements of the complex R2cS1 ..... *84*
D.2.3.1 ESR measurement 84
D.2.3.2 MCD and absorbance measurement 85

D.2.3.3 DFT calculation 85
D.2.3.4 Fluorescence measurement 86
D.2.3.5 Elemental analysis 90
D.3 SUMMARY AND CONCLUSION 91

E) APPENDIX ..... - 92 -

E.1 ESI-MS SPECTRA ..... - 93 -
E.1.1 Reaction A ..... - 93 -
E.1.2 Reaction B ..... - 99 -
E.2 PREPARATION PROCEDURE FOR CHANGING OLEUM CONCENTRATION ..... - 103 -
E.3 THE BEER-LAMBERT LAW & PREPARATION OF SAMPLE FOR YIELD CALCULATION ..... - 103 -
E.4 DFT CALCULATION ..... - 104 -
E.4.1 DFT calculation R2cS1-orbitals: ..... - 104 -
E.4.2 DFT calculation SiPc-orbitals ..... - 105 -
E.4.3 HOMO and LUMO energy calculation of R2c and R2cS1 ..... - 105 -
E.5 TLC ARRAYS ..... - 108 -

F) TABLE OF ILLUSTRATIONS ..... - 109 -

G) REFERENCES 113

A) Formula Schemes

A.1 Synthesis of mono-sulfonated silicon(IV)phthalocyanine

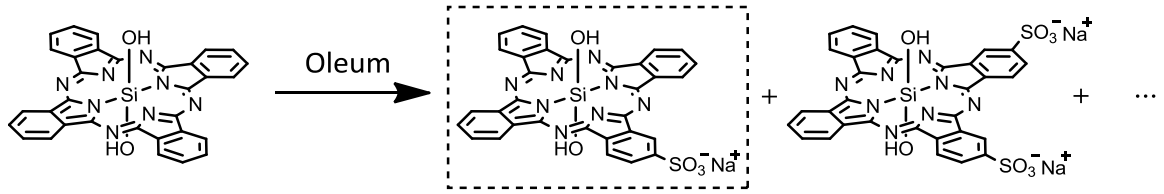

Figure 3: Formel schema of the first step reaction - the synthesis of SiPcS1

A.2 Synthesis of mono-sulfonated silicon(IV)phthalocyanine covalently linked to two TEMPOL radicals

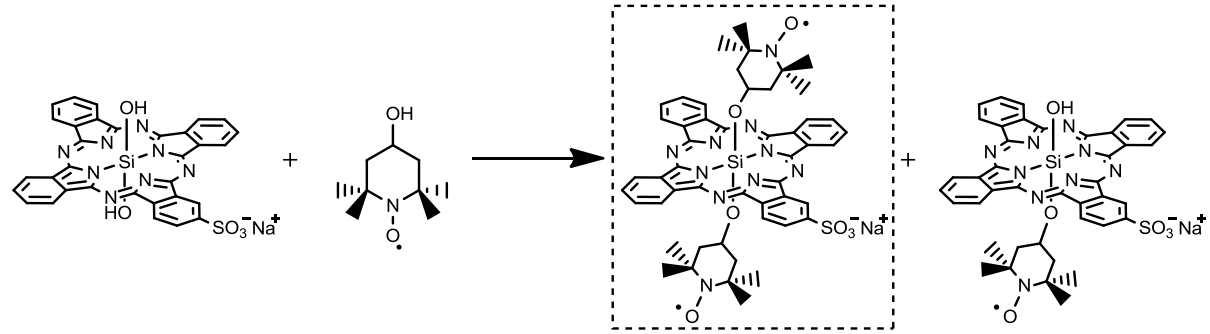

Figure 4: Formel schema of the second step reaction for the synthesis of R2cS1

A.3 Reaction of R2cS1 with ascorbic acid

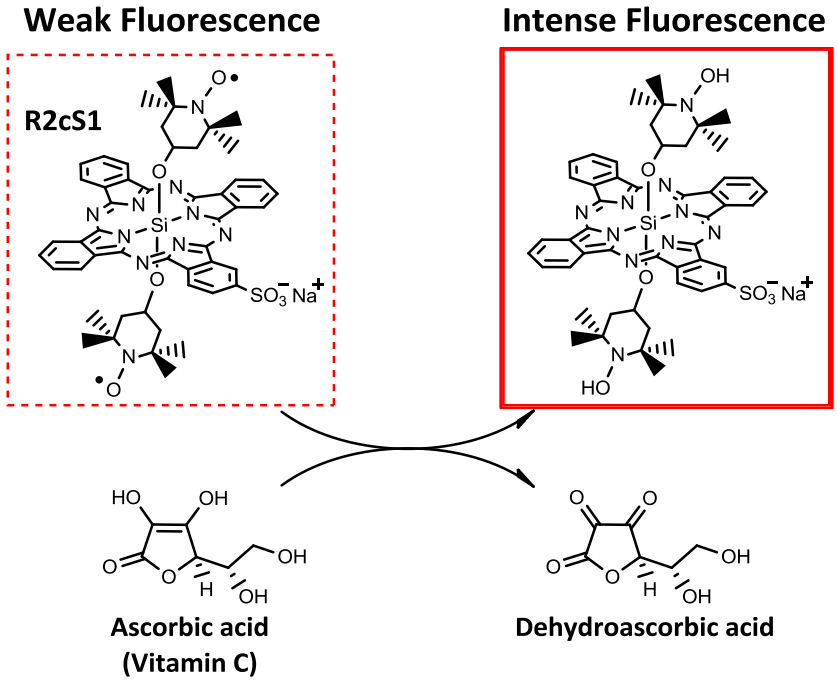

Figure 5: Increaced fluorescence after the reaction of R2cS1 with ascorbic acid

B) General Aspects

B.1 What are phthalocyanines?

The phthalocyanine (Pc) complex is a chemical substance similar to that of porphyrin (Por) complex. Both complexes exhibit unique physical, chemical and spectral properties. [2] It is the fundamental chemical backbone of many important enzymes and chemical compounds in nature (such as hemoglobin or chlorophyll). The basic structure of Pc and Por can be seen below in Figure 8.

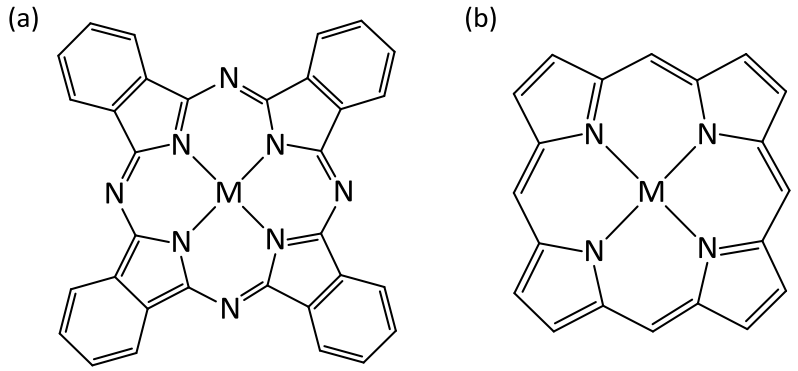

Figure 6: Basic structure of (a) metal-phthalocyanaine and (b) metal-porphyrin complex

Phthalcyanines and porphyrins are groups of heterocyclic macrocycle organic compounds. Porphyrins are composed of four modified pyrrole subunits interconnected at their α-carbon atoms via methine bridges (=CH−). [3]

Phthalocyanines are similarly composed of four isoindole-units in which the pyrrole parts are cross-linked via nitrogen atoms forming a 16-membered ring. The planar porphyrin macrocycle as well as the planar phthalocyanine macrocycle have 18 (delocalized) π electrons which are involved in the delocalization pathway. [4, 5] This is in accordance with the Hückel´s rule for aromatic systems (4n+2 π electrons n=4, for the shortest cyclic path). [6]

Despite the big importance of Pc related compounds in the field of medicine as of photosensitizers for single oxygen generation, in the photodynamic cancer therapy (PDT) or its use as fluorescence bioimaging method in the photodynamic diagnosis (PDD), the success of this compound has a long history. [7]

B.1.1 Historical background of phthalocyanines

Phthalocyanine is derived from the Greek term for naphtha (rock oil) and cyanine (dark blue). [8]

The first Pc compound was reported from the two chemists Braun and Tcherniac in 1907 during a high temperature experiment in which they wanted to obtain o-cyanobenzamid. This blue colored compound was (as we know today) a metal-free form of phthalocyanine. [9]

The discovery of Pc as a dye was also incidentally when in 1928 the Scottish company Scottish Dyes Ltd. (ICI) in Grangemouth tried to produce phthalimid from phthalic anhydride and ammonia in an enameled iron kettle. At one part where the enamel was destroyed and the chemicals came in contact with the iron of the kettle, a dark blue substance was formed. [8]

In the following experiments it was discovered that this blue colored compound could be obtained not only with iron but also by reaction of phthalonitrile with other metals such as copper, nickel or their salts. A year earlier in 1927 H. de Diesbach and E. von der Weid had reported in the journal Helvetia Chimica Acta on the synthesis and the brilliancy of color of copper phthalocyanine. [10] But they have not realized its economic potential of these complexes as a pigment at that time. The porphyrin like structure of phthalocyanine which was postulated by R. P. Linstead in 1933 was finally proven in 1935 by J. M. Robertson by X-ray structure analysis. [11, 12] Since then it was clear that the chemical structure of phthalocyanines have similarities to biologically relevant metal complexes such as the red blood pigment hemin or the chlorophyll of plants. [8]

Phthalocyanines and their derivatives have long been used mainly as dyes and coloring agents. The renaissance of the phthalocyanine chemistry during the last 30 years was caused by their extraordinary physical properties interesting for applications in materials science. [13]

B.1.2 Usage of phthalocyanine complexes nowadays

Nowadays Pc has attracted much attention as a result of their diverse electronic and optical properties. They offer applications in the fields of luminophores, sensors, nonlinear optics, photo-sensitizers for singlet oxygen generation, photovoltaic cells, artificial photosynthesis, red or near-infrared (IR) light absorbers, in optical data storage systems (such as CD-R) and

photoconductor devices in laser printers. Furthermore Pc has been established as essential chemicals in the field of medical science. Very important and sharply developing field of application of phthalocyanines is medicinal chemistry in particular, photodynamic therapy (PDT). Some of them are currently used in PDT (e.g., Photosens®) or tested in clinical trials. Therefore the production of Pc related compounds including pigments are now exceeding 60 million tons per year. [14]

B.2 Chemistry of phthalocyanine complexes

Before I am going to elaborate in detail the application of the actual complex that was synthesized in this master thesis, I will firstly describe the chemical and photophysical properties of Pc complexes in general and compare them with Por complexes. After the introduction of the basic knowledge of the properties of Pc complexes I will focus on the applicational use of this complex in the field of photodynamic diagnosis (PDD) in which fluorescence bioimaging methods are used to detect ascorbic acid in vitro as well as in vivo. This fluorescence bioimaging method can be used for early cancer detection.

B.2.1 Chemical properties of phthalocyanine complexes

B.2.1.1 Central atoms

The chelate system of the Pc macrocycle can form complex bonds with numerous main group elements (such as Na(I), K(I), Mg(II), Ca(II), Ba(Il), B(III)*, Al(III), Si(IV), Ge(IV), As(V) and P(V)) as well as with many transition metal elements (such as Fe(II), Zn(II), Co(II), Pt(II) and Cu(II)).[15]

B.2.1.2 Stability

Metal Pc complexes show a high thermal stability and are sublimable in a high vacuum at temperatures up to 600 °C without decomposition. Also the chemical stability is very high. Pcs are very resistant against non-oxidizing acids, alkalis and organic solvents. In the presence of atmospheric oxygen, they can be destroyed at temperatures over 150 °C. Furthermore Pc has a limited stability against strong oxidizing agents. [15]

* In the case of boron Pc, it forms a special so-called subphthalocyanine, which consists only of three isoindolenin units.

An undesirable property of phthalocyanines is the natural degradation during irradiated with light. Depending on the reaction conditions, this degradation leads to the complete destruction of the Pc photosensitizer. Since it is a degradation in which phthalimide is formed as a product, it is believed that the decomposition of the dye is caused by a [4+2]-cycloaddition of singlet oxygen on the macrocycle. [15, 16]

B.2.1.3 Solubility

Phthalocyanine complexes are generally insoluble in most common solvents. Some exceptions are for example chloronaphthalene, chlorobenzene or strong inorganic acids, such as H_2SO_4 and HF. In this case, a protonation of the nitrogen atoms is occurring. The resulting salts are charged and consequently soluble. By installing some appropriate substituents onto the Pc base structure, the solubility can be significantly increased. For increasing the solubility in non-polar solvents, long alkyl groups can be installed. To increase the solubility for polar or protic solvents, Pc can be modified by carboxyl, sulfonic or quaternary ammonium salts groups. [15]

One of the most unpleasant features of phthalocyanines is the formation of oligomers and Pc clusters for example in aqueous solutions. This process is called aggregation. The tendency of Pc to form agglomerates can be dependent on the solvent, as well as on the temperature and the pH value of the solvent and the nature of the central metal. By adding appropriate organic solvent (for example DMF) or by addition of detergents, the aggregation can be suppressed. The aggregation effect results a band broadening of the Q-band in the UV/VIS-spectrum (for the explanation of the different bands see **Chapter B.2.2**). This makes the assignment of the peak maximum very difficult. In addition, the extinction of the Q-band decreases significantly if aggregation occurs. [15]

B.2.1.4 Color

The distinctive color of phthalocyanines is the result from their extended conjugated π-electron system. The color spectrum is dependent on:

- the substituents
- the central metal ion
- the solvent in which the compound is solved

Depending on the central atom in solution the colors can reach from blue to green and in the solid state the colors range from violet-black to green-black for the different Pc complexes. [15]

B.2.1.5 Symmetry*

Pcs with one central metal ion show a D_{4h} symmetry. Those complexes with two chelate bounded central metal ions (e.g. Li-phthalocyanine) or metal-free derivatives (e.g. H_2-phthalocyanines) have D_{2h} symmetry. The different symmetry behavior results in different UV/VIS spectra. The species with D_{4h} symmetry show one HOMO/LUMO transition and associated to that one absorption band, while derivatives with D_{2h} symmetry split into two smaller bands at different wavelength. [15]

B.2.1.6 Modification possibilities

In the metal-free Pc there are two hydrogen atoms in the center bonded to the two nitrogen atoms which are interchangeable with various metals. There are more than 60 kinds of elements from the periodic table (shown in Figure 9) which can be introduced into the center of the Pc complex. [15]

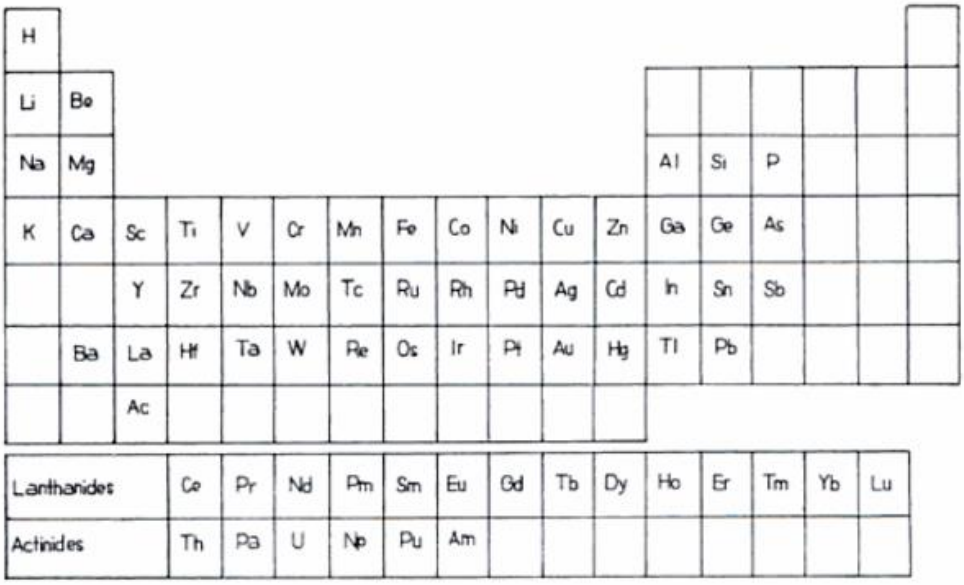

Figure 7: Metals that have been used to make metal phthalocynanines [8]

*This aspect will be of importance for the in this thesis synthesized new Pc complex.

In case of use of multivalent metal in the center of the Pc complexes, it is also possible to impart also a big variety of compounds as axial ligands. The peripheral positions of the macrocycle can be also substituted by a big variety of groups in order to allow fine tuning of their physical properties. By installing some appropriate substituents onto the Pc base structure, the solubility can be significantly increased (see **Chapter B.2.1.3.**).

Furthermore as shown in Figure 10, Pcs can have substituents at α and β positions of the four benzene rings.

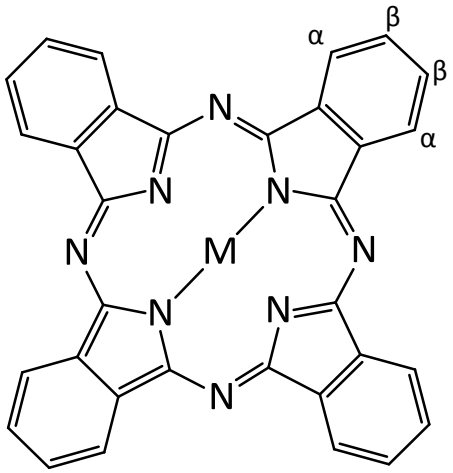

Figure 8: Molecular structure of Pc

Hence

- the large number of different forms of isomers, which can be formed by the different positions of the substituent,
- the large number of different central atoms and
- the possibility of imparting different axial ligands attached to the central metal of the Pc molecule

opens up a huge variety of opportunities to synthetically modify the complex and tune the chemical and photophysical properties to a desired demand. [17]

B.2.2 Photophysical properties of phthalocyanine complexes

B.2.2.1 Electronic transitions schema of the absorption sprectrum

In Figure 11 you can see the electron transitions of a Pc complex from lower into higher electronic configurations and their appropriate notation. Depending from which configuration to which electronic state the electrons become excited, a peak can be seen in the absorption spectrum at the according wavelength. The transitions of π → π* and n → π* are essentially responsible for the absorption process of Pc. [15]

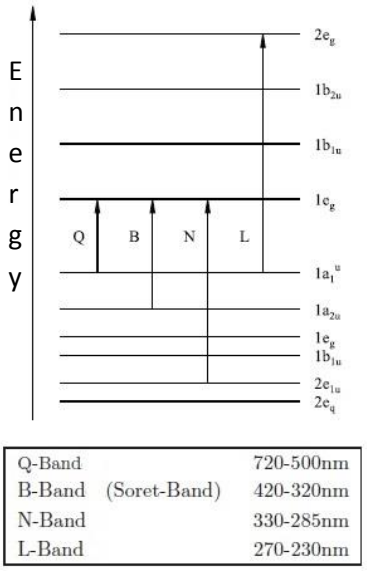

Figure 9: Electron transitions and associated wavelength of Pc [15]

One typical electronic absorption, fluorescence, phosphorescence, and triplet–triplet (T–T) absorption spectra of a silicon(IV)phthalocyanine dihydroxide is shown in Figure 12.

These are typical spectra for Pcs having a main group element as the central atom. Intense absorption bands (700 and 350 nm) due to electronic transitions from ground state S_0 to the excited S_1 and S_2 states are called the Q- and B- (also called Soret-) band, respectively. Mainly the Q-band and not so much the Soret-band is responsible for the pronounced color of the Pc.[15]

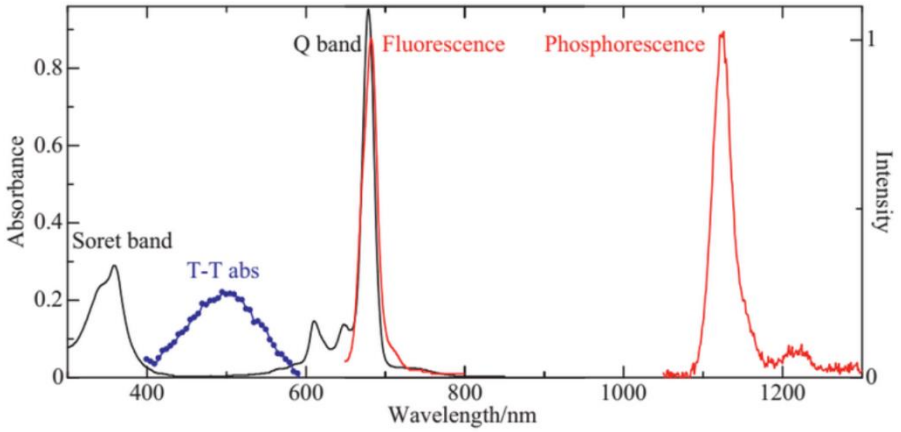

Figure 10: Electronic absorption (black), fluorescence (red), phosphorescence (red), and T-T absorption (blue) spectra of Si(IV)t-BuPc(OH)$_2$ in toluene [19]

Fluorescence is observed at around 700 nm and the decay time corresponds with the lifetime of the S_1 state (the different states of Pc will be explained in more detail in **Chapter B.2.2.2.**). The Stokes shift* is small, because the extent of the rearrangement of atomic coordinates by the photo-excitation of normal Pcs is small. [17, 18, 19]

Phosphorescence is observed for Pc complexes at 77 K, in the near-IR region at around 1100 nm. The excited-state dynamics and photophysical properties of Pc complexes are strongly dependent on the central atom. [20]

The phosphorescence efficiency of MPcs where M = Mg, Zn, or Cd is very low, in contrast to the strong phosphorescence of the platinum group, which can be seen even at room temperature. Because of the difficulty in observing phosphorescence at room temperature, the lifetime of the T_1 state is generally determined by the T–T absorption at around 500 nm. [19]

For an general overview the S_2, S_1 and T_1 states are located at around 27.000, 14.500, and 9000 cm^{-1}(= 370 nm, 690 nm and 1111 nm) respectively. [19, 20]

B.2.2.2 Explanation of the excited-state energy diagram of Pc

The absorption of ultraviolet or visible light by a Pc molecule causes the excitation of an electron from an initially occupied, low energy orbital to a high energy, previously unoccupied orbital. [21]

One of the excited electronic states is the excited singlet state where the electron spins are anti-parallel without spin magnetic moment. The other state is the excited triplet state where the electron spins are parallel, resulting in a net spin magnetic moment. The low-lying excited states with anti-parallel and parallel spins are termed the lowest excited singlet (S_1) and triplet (T_1) states, respectively. These excited-state energies are measured by steady-state electronic absorption and luminescence spectra. Excited-state energy diagram and decay kinetics of a typical Pc complex is shown in Figure 13. [21]

***** Stokes shift is the difference (in wavelength or frequency units) between positions of the band maxima of the absorption and emission spectra (fluorescence and Raman being two examples) of the same electronic transition. [V]

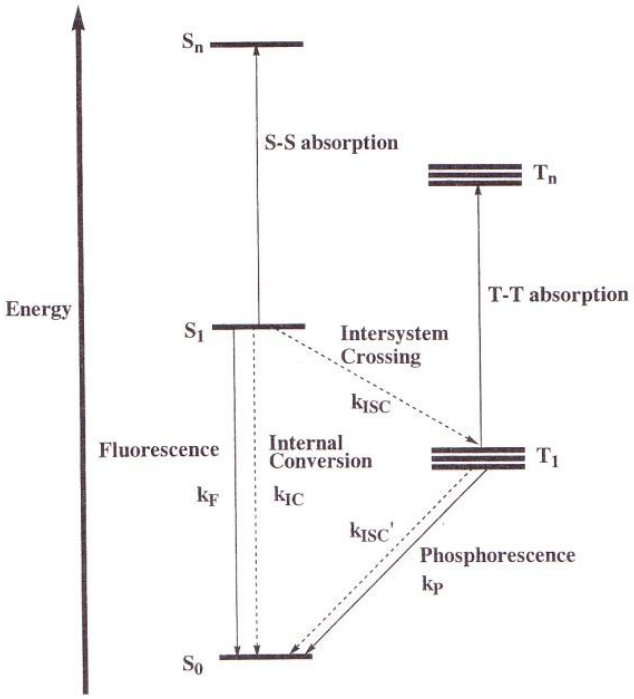

Figure 11: Excited-state energy diagram and decay kinetics of Pc with closed-shell atoms [21]

After photoexcitation, the important photophysical processes are classified as the following radiative and radiationless processes:

1. "Allowed" or singlet - singlet emission, called fluorescence ($S_0 \rightarrow hv + S_0$), characterized by a radiative rate constant k_F;
2. "Forbidden" or triplet - singlet emission, called phosphorescence ($T_1 \rightarrow hv + S_0$), characterized by a radiative rate constant k_P;
3. "Allowed" transitions between states of the same spin, called internal conversion, IC ($S_1 \rightarrow S_0$ + heat), characterized by a non-radiative rate constant k_{IC};
4. "Forbidden" transitions between triplet and singlet states, called intersystem crossing, ISC ($S_1 \rightarrow T_1$ + heat, $T_1 \rightarrow S_0$ + heat), characterized by a non-radiative rate constant k_{ISC} ($k_{ISC'}$). [21, 20]

The radiative rate constant is related to the extinction coefficient for electronic absorption. The non-radiative rate constants will be related to the Franck- Condon overlap of the nuclear wavefunctions. This Franck-Condon factor becomes increasingly unfavorable with increasing energy separation, and therefore the rate of a radiationless transition will fall exponentially as the energy separation increases, which is called the energy gap law. [21]

For radiationsless and spin-forbidden transitions, ISC ($S_1 \rightarrow T_1$ + heat), spin-orbit coupling (SOC) on the central atom is the most probable general mechanism which provides a magnetic torque (generated by the electrons orbital motion) capable of "flipping" the electron's spin magnetic moment. In order to conserve total momentum from the coupling, a spin-flip compensating orbital jump occurs. In other words, the momentum change due to the change in spin momentum can be exactly balanced by a change in orbital momentum. [21]

B.2.2.3 Calculation of the different observable parameters

These dynamics in the S_1 and T_1 states are characterized using observable parameters, excited state lifetimes (τ_S, τ_F, τ_T, τ_P), luminescence efficiency (φ_F, φ_P), and triplet yield (φ_T) as follows.

$$\tau_F = \tau_S = \frac{1}{k_F + k_{IC} + k_{ISC}} \quad (1)$$

$$\tau_P = \tau_T = \frac{1}{k_P + k_{ISC'}} \quad (2)$$

$$\phi_F = \frac{k_F}{k_F + k_{IC} + k_{ISC}} \quad (3)$$

$$\phi_T = \frac{k_{ISC}}{k_F + k_{IC} + k_{ISC}} \quad (4)$$

$$\phi_P = \frac{\phi_T * k_P}{k_P + k_{ISC'}} \quad (5)$$

Here k_F and k_P are the radiative decay rates of fluorescence and phosphorescence, respectively. k_{IC}, k_{ISC} and k'_{ISC} are the rate constants of $S_1 \rightarrow S_0$ internal conversion (IC), $S_1 \rightarrow T_1$ and $T_1 \rightarrow S_0$ intersystem crossing (ISC), respectively.[20, 21]

B.2.2.4 Measurement methods of the observable parameters

The luminescence efficiency (φ_F, φ_P) is determined by steady-state luminescence measurements. The excited-state lifetimes (τ_S, τ_F, τ_T, τ_P) are measured by time-resolved spectroscopy, where an intense pulse of light is very quickly introduced into a Pc-complex and then the time-evolution of the electronic absorption and luminescence signals is

analyzed. The lifetime of the S_1 state, τ_S (= τ_F), can be determined by the time-evolution of the transient absorption from the S_1 state to the higher S_n state or fluorescence from the S_1 state to the S_0 ground-state. In a similar manner, the lifetime of the T_1 state, τ_T (= τ_P) is also obtained by the time-resolved measurements of the T-T absorption from the T_1 state to the higher T_n states or phosphorescence from the T_1 state to the S_0 ground-state. In the case of non-luminescent compounds, the values of τ_S and τ_T are evaluated by singlet-singlet (S-S) and triplet-triplet (T-T) transient absorption measurements, respectively. [20, 21]

B.2.3 Comparison of Pc and Por complexes

B.2.3.1 Spectroscopic comparison Pc & Por

In Figure 14 an example of an electronic absorption spectrum of Zn(II)Pc and Zn(II)Por complex is shown. The Zn(II)Pc complex shows an intense absorption Q-bands at 700 nm and B-band at 350 nm which is due to the electronic transitions to the S_1 and S_2 states. The Zn(II)Por has just a weak Q-band at 500 nm to 600 nm. The intense absorption of light in the visible red or near-IR region is an important advantage of Pc complexes compared to Por complexes. Light in this region can more easily penetrate biological tissue such as skin (this fact will be explained in detail in **Chapter B.2.3.2**). Hence, Pc complexes are useful for biological applications such as PDT (photodynamic therapy) and PDD (photodynamic diagnosis). [20]

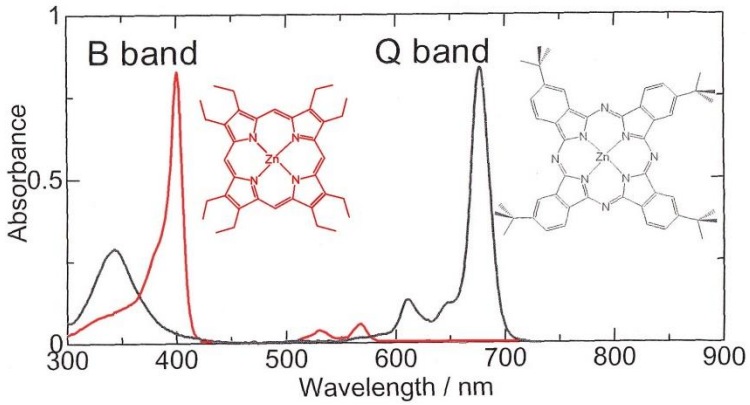

Figure 12: Electronic absorption spectra of Zn(II)tBuPc (black line) and Zn(II)PEP (red line) [20]

The mechanism of these electronic absorption spectra can be reasonably explained by the four frontier π-molecular orbitals (MOs) shown in Figure 15.

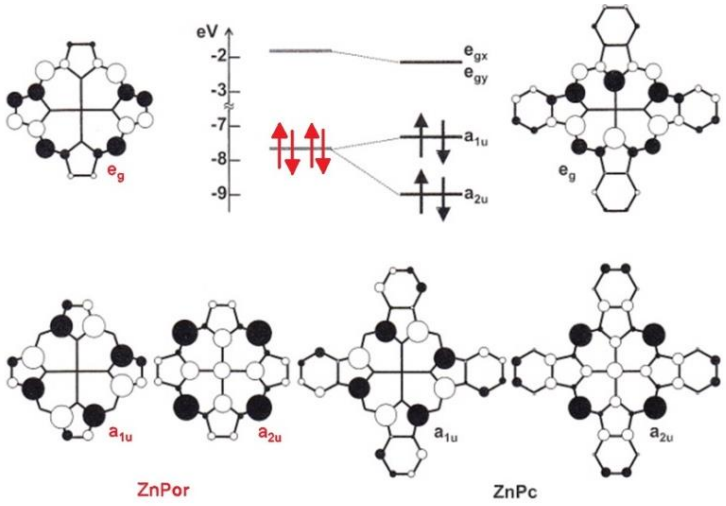

Figure 13: Molecular orbitals of Zn(II)PC and Zn(II)Por [20]

Compared with the porphyrin (Por) skeleton, the important structural features of Pc complexes are the meso-nitrogen atoms and the fused benzo-rings.

The a_{2u}, e_{gx} and e_{gy} orbitals, which have high electron density at the *meso*-positions, are stabilized compared to Por. This is caused by the substitution of the nitrogen atoms, whose electronegativity is bigger than that of carbon atoms from the Por complex. On the other hand, the fused benzo-rings destabilize the a_{1u}, e_{gx} and e_{gy} orbitals and the destabilized energy is larger in the a_{1u} orbital than that in the e_g orbitals. Thus, one of the important electronic properties in Pcs is the large energy separation between the a_{1u} and a_{2u} orbitals, in contrast to the quasi-degeneracy of the a_{1u} and a_{2u} orbitals in Pors. [19]

The S_1 state (which is responsible for the pronounced Q-band in the absorption spectra) of Pcs mainly originates from the ($a_{1u}e_g$) configuration, because the large energy difference between the a_{1u} and a_{2u} orbitals results in a small interaction between the $a_{2u}e_{gy}$ and $a_{1u}e_{gx}$ configurations; therefore, the absorbance of the Q-band is intense. On the other hand because of the small energy difference between the a_{1u} and a_{2u} orbitals of Por it develops just a weak Q-band. [20, 21]

Thus, this spectroscopic difference between Pcs and Pors can be reasonably explained by the change in the MOs due to the *meso* nitrogen atoms and fused benzo rings. [19]

In contrast to the Por complexes, the S_1 and T_1 states of MPcs are entirely derived from the $^1(a_{1u}e_g)$ and $^3(a_{1u}e_g)$ configurations, respectively, where the a_{1u} and e_g orbitals denote the HOMO (π) and LUMO (π*) of the Pc ligand, respectively (see again Figure 13). [20]

A higher bathochromic effect* for the transition from Por to the higher fused systems of Pc is explained by the increase in the π-system, resulting in a lowering of the HOMO/LUMO difference (this fact is explained in **Chapter B.2.2.1** in detail). [15]

B.2.3.2 Permeability of radiation of biological tissue

Especially for applications in the field of medicine the Pc has big advantages over the Por complex. In the context of tissue permeability the photophysical properties of Pc complexes are particularly noteworthy.

In Figure 16 below, the molar extinction coefficients for the absorption predominantly responsible substances in living tissue are plotted against the wavelengths. According to that figure, it can be seen that pronounced absorption bands are caused by water at high and low wavelength (< 300 nm, > 1200 nm). There are also absorption bands of the natural pigment melanin (between 300 nm – 600 nm) and of the blood pigment hemoglobin (around 250 nm – 600 nm). This fact leaves just a small window open in which the best permeability of radiation in biological tissue can be found. Therefore the wavelength range with the best permeability of radiation of biological tissue is for wavelengths between 600 to 1200 nm. [15]

***** Bathochromic shift is a change of spectral band position in the absorption, reflectance, transmittance, or emission spectrum of a molecule to a longer wavelength (lower frequency). [22]

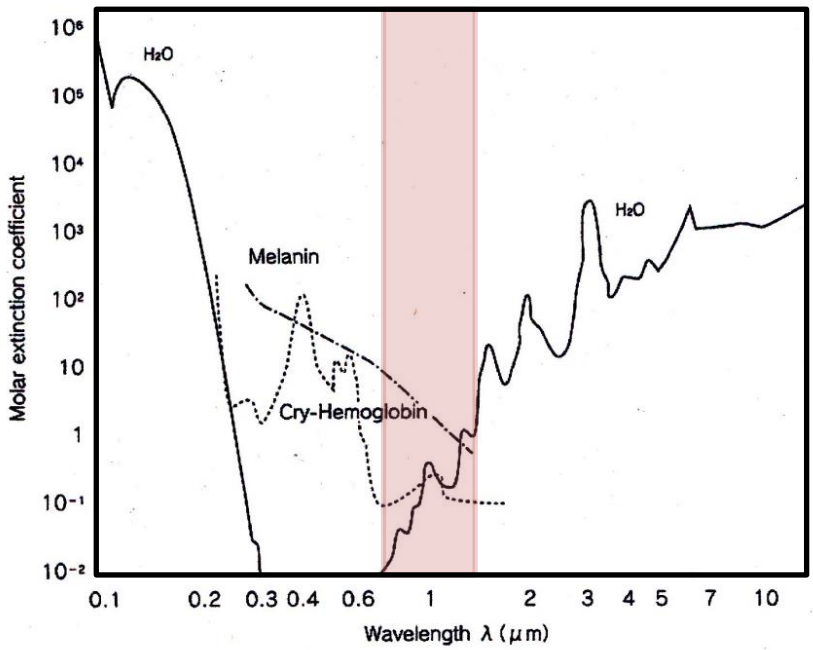

Figure 14: Absorption behavior of the different substances in biological tissue [17]

Especially red light with wavelengths of 650 nm – 700 nm imply following advantages for biological applicability:

1. it has a high biological tissue permeability,
2. this light is in the visible range,
3. it is an optimal wavelength range, which can be used for in vivo applications and is suitable for detectors in conjunction with photomultipliers.

Hence this wavelength region can be used for fluorescence imaging methods and it is of special interest in the field of medicine. [19]

As already mentioned Pc is one of very few dyes that have an excitation and an emission peak which are both in the red light region. Pc has a long-wavelength absorption maximum at approximately λ_{max} = 650 - 700 nm, with a high molar extinction coefficient ($\varepsilon \approx 10^{5\text{-}6}$). It has a low cytotoxicity, a high chemical stability and because of its good emission quantum yield it is perfectly suitable for the process of fluorescence bioimaging. [19]

Because of these outstanding properties of Pc, it is used for various applications in the field of medicine (such as photodynamic therapy (PDT) and photodynamic diagnosis (PDD)). Phthalocyanine derivatives have a bigger absorbance capability at longer wavelengths than porphyrin and most of them are capable of photo-induced singlet oxygen generation which

can be used for PDT. In addition, their properties can be altered and influenced through the addition of substituents to the periphery of the macrocycle or the variation of axial ligands to the chelated central metal ion. [19]

B.3 Application of phthalocyanines

This chapter is describing just one area of application of Pc in the field of medicine. The actual applicability of Pc complexes is of course much wider (as already mentioned in the **Chapter B.1.2**). The application that will be discussed in this chapter is the application of Pc for the use as fluorescence bioimaging method for the photodynamic diagnosis (PDD). The compound that was synthesized for this thesis was part of this field of research.

B.3.1 Characteristic Bioimaging Applications

As already mentioned in **Chapter B.2.3.2** the fluorescence properties of Pcs are important for the biological use. The wavelength of the Q-absorption band and the fluorescence emission wavelength of Pc are in regions in which the light can easily penetrate biological tissues. Therefore Pc complexes have the fundamental properties of being used for the photodynamic diagnosis (PDD). [20]

B.3.1.1 Principle of PDD

Pcs tend to concentrate in tumor tissues, which can be detected by the fluorescence of Pcs via PDD. PDD is based on the combined use of the selective uptake of photosensitizers into malignant tissues and the detection of emitted light (≥ 650 nm), which significantly penetrates through living tissues. This light is detected and measured and it can be used for the diagnosis of tumor tissues. In the case of Pc compounds, both the excitation light and fluorescence light have similar wavelengths over 650 nm and can significantly penetrate through living tissues. This is an important advantage for the use of fluorescence probes to detect biologically important chemicals. Fluorescence detection has several advantages including high sensitivity and high spatial resolution with microscopy. The development of potential fluorescence probes is therefore highly important. [20]

Ishii et al. from the University of Tokyo has developed a fluorescence probes to detect ascorbic acid (vitamin C) in biological systems by employing SitBuPc linked to two TEMPO radicals. [20]

B.3.1.2 Previous research of SitBuPc fluorophore

A new method for quantitative analysis of vitamin C in biological and chemical liquids was proposed by Ishii et al. Two hybrid molecules consisting of chromophore and nitroxide parts were employed. The machanism of fluorescence vitamin C detection is based on two physico-chemical phenomena (see Figure 17):

- intramolecular quenching of the fluorophore by the nitroxide fragment which reduces the fluorescence and
- chemical reduction of the nitroxide by ascorbic acid which enhances the fluorescence intensity by eliminating the quenching effect of the nitroxide radicals.

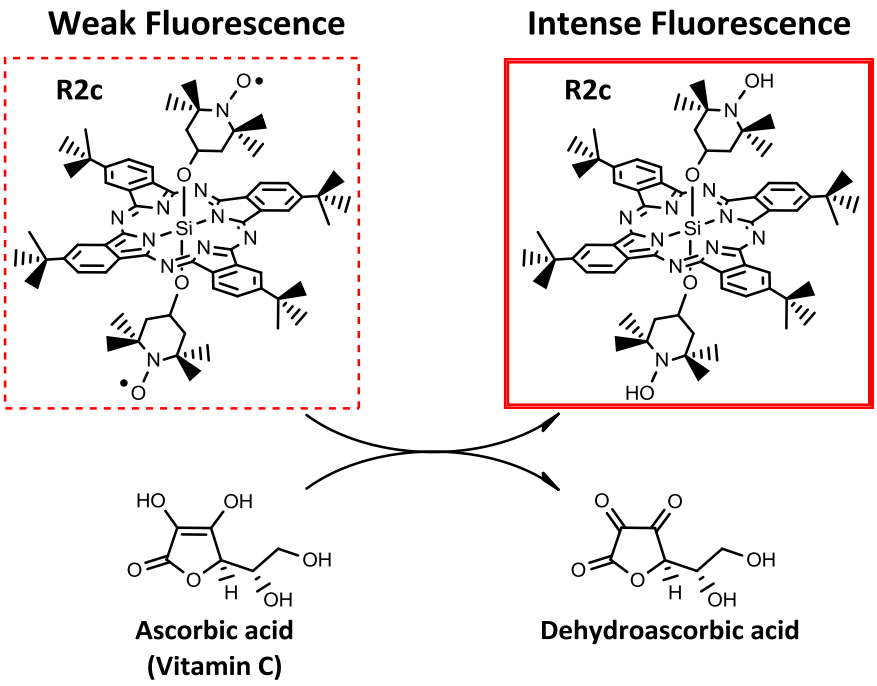

Figure 15: Reaction of vitamin C with the nitroxides of the SitBuPc-complex

These probes were encapsulated in liposomes for application to aqueous solutions and were measurement in HeLa cells. [23]

Fluorophores linked to nitroxide radicals exhibit potentially useful properties based on the fact that such radicals have both efficient fluorescence quenching and favorable reactions with ascorbic acid.

HeLa cells treated by the Pc-compound showed negligible fluorescence before ascorbic acid addition, indicating that the TEMPO radicals of hydrophobic Pc complex resulted a

quenching before reacting with ascorbic acid. Nevertheless, fluorescence was observed at 30 minutes after adding ascorbic acid to the Pc complex. [20]

B.3.1.3 Photophysical properties of phthalocynanines linked to nitrodixe radicals

Interactions between Pcs in the T_1 state and other paramagnetic molecules result in some important phenomena in photophysical and photochemical processes.

- **One** example is the quenching of Pcs in the S_1 and T_1 states. This quenching occurs when the concentration of the T_1 Pc is high (T-T annihilation) or when paramagnetic metals (such as CuPc) or radicals exist. [Booklet]
- The **second** phenomenon is the formation of excited singlet oxygen. T-T annihilation between the T_1 Pc and triplet oxygen results in an energy transfer to yield the excited singlet oxygen. This mechanism has been applied to photodynamic cancer therapy (PDT). [21]
- A **third** phenomenon is photo-induced population transfer (PIPT) between the singlet and triplet ground states, observed for (phthalocyaninato)silicon covalently linked to two doublet nitroxide radicals. This PIPT results from selective decay from the excited states to the triplet ground state, and is, therefore, attractive as a new concept for controlling magnetic properties by photoexcitation. [24]

Since a key feature of these phenomena is the formation of excited multiplet states constituted by the T_1 Pc and other paramagnetic molecules, it is important to investigate when the excited multiplet states such as the lowest excited doublet (D_1) and quartet (Q_1) states consisting of the T_1 chromophore and doublet nitroxide radical (NR) are formed. [24]

In order to discuss the electron spin dynamics simple excited-state diagrams are shown in Figure 18. The doublet ground (D_0) state consists of NR in the D_0 state (^{2}NR) and Pc in the singlet ground S_0 state (^{1}Pc). A pair of ^{2}NR and Pc in the S_1 state (^{1}Pc*) provides the excited doublet (D_n) state. On the other hand, the D_1 and Q_1 states are generated by an interaction between ^{2}NR and Pc in the T_1 state (^{3}Pc*). [21]

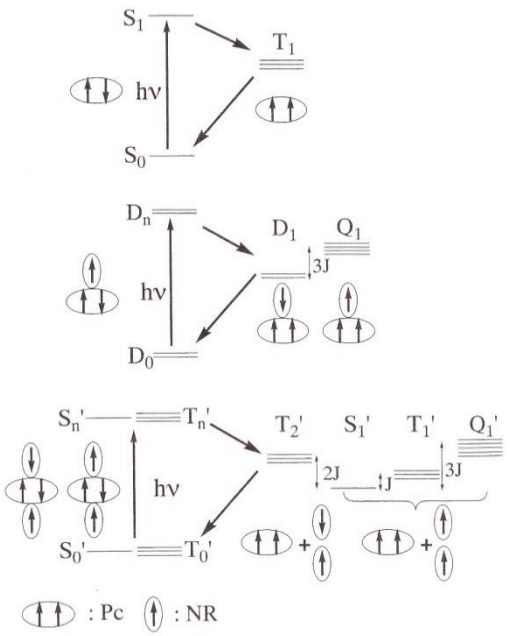

Figure 16: Excited-state diagrams of Pcs linked to one (middle) and two (lower) nitroxide-radicals with that of normal Pc (upper) [21]

Many studies have been carried out about this topic and in conclusion, it was shown experimentally that the decay rate of the $D_1 \rightarrow D_0$ transition is well correlated with the magnitude of the electron exchange interaction between the excited triplet SiPc and doublet NR. [21, 24]

Recently, a novel phenomenon originating from the formation of the excited multiplet states has been observed for SitBPc covalently linked to two TEMPO radicals, $SiPc(TEMPO)_2$. The excited state diagram of Pc linked to two nitroxide radicals, $SiPc(TEMPO)_2$, is shown in Figure 19. The singlet (S'_0) and triplet (T'_0) ground states are generated by an interaction between two ^{2}TEMPO radicals. The excited singlet (S'_n) and triplet (T'_n) states are constituted by ^{1}SiPc* and two ^{2}TEMPO. The interactions among ^{3}SiPc* and two ^{2}TEMPO produce the lowest excited singlet (S'_1), triplet (T'_1), quintet (Q'_1), and second lowest excited triplet (T'_2) states. Here, the two ^{2}TEMPO radicals exhibit triplet and singlet characters in the T'_1 and T'_2 states, respectively. [21]

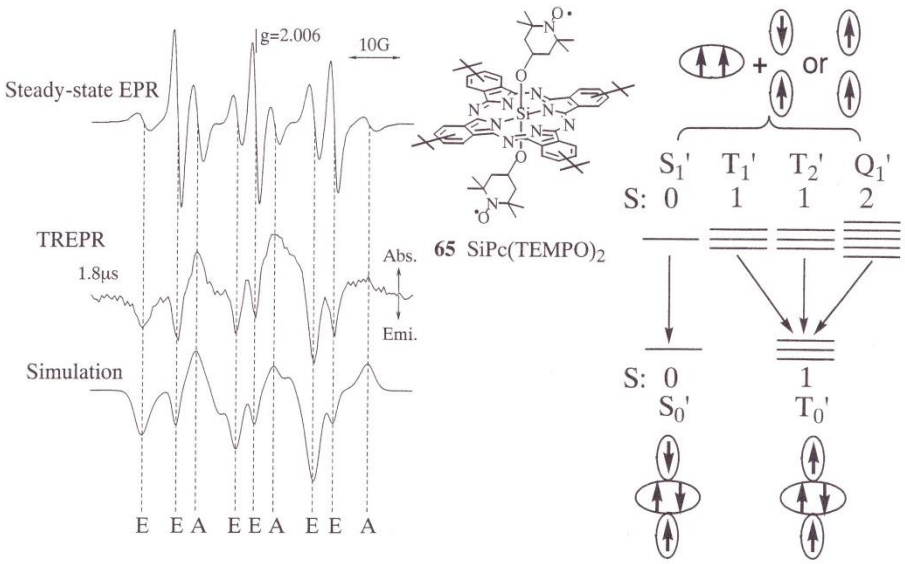

Figure 17: Steady-state EPR and TREPR spectra of $SiPc(TEMPO)_2$ and decay dynamics from the excited multiplet states [21]

A TREPR spectrum of $SiPc(TEMPO)_2$ at 293 K, observed at 1.8 μs after laser excitation, is shown in Figure 19. By comparison with the steady-state EPR spectrum, these signals are assigned to a spin-correlated radical pair in the ground state. The TREPR spectrum at 1.8 μs shows an EEA EEA EEA polarization pattern, which can be reproduced by selective population to three triplet sublevels in the ground state. [21]

The decays from the T'_1, T'_2, and Q'_1 states, except for the S'_1 state, should be selective to the T'_0 state rather than those to the S'_0, state, because of the spin quantum number. The EEA polarization is reasonably interpreted by selective decay from the excited multiplet states in the Boltzmann distribution to three triplet sublevels in the ground state. The time-profile of this ESP is analyzed where the rising and decaying parts are the spin-lattice relaxation time of the ground state and the lifetime of the excited multiplet states, respectively. In general, it is very difficult to vary the difference in population between the S'_0 and T'_0 states by varying the temperature. [21]

Accordingly, it is noteworthy that the ground state generated via the excited multiplet states has more triplet character than that in the absence of photoexcitation, even at room temperature. Furthermore, this is different in principle from the previous mechanisms, where the magnetic properties are varied by changing the electronic or chemical structures, to control the magnetic properties by the photo-induced population transfer between the S'_0 state and the T'_0 state, where the electronic configuration is the same as that in the S'_0 state. Therefore, this mechanism is not only attractive in terms of the excited state dynamics

but is also a novel concept for controlling the magnetic properties in the ground state by photoexcitation. [21]

B.3.1.4 Electronic absorption, MCD, and fluorescence spectra

Typical UV/VIS absorption, MCD, and fluorescence spectra of SiPc, SiPc-TEMPO, and SiPc-$(TEMPO)_2$ are compared with each other in this chapter.

The **absorption** data of SiPc-TEMPO and SiPc-$(TEMPO)_2$ are very similar to those of SiPc, indicating that electronic interactions between the doublet TEMPO and the excited singlet SiPc are weak.

The **MCD** data of SiPc-TEMPO and SiPc-$(TEMPO)_2$ are almost identical with those of SiPc, in analogy with the absorption spectra. This result can be reasonably explained by the fact that the MOs, which provide the orbital angular momentum, are localized on the Pc ring, and exhibit little interaction with the spin angular momentum of the TEMPO radicals. In contrast, **fluorescence** quantum yield (φ_F) values are remarkably dependent upon the number of TEMPO radicals. The φ_F values of SiPc, SiPc-TEMPO, and SiPc-$(TEMPO)_2$ are 0.57, 0.21, and 0.012, respectively. The decrease in the φ_F values is reasonably assigned to the change in ISC rate from ^{1}SiPc* to ^{3}SiPc*. The energy diagram of SiPc-TEMPO is different from that of SiPc, as shown in Figure 20. [25]

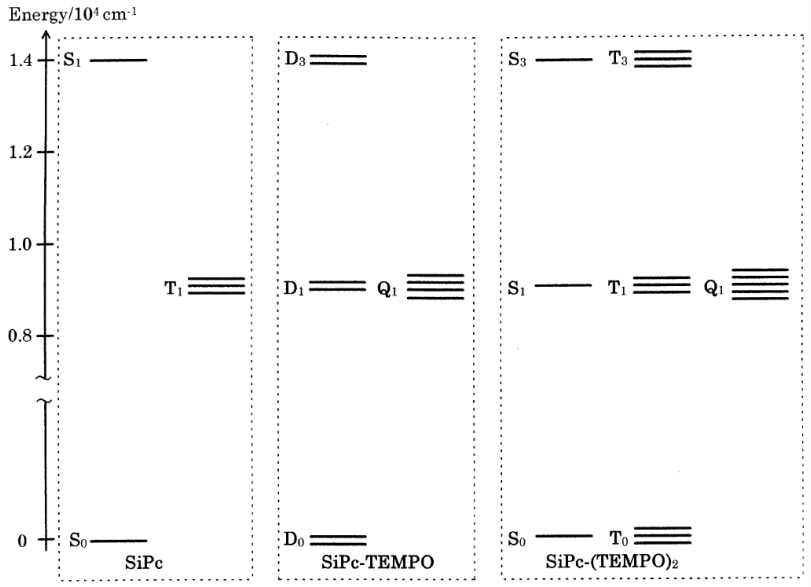

Figure 18: Energy diagrams of SiPc, SiPc-TEMPO and SiPc-$(TEMPO)_2$. The D_3 state of SiPc-TEMPO and the S_3 and T_3 states of SiPc-$(TEMPO)_2$ are constituted by the excited singlet SiPc and doublet TEMPO radicals. The D_1 and Q_1 states of SiPc-TEMPO and the S_1, T_1 and Q_1 states of SiPc-$(TEMPO)_2$ are constituted by the excited triplet SiPc and doublet TEMPO radicals. [25]

For SiPc-TEMPO, the D_3 state is constituted by ^{1}SiPc* and ^{2}TEMPO. In contrast, the D_1 and Q_1 states are generated by the interaction between ^{3}SiPc* and ^{2}TEMPO. For SiPc the decay from ^{1}SiPc* to ^{3}SiPc* is spin-forbidden. However, the decay from ^{1}SiPc* to ^{3}SiPc* partially turns out to be a spin-allowed transition ($D_3 \rightarrow D_1$) for SiPc-TEMPO. Therefore, the decrease in the φ_F value of SiPc-TEMPO is rationalized by the formation of the $D_3 \rightarrow D_1$ decay. [25]

The smallest φ_F value of SiPc-$(TEMPO)_2$ is considered in a similar manner. The energy diagram of SiPc-$(TEMPO)_2$ is also shown in Figure 20. The S_3 and T_3 states are constituted by ^{1}SiPc* and two ^{2}TEMPO radicals. Further, the S_1, T_1 and Q_1 states are generated by the interactions among ^{3}SiPc* and two ^{2}TEMPO radicals. Although nine spin sublevels are generated from ^{3}SiPc*, the spin quantum numbers of four sublevels are identical with that of the S_3 or the T_3 state. On the other hand, only two sublevels of the D_1 state out of six sublevels have the same spin quantum number as the D_3 state for SiPc-TEMPO. Therefore the probabilities of spin-allowed sublevels are 1/3 and 4/9 for SiPc-TEMPO and SiPc-$(TEMPO)_2$, respectively. Hence the decay from ^{1}SiPc* to ^{3}SiPc* for SiPc-$(TEMPO)_2$ is faster than that for SiPc-TEMPO. [25]

B.3.1.5 Steady state EPR spectra of SiPc derivatives

Steady state EPR spectra of SiPc-TEMPO and SiPc-$(TEMPO)_2$, observed at 293 K, are shown in Figure 21a and b, respectively. Three signals, split by hyperfine coupling of a nitrogen nucleus (I=1), are observed for SiPc-TEMPO, indicating the presence of one TEMPO radical. On the other hand, SiPc-$(TEMPO)_2$ shows more complex EPR signals compared to the three signals of SiPc-TEMPO. Additional new signals are due to a spin-correlated radical pair constituted by two TEMPO radicals. [26] The observed spectrum was also simulated as shown in Figure 21c.

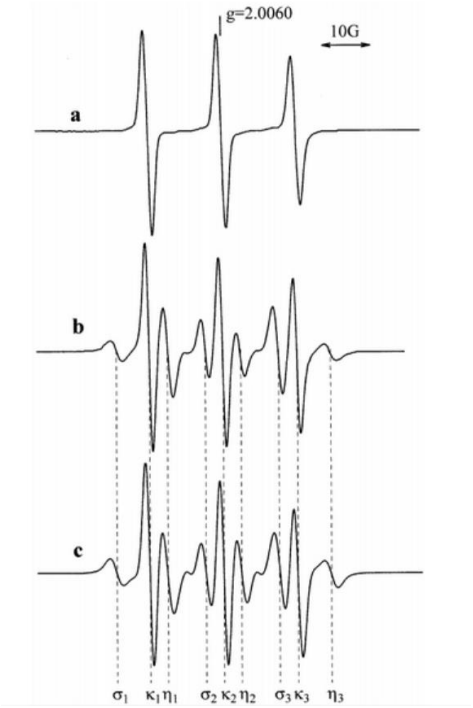

Figure 19: Steady state EPR spectra of SiPc-TEMPO (a) and SiPc-$(TEMPO)_2$ (b). A simulation spectrum (c) was calculated as a spin-correlated radical pair [26]

C) Specific Part

C.1 Introduction to vitamin C detection

Ascorbic acid (Vitamin C) is a well-known and essential nutrient in relation to biological functions such as carnitine biosynthesis and scurvy prevention; moreover, it is also used in health care supplements as anti-oxidizing agents or anti-aging agents. In particular, recently, ascorbic acid has attracted considerable attention for its uses in modern cancer therapy. Although it has become necessary to directly detect ascorbic acid today, no fluorescence bioimaging technique has been established thus far. This has led to many limitations; for example, investigations on cellular uptake of ascorbic acid had been restricted only to indirect techniques such as radiometric measurements of cells including radioactive ascorbic acid or high-performance liquid chromatography-electrochemical detections of ascorbic acid extracted from cells. Thus, it is extremely important to develop fluorescence probes to detect ascorbic acid for clarifying the biological roles. [1]

Fluorophores linked to a nitroxide radical (FN systems) are promising candidates as the fluorescence probes for detecting ascorbic acid. The nitroxide radical provides efficient fluorescence quenching and the standard redox potential of nitroxides is high enough (E°=0.54 V vs SHE for piperidine) to oxidize ascorbic acid. [26] Thus, the FN-based probes have been expected to be applied to the quantitative determination of ascorbic acid in aqueous solutions. However, in contrast to aqueous solutions, improvements are required to apply the FN probes to the detection of ascorbic acid in biological environments, since, in addition to ascorbic acid, the nitroxide radical easily reacts with some biological reductants such as mitochondrial NADH and superoxide. [1]

C.2 Aim of the thesis

The aim of the research project of this master thesis was to develop and synthesize a new SiPc complex that could detect ascorbic acid (vitamin C) by emitting fluorescence radiation. This new complex should be able to detect even smaller amounts of ascorbic acid compared to an already developed first generation of this complex which has these capabilities. In Figure 22 the two generations of vitamin C detecting complexes can be seen.

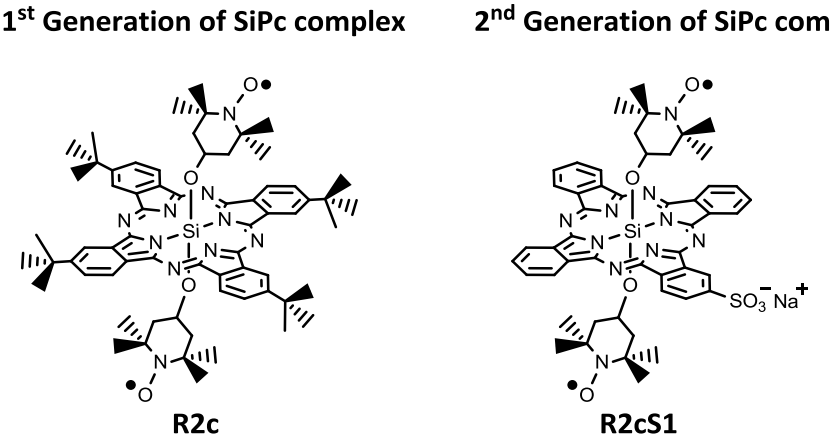

Figure 20: First (left) and second (right) generation of the vitamin C detecting complex

The improvement of the second generation of the SiPc complex should be achieved by increasing the hydrophilicity of the complex by attaching one hydrophilic sulfate group on the complex. The reason behind this improvement will be explained in **Chapter C.1.2**. A higher sensitivity towards vitamin C should enable that complex to detect even lower concentrations of ascorbic acid compared to the first generation of the complex.

C.2.1 Synthesis of the Pc complex

C.2.1.1 First reaction step

The complex is prepared in a two-steps synthesis. In the first reaction step (Reaction A) $SiPc(OH)_2$ is sulfonated on one of the four fused benzyl rings of the SiPc complex a reaction with oleum.

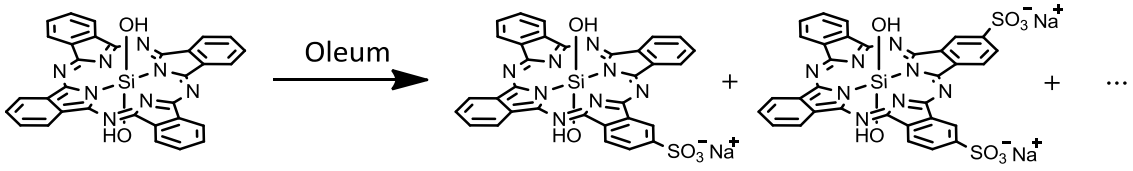

Figure 21: Reaction A: First step of the synthesis of the complex R2cS1

This sulfate group causes a higher hydrophilicity of the complex. The main challenge of the first reaction step is to find the optimal reaction conditions in which the formation of mono-sulfonated SiPc complex is favored particularly. This can be achieved by changing the following variable parameters: reaction time (t), temperature (T), and concentration of

oleum (c). The parameters are optimized in a way that the largest possible yield from the SiPcS1 complex is formed.

The second challenge of the first reaction step after the optimum reaction conditions are found, is the separation of the desired product SiPcS1 from the higher substituted SiPcSx (x = 2-4) complexes. After that, the purified complex SiPcS1 is characterized by ESI-MS and absorption measurement.

C.2.1.2 Second reaction step

In the second reaction step, two 4-hydroxy-TEMPO radicals are attached to the silicon central atom of the SiPcS1 complex. In this reaction step there are two reaction products formed: R1cS1 and R2cS1.

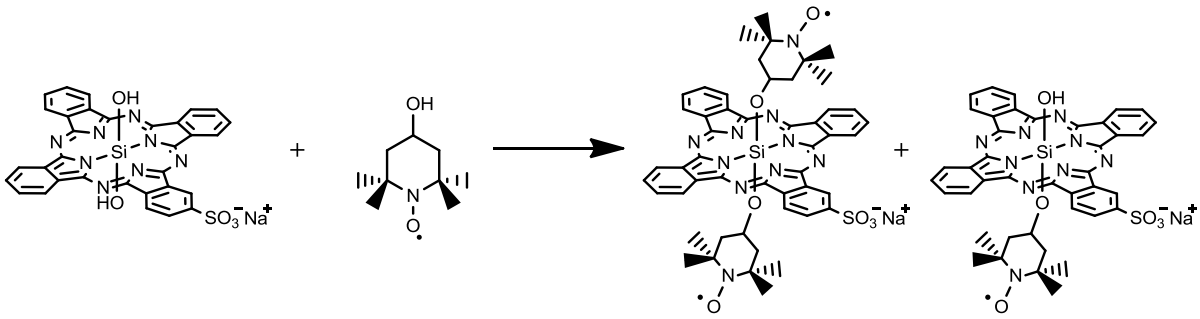

Figure 22: Reaction B: Second reaction step for the synthesis of the complex R2cS1

The purpose of the two TEMPOL radicals is that they cause a fluorescence quenching of the complex R2cS1 after its excitation at an appropriate wavelength. Also for this reaction step the reaction mixture will have to be separated, purified and finally characterized by an ESI-MS-measurement, an absorption spectrum and an ESR-measurement. Finally the fluorescence development is compared with that of the old first generation of the complex R2c.

C.2.1.3 Reduction of the Pc complex

To be able to detect ascorbic acid in biological environments, R2cS1 complex is encapsulated in liposomes and micelles. This spherical vesicles composed of phospholipids prevent the nitroxide radical to react with some biological reductants such as mitochondrial NADH and superoxide. [1] Then the last and final reaction step, the reduction reaction of the newly synthesized complex with vitamin C is carried out. The reduction eliminates the two nitroxid radicals. This results in a termination of the quenching effect of these radicals and since the radical sites of the complex no longer exist the complex will develop its high fluorescent effect. This change in fluorescent activity is measured and monitored over time and is also compared with the first generation of the fluorescent complex R2cS1 (see Figure 25 left side) under the same conditions.

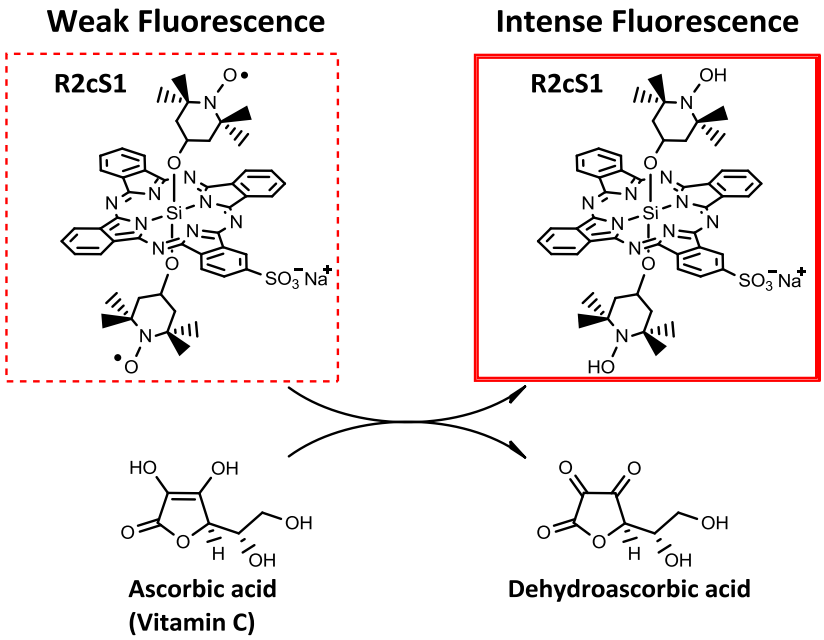

Figure 23: Reduction reaction of the complex R2cS1 with vitamin C which causes a stronger fluorescence signal

C.2.2 What is the difference between the 1st and 2nd generation of the Pc complex?

As it can be seen in Figure 25 above, the only difference between the two complexes is that the second generation of the vitamin C detecting complex is more polar than the first generation of that complex due to the installed polar sulfate group.

The four isobutyl groups attached to the fused benzyl groups of the SiPc complex are replaced for one sulfate group. This change increases the polarity of the complex and therefore changes also its solubility properties. Since the complex still has to be protected from reactive species when injected into a biological system, it is incorporated into bilayered liposomes or micelles (see Figure 26). Due to the changed polarity of the new complex, the probability of positioning of the complex closer to the outer polar regions of the liposome is much higher. This is believed to increase the reactivity with the polar vitamin C which is also more probable located at the outer regions of the liposomes. Because of this theory the hypothesis of this research project is that an increased polarity of the SiPc-complex could be the reason for an increased and stronger fluorescence emission for the second generation of the complex compared to the first generation.

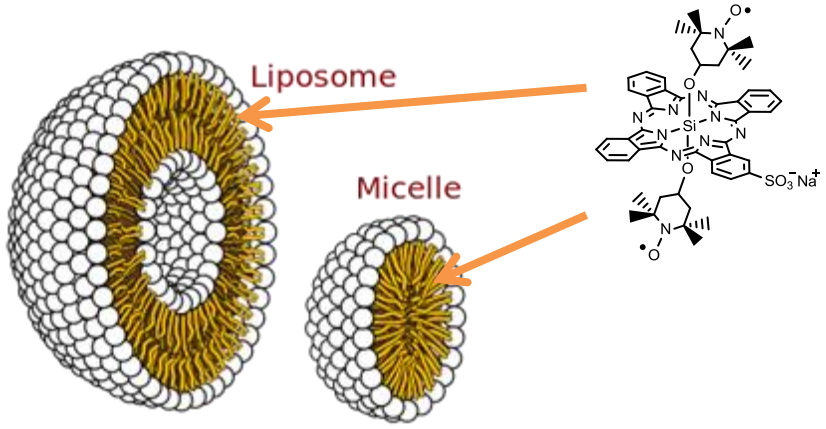

Figure 24: The new synthesized complex will be encapsulate in liposomes and micelles which should protect the radical sites to react with reactive species in a biological environment [28]

D) Experimental Part

D.1 General remarks

All reagents, which were purchased from commercial suppliers, were used without prior purification.

D.1.1 Chromatographic methods

D.1.1.1 Thin layer chromatography

TLC was performed by using TLC aluminum foil Merck, Silica gel 60 F_{254}, Silica gel 60 RP-18 F_{254}s and Aluminum oxide 60 F_{254}.

D.1.1.2 Column chromatography

The glass columns were packed with either silica gel (Kanto Chemical Co, 63-200 µm) or aluminum oxide 90 active basic (Merck KGaA, 63 - 200 µm). The solvents, which were used for column chromatography, were either purchased from commercial suppliers or redistilled before use. The composition of the mobile phase in each experiment as well as the amount of silica used are given in the respective synthesis.

D.1.2 Analysis methods

D.1.2.1 Spectrophotometric assay

The Absorbance measurements were done on a JASCO V-570 (UV/VIS/NIR spectrometer). The spectra were measured from 300 to 800 nm at room temperature using quartz glass cuvettes with a diameter of 1 cm. For the measurement of the spectrum, in each experiment are given in the respective description.

D.1.2.2 ESI-MS

The ESI-MS was measured on a BRUKER HCT ultra 12S. The samples were prepared in a 1, 0.1, 0.01 ppm solution with MeOH as a solvent. The concentrations were set up with the help of absorption measurement on the UV/VIS spectrometer. After each measurement the tubes were conscientiously cleaned with MeOH and water.

D.1.2.3 ESR measurement

The ESR spectra were recorded on a JEOL JES-FE2XGS Electro Magnet at T = 297 K. The sample was dissolved in absolute toluene before the measurement. After this liquid samples were drawn into 5 mm I.D. glass tube sealed at the bottom. All experiments were conducted with the following parameters: 9.40 GHz microwave frequency, 20.12 mW non-saturated microwave power, 100 kHz field modulation of 1 G amplitude.

D.1.2.4 Fluorescence measurement

For fluorescence measurements the liposome solution was transferred in cuvette. The solution was stirred by a magnetic stirrer and excited by a diode laser (LDX Optronics LDX-2515-650; 650 nm) with a mechanical chopper. The fluorescence was detected by using a monochromator (JASCO CT-25CP) and a photomultiplier (Hamamatsu Photonics R928), and subsequently, the time- profiles of the signals obtained through a lock-in-amplifier (Stanford Research SR830) were recorded using a digital oscilloscope (Iwatsu-LeCroy LT342). The experimental setup can be seen in Figure 27.

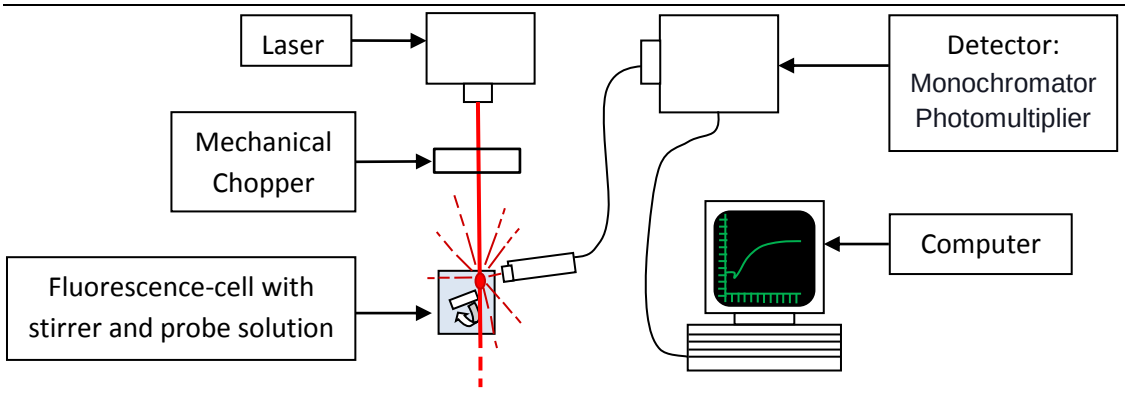

Figure 25: Experimental setup for measuring the time dependent fluorescence development after adding vitamin C to the in PBS dissolved complex solution

D.1.2.5 MCD measurement

MCD measurements were performed by using JASCO E-250 equipped with a JASCO electro magnet (+1.35 or – 1.35 T).

D.1.2.6 Elemental analysis

The elemental analysis was recorded on a Thermo Fisher SCIENTIFIC FLASH 2000 Organic Elemental Analyzer.

D.2 Experimental procedures

This chapter describes the experimental procedure for the synthesis of the compounds SiPcS1 and R2cS1 in the following structure: hypothesis tested – methodes used – conclusion drawn and new open questions emerging, which are considered in the next iteration round. Due to the fact that the two newly synthesized compounds SiPcS1 and R2cS1 have never been described in any literature before, it came to numerous obstacles throughout the research project that could not be overcome immediately. The following subchapters describe the experimental procedures of the individual experiments and the hypotheses that were made in respect to overcome these obstacles.

Furthermore some reactions were repeated under exactly the same reaction conditions but different measurements were performed with those reaction products the results of these measurements and the gained knowledge are summarized in one reaction. At the end of this chapter a fully working and optimized synthetic procedure is provided which lead to the successful synthesis of the complex R2cS1.

D.2.1 Experiments carried out for the discovery of the synthesis of mono-sulfonated silicon-phthalocyanine

D.2.1.1 Reaction A01

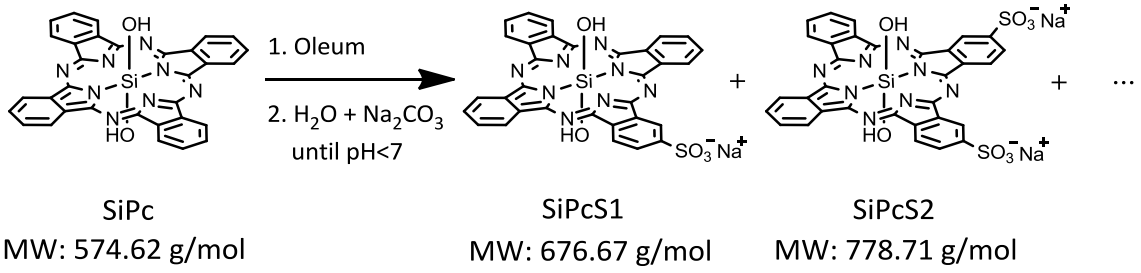

Figure 26: First reaction step: Synthesis of SiPcS1

Hypothesis:

- In an one-hour small scale reaction of SiPc with 30 % oleum at room temperature should form the desired product SiPcS1 and higher substituted SiPcSx (x=2-4) compounds.
- The starting material (SM) SiPc is very hydrophobic. But with an increasing number of sulfate groups installed on the SiPc complex, the compound should become more and more water-soluble. It is believed that the SM and SiPcS1 are not dissolving in water, but the higher substituted compounds would dissolve in water. Therefore, the separation of SiPc and SiPcS1 from the higher sulfonated complexes should be achieved by normal filtration.
- The third hypothesis is that only the SiPc complex would be soluble in $HCCl_3$. Thus, by extraction of the complex mixture with $HCCl_3$, H_2O and MeOH a separation of SiPc and SiPcS1 should be achieved.

Experimental implementation:

In this first synthetic experiment 3.75 mg (= 5 mg of 75 % SiPc; $6.52*10^{-6}$ mol) SiPc was weighed into a 10 ml flask and 1 ml of 30 % oleum was added afterwards. The flask was sealed with a glass stopper and the reaction was stirred for one hour at room temperature using a magnetic stirrer. After one hour, the reaction was terminated by the addition of H_2O. When the water was added to the reaction solution a strong exothermic reaction was observed because the SO_3 molecules which were dissolved in sulfuric acid reacted with H_2O to H_2SO_4. As a consequence the reaction solution heated up for a short time. Then Na_2CO_3 was added to the aqueous solution. A strong foam formation was observed due to CO_2 release. After the pH value of the solution reached a value smaller than 7 and no more CO_2 formation was observed, the reaction solution was examined for products.

General explanation of the TLC separation procedure:

TLC experiments were carried out with the reaction solution to analyze the product mixture for their different products. In theory by the right choice of a suitable solvent mixture and the appropriate TLC solid phase, it is possible to separate the various reaction products by TLC. This allows getting an insight into how many products are formed in a reaction and how the product-ratios of the reaction are.

The assumption was that the starting material SiPc would not be move from the mobile phase on TLC plate, as it is not soluble in most solvents. Therefore it was expected that SiPc remains at the starting spot of the TLC plate. However, the various substituted products should show different solubility in the used solvents. The different number of sulfate groups of the SiPc complex would show a different retention behavior on RP (reversed phase) and NP (normal phase) –TLC. Following these assumptions, the reaction products with NP and RP-TLC would have the following retention behavior (see Figure 29).

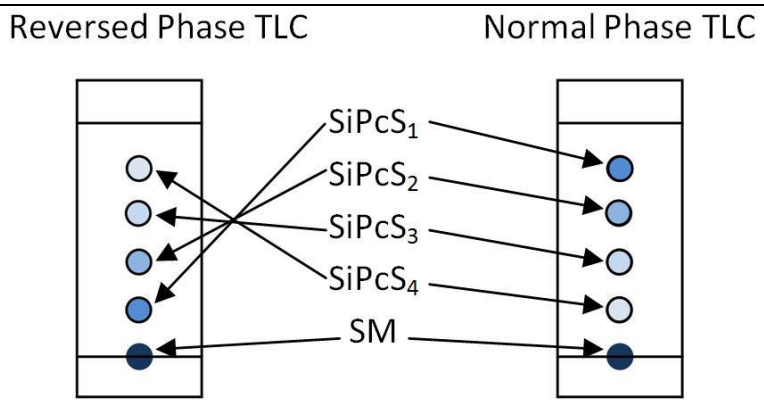

Figure 27: Retention behavior of the first-step reaction product mixture for reversed phased TLC (left) and normal phased TLC (right)

In order to find a suitable separation method, many different solvents and different solvent mixtures in different ratios were tried out as a mobile phase for the TLC separation.

Especially the methanol-water (2:1) RP-TLC 2a successfully separated some compounds and showed various spots.

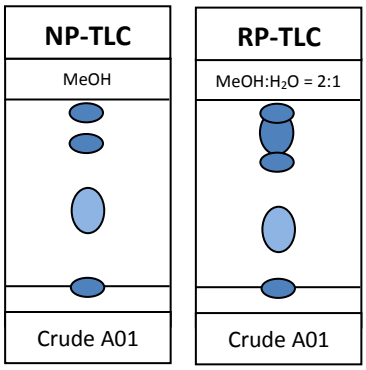

TLC-1a TLC-2a

Filtration:

The aqueous solution, which was created during the neutralization reaction, was then filtered through filter paper and a funnel. A bluish solution and a blue solid material could be separated. The filter cake was washed thoroughly with water until the water flowing through the filter showed no more blue color change. Both from the filter cake and the filtrate TLC were made to control the separated compounds. However, it became clear that in both fractions, the filter cake (this was dissolved again in toluene) and in the filter solution, the starting material was still present. Nevertheless different product spots could be separated with normal phase TLC using methanol as a mobile phase.

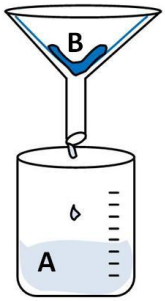

Figure 28: Illustration of the filtration of the first synthesis

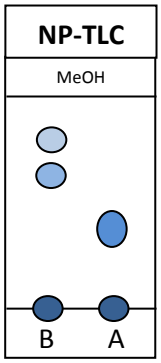

TLC-3a

According to theory, the spots at higher Rf values on the NP-TLC should be the product spot SiPcS1 (based on Figure 29). Therefore it was concluded that the aimed reaction product had to be present in the filter cake.

Extraction:

For this reason, a liquid-liquid extraction (using $HCCl_3$ and MeOH) was carried out with the filter cake. However, since these two solvents were miscible and trained no phase boundary, H_2O has been added as a third extraction solvent.

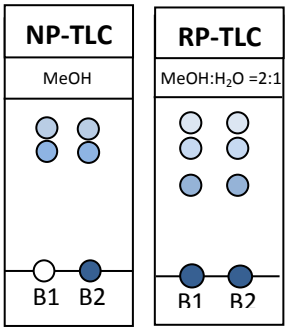

TLC-4a TLC-5a

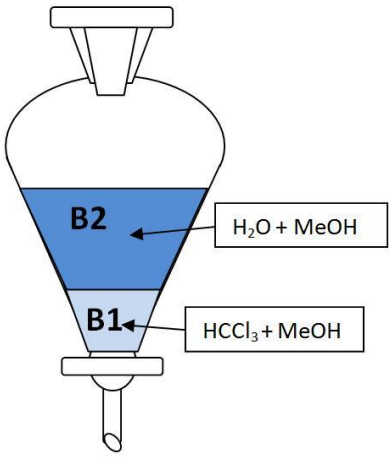

Figure 29: Illustration of a liquid-liquid extraction for the first synthesis

The subsequent TLC control showed that in the lower liquid phase B1 no starting material was left, but in both phases (B1 and B2) the presumed product spots were found. In addition, in a RP-TLC experiment using MeOH and H_2O as solvents, three spots were observed (the same as in TLC-2a). These TLC experiments indicated that the separation method of extraction with those solvents was not working. However, the fine separation of the individual spots on the TLCs opened up the possibility to separate the products later with the help of a larger scale TLC-plate separation and maybe even in a column chromatography for following large scale reactions.

Workup reaction A01:

For this reason, all fractions of the extraction were reunited and the solvent was removed on evaporator. Just before all of the solvent was completely removed from the flask, the formation of a white solid on the glass wall was observed. When it was tried to dissolve the solids in MeOH (it was already known that MeOH could solve all the reaction products except the SM) this white solid was not dissolved and remained on the flask wall. After a second filtration and thorough washing with MeOH, the solvent was again reduced to a minimum. The filtration had the result, that a large proportion of SM was separated. After that a RP-TLC separation (MeOH:H_2O = 2:1) was performed.

TLC separation A01:

After the evaporation the product mixture was again dissolved in a very small amount of MeOH and it was then applied on a 25 cm long RP-TLC plate. The TLC plate was put into a TLC chamber filled with a solvent mixture (MeOH:H_2O = 2:1) for separation. Thus, the entire concentrated product-solution was applied onto several TLC plates and separated in the TLC chamber. Since the concentration of the product on the big TLCs was much bigger than that of the small TLC experiments, the spots were also much more intense but also the separation of the spots was worse and not 100 % indistinguishable between the different product spots. Subsequently, the all spots from the solid phase of the TLC plate were scraped down and separated with a spatula, were extracted with MeOH and the solid particles were separated by normal filtration. Finally four fractions and samples were collected and prepared: SiPcS1, a mixture of SiPcS1 and SiPcS2 and a mixture of all other fractions SiPcSx (x=2-4).

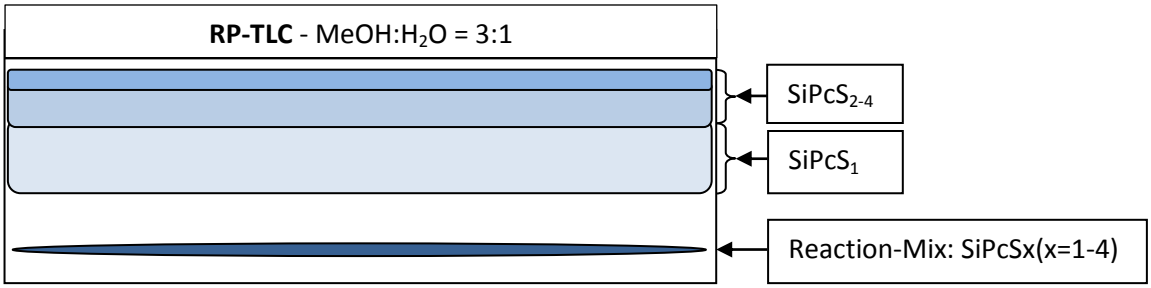

TLC-6a: First RP-TLC big scale separation of the different reaction products

The solvent used for the extraction was again removed on an evaporator and the product was dried under high vacuum. The yield of the collected sample of SiPcS1 according to balance was 0.8 mg which was a total yield of 18 %. (This was a misleading result. The reason for that will be explained in a later chapter). After the TLC separation an ESI-MS measurement was performed.

ESI-MS measurement:

Even though many fragment peaks of the complex were observed in the ESI-MS measurements there was also the product peak of SiPcS1 measured for the TLC-spot number 1. The product peak was found by a m/z value of 653 n the negative spectrum of the measurement. This peak corresponds to the product SiPcS1 minus one times the mass of sodium. The isotopic pattern which was previously calculated using the Chemdraw software verified the result. The relevant measured spectra from this measurement can be found in Appendix E.1.1.

Conclusions of the reaction A01:

- An one-hour reaction of SiPc with 30 % oleum formed the reaction product SiPcS1 with a yield of 18.8 %, according to the balance (this will be revised and corrected in later experiments).
- The filtration and extraction separation method did not lead to a successful separation.
- The separation of the various products of SiPcSx by RP-TLC (MeOH: H_2O 2:1) could be achieved.

Open questions:

- Which parameters must be changed in order to obtain an even better yield of the product SiPcS1? (Variables: reaction time t, temperature T or H_2SO_4 concentration)

- How could be the product of a big scale reaction successfully separated with the help of column chromatography?

D.2.1.2 Reaction A02

Hypotheses on reaction A02:

- The yield of the reaction is dependent on the reaction time. Therefore throughout the reaction time small samples should be taken at regular intervals.
- The yield of the small samples during the reaction will be monitored with RP-TLC (MeOH:H_2O = 2:1) by comparing the intensity of the color of the individual product TLC-spots.

Experimental implementation:

In the second synthetic experiment (A02), the same experimental implementation was performed as in reaction A01. The only difference was that small samples were drawn in regular intervals during the reaction. The samples were subjected to same workup procedure and then they were examined with the help of RP-TLC to the desired product. The separated product spot number one which contained the desired product SiPcS1 served as a reference material on the TLCs plate.

3.75 mg (= 5 mg of 75 % SIPC 6.52 * 10^{-6} mol) SiPc was weighed in a 10 ml flask and then 1 ml of 30 % oleum was added. The flask was sealed with a glass stopper and every 10 minutes a 150 µl sample of the reaction solution was taken by using a calibrated Pasteur pipette. The samples were mixed with 2 ml of water and neutralized with Na_2CO_3 to a pH > 7. Then RP-TLCs were measured. The results of the TLC experiments were surprising. Up to the reaction time of one hour (the time when the first reaction was stopped) no SiPcS1 product peak was found. The spots on the TLC plates only showed the by-product spots which presumably could be SiPcS3/4 but no mono-substituted SiPcS1 product spot could be found this time (see TLC-7a).

Due to this fact the reaction was not stopped after one hour. It was continued and further samples were taken at regular intervals and were checked for product formation. After a reaction time of 17 hours the product spot could be found on the TLC plate.

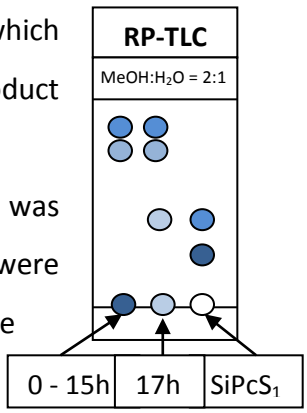

TLC-7a

In order to observe the whole reaction process, the reaction was stopped after 3 full days and worked up as described in the previous reaction A01.

Work up instructions:

Water was added and then the reaction solution was neutralized with Na_2CO_3 to a pH value >7. The solvent was removed on the evaporator and the resulting solid salt-product mixture was extracted with MeOH and filtered off. The blue MeOH solution was then again evaporated and the product was separated again by TLC separation in the same manner as in reaction A01.

Since in this experiment, a large part of the reaction solution was taken for the small scale tests, no significant yield determination was possible. Surprisingly, in this reaction mainly the second spot was produced but hardly the first one. Furthermore in the comparative sample of the reaction A01 another spot was observed which raised new questions (see TLC-8a)

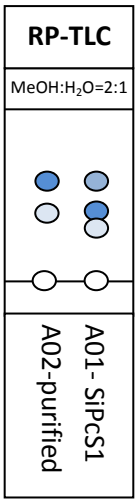

TLC-8a

Solid formation in old samples:

Another observation worth mentioning was the fact that over time a dark blue solid precipitated from already neutralized small samples. When it was tried to filter this solid particles the solid dissolved again while washing the filter with water. From this small experiment it can be reasonably assumed that the solid particles in the solution were macroscopic agglomerates of the complexes.

TLC spots displacement:

Another finding was obtained during this experiment. Since the comparison product SiPcS1 from the reaction A01 was dissolved in MeOH and the solvent of the second reaction was H_2O, there was a displacement effect of the spots observed on the TLCs. As it can be seen in TLC 9a, the product spots of the reaction A01 compared to those of the co-spot have different Rf values. This effect was due to an insufficient drying of the solvent on the TLC plate. When the TLC plate was dried for 5 minutes with a blow drier this effect disappeared as it can be seen in TLC 10a.

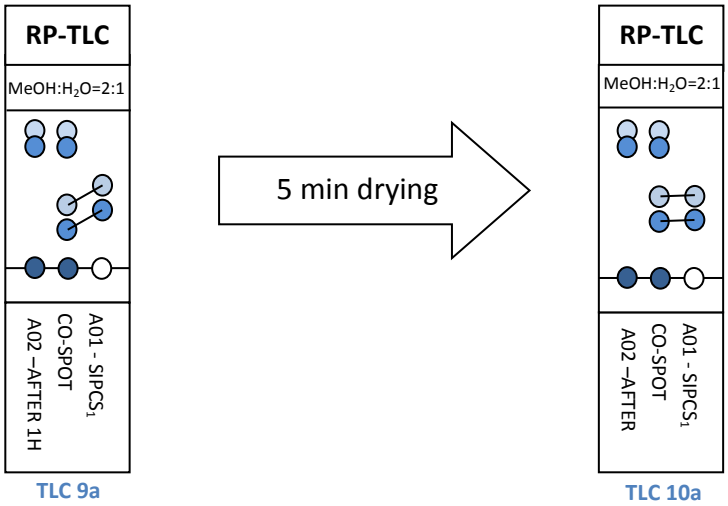

Conclusions of the reaction A02:

- Not the same results as for the first reaction (A01) could be reproduced. In this reaction longer reaction times seem to lead to bigger product yields.
- In the neutralized aqueous solution agglomerates are formed over time.
- If there is insufficient drying of the TLC plate it leads to a shift of the Rf value due to solvent residues on the TLC plate.

Open questions:

- Why was the product formation in reaction A01 much faster (after 1 hour) than in reaction A02 (after 17 hours)?
- Why did a third spot appear on the TLC for the purified product of reaction A01 (TLC-8a)?
- Why did reaction A02 almost formed only the second product spot, but not the first product spot?
- Why have large amounts of high substituted byproducts already been formed after a few minutes after the reaction started (TLC 7a)

D.2.1.3 Reaction A03

Hypotheses on reaction A03:

- The higher substituted byproducts SiPcSx (x=2-4) might form because of a rapid temperature increase at the reaction start (when the oleum is added). This might promote the formation of higher substituted compounds.

Experimental implementation:

In this experiment, 1 ml of oleum was first filled into a 10 ml flask. This flask was then cooled with ice water to 0 °C. This procedure should prevent a rapid rise in temperature at the beginning of the reaction after addition of the starting material. Subsequently, 3.75 mg (= 5 mg of 75 % SiPc 6.52 * 10^{-6} mol) SiPc was added to the oleum in the flask. The reaction was continued at 0 °C to observe the reaction behavior at low temperature. After 15 minutes, the first sample was taken and worked-up following the instructions of reaction A02. Nevertheless, the same two spots were found at high Rf values on TLC (TLC-7a). This proved the above hypothesis to be false.

However, even after 10 hours no significant changes on the TLC could be detected compared to the first sample. Overnight when the reaction could no longer be cooled down a higher substituted product spot with the lower Rf-value was detected after a reaction time of 24 hours. This reaction was also extended up to a reaction time of three days. The result of that reaction was comparable with the result of the reaction A02. Only after long reaction times of about 15 hours at room temperature the product spot was observable. The reaction was then worked up in the same way as reaction A02 by neutralization with water and Na_2CO_3, and then removing the solvent, extraction of the formed solid with MeOH, followed by filtration and separation by big RP-TLC plates.

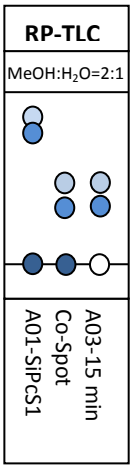

TLC-11a

Summary of the reaction products so far:

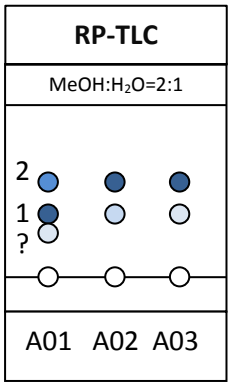

TLC-12a

On TLC 12a all three purified reaction products of the first three reactions can be seen. Only the first reaction produced a relatively good yield of the desired product SiPcS1 (TLC-spot No. 1). In addition, it can be seen that both experiments with longer reaction times were more likely to form the second reaction product. For that spot it was not yet clarified if this is also the product spot or the twice substituted SiPcS2 complex.

The cooling of the reaction also did not affect the product formation positively. In addition for reaction A01 it was still unclear, what the spot with the lowest Rf value was and why it was formed over time. Another question that couldn´t be answered at that point was, why did the first reaction form already a big amount of product after one hour, but not the reaction A02 and A03.

Another challenge which could be seen on the TLC 12a is that the separation method using RP-TLC (with MeOH:H_2O = 2:1) could separate well the higher substituted compounds, but could not separate the first from the second spot.

Second ESI-MS measurement of the reaction products of A:

Since the reaction product composition of A02 and A03 were very similar they were combined together. Subsequently, the mixture was separated again with RP-TLC. This time it was possible to collect the spots 1 and 2 separately by scraping the product spots from the solid phase from the TLC plates. After extraction with MeOH and filtration of the particles samples for ESI-MS measurements were prepared. These two samples and an additional sample with a mixture of higher substituted byproducts were then measured by ESI-MS.

ESI-MS measurement of TLC-spot No. 2:

The result of the measurement of spot No. 2 showed numerous fragments of the Pc-complex, but also in the negative spectrum at m/z ratio of 653.2, the product fragment of SiPcS1. However, the higher substituted fragments of SiPcS2 could not be found.

ESI-MS measurement of TLC-spot No. 1:

The ESI-MS sample of the product spot No. 1 was hard to distinguish from the first measurement. In positive spectrum there were just fragments found, link in the previous measurement. However, in the negative spectrum there was again the peak found at m/z ratio of 653.2, which was the product peak of SiPcS1.

ESI-MS measurement of the byproduct spot mixture:

As a third ESI-MS mixed byproducts sample was measured no product peaks were found neither in the positive nor in negative spectrum for any SiPcSx products. Therefore, it was assumed that the higher substituted SiPc complexes could not be found in the measurement. Due to their high molecular mass they disintegrate during the measurement. The measured ESI-MS spectra can be found in the Appendix E.1.1.

UV/VIS absorption measurement:

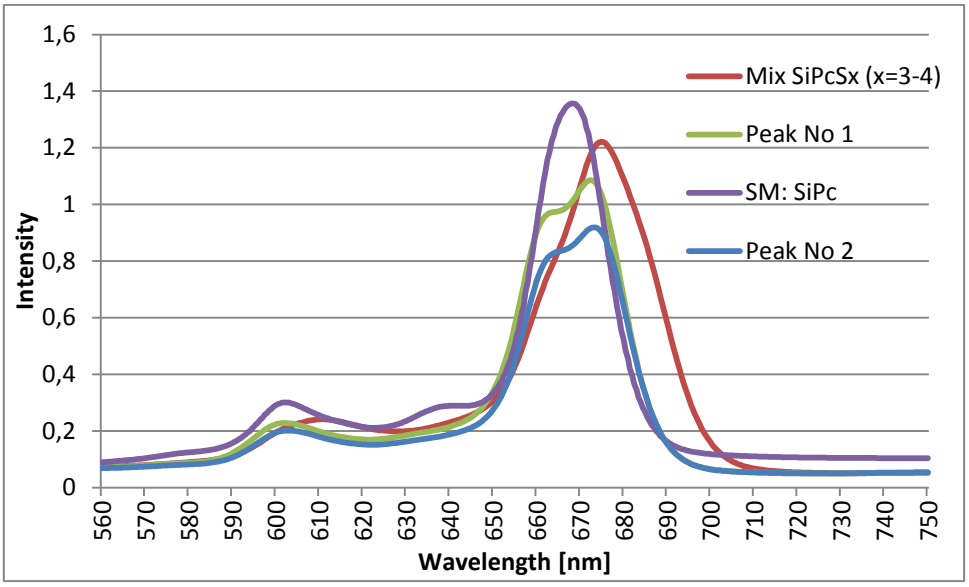

Figure 30: Absorption spectra of the different peaks after separation with RP-TLC

In this diagrams (shown in Figure 31 and 32), the absorption measurements of the three different fractions of the different collected spots and the starting material are shown. Interestingly the fractions of the first spot and the fraction of spot number 2 showed the same absorption pattern. This consolidated the assumption that both collected TLC spots could be the same substance. The mixture of higher substituted SiPcSx complexes and the sample of the starting material resulted in a different absorption pattern. The focus of these

spectra is on the Q-band region because this is the most important and most informative region for this compound.

One could clearly see that the individual spots show some fundamental differences. On the one hand the absorption maximums as well as for the vibronic bands were at different wavelength. On the other hand there was a distinctive difference in the spectrum of the spots number 1 and 2, compared to the higher substituted complexes and also compared to the starting material. The measurement of spots 1 and 2 showed a splitting of the Q band. At this point it was not clear whether this phenomenon was caused by contamination or whether it had a different cause. (The explanation was found later in the research by using a MCD measurement and by applying a DFT calculation) The absorption maximum of the spot number 1 and 2 was observed at a wavelength of 672.5 nm and the second spot of the Q-band was at 661 nm. For the byproduct mixture the spot maximum was observed at 675 nm and the spot for the SM SiPc it was at 668.5 nm.

Conclusions of the reaction A03:

- The hypothesis that an increasing reaction temperature during the process of mixing SM and oleum leads to higher substituted SiPc complexes was falsified.
- The reaction proceeds slower at low temperatures and thus formed almost no low-substituted complexes.
- Longer reaction times lead to larger product yields of SiPcS2
- The ESI-MS measurement showed that for spot No. 1 and 2, the same product peaks were measured. Higher substituted compounds could not be detected.
- Due to the similar absorption spectra of spot No. 2 and No. 1 and the identical results for the ESI-MS measurements it seemed likely that spot No. 1 and No. 2 were the same substance and thus both of them could be the desired product SiPcS1.

Open questions:

- How could the reaction conditions be optimized to increase the yield of the SiPcS1 product and reduce the amount of high substituted SiPcSx (x = 2-4) products?
- How could it be proven that spot No. 1 and No. 2 were the same substance?
- What could be the reason that one substance shows two or even three different Rf values on the TLC?

D.2.1.4 Reaction A04

Hypotheses on reaction A04:

- Previous research on similar Pc-complexes had shown [29] that the degree of sulfonation could be controlled by changing the oleum concentration for the reaction. Therefore the following small scale synthesis should examine the effect of lower concentrated oleum for the sulfonation reaction.
- It could be assumed that the reason for the fact that at the beginning mainly high substituted products were formed and then after long reaction times the mono-substituted product SiPcS1 formed seem illogical. Another new hypothesis should be examined that the higher substituted products, which were formed at the beginning, disintegrated over time to the product SiPcS1 because of light radiation. That would explain, why higher substituted SiPcSx were formed first and later the low-substituted compounds SiPcSx followed.

Experimental implementation:

In order to get a lower oleum concentration from the existing 30 % oleum solution a certain amount of water had to be added. The water reacts with the SO_3 gas which is dissolved in the sulfuric acid and forms more H_2SO_4, thereby reducing the SO_3 concentration in the oleum. (The calculation for producing a 5 % oleum concentration from a 30 % oleum solution can be found in Appendix E.2)

For this synthetic experiment 1ml 30 % oleum was pipetted into a 10 ml flask. Subsequently, 107 µl H_2O was added, whereby the oleum concentration was lowered to 5 %. After that 3.75 mg (= 5 mg of 75 % SiPc, 6.52 * 10^{-6} mol) SiPc was added to the oleum.

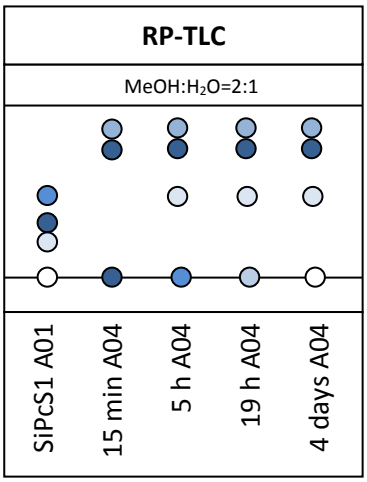

TLC-13a

After 15 minutes the first sample was taken and processed in accordance with the workup instructions of reaction A2. The RP-TLC 13a control showed that also for that reactions only the higher substituted SiPcSx (x=2-4) complexes with high Rf values were formed. SM was still sufficiently present and consequently the reaction was not yet terminated.

Further samples were taken after 5 hours and after 19 hours and were also tested with TLC experiments. Since the results of these TLC experiments did not show good results in respect to SiPcS1 product, the reaction was continued and finally terminated after 4 days. Afterwards the reaction solution was worked up according to the instructions of reaction A02. After the 4 days reaction time the entire SM was consumed. However, the intensities of the desired product spot remained almost equal over the entire period of 5 hours to 4 days.

Radiation decomposition theory:

To test the hypothesis of decomposition product, one bigger sample had been drawn after 19 hour and was placed into a UV chamber. The irradiated at a wavelength of 253 nm was applied to the sample vassal. During the irradiation time samples for TLC experiments were drawn at regular intervals. The results were compared with each other over time. However, as it can be seen in TLC 14a the intensities of the TLC-spots showed little difference. Therefore the hypothesis has been falsified.

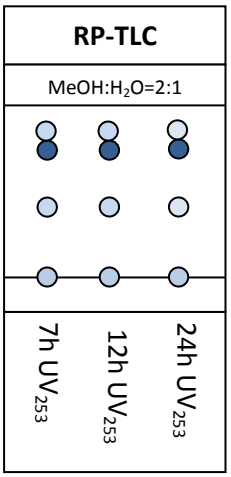

TLC-14a

Conclusions of reaction A04:

- A lower oleum concentration has a poor effect on the yield of the formation of low-substituted SiPcSx complexes.
- The effect of UV_{253} radiation on a sample did not cause decomposition of higher-substituted SiPcSx complexes to form lower-substituted complexes.

D.2.1.5 Reaction A05

Hypothesis on reaction A05:

- Increased reaction temperatures could accelerate the reaction and could therefore improve the yield for low-substituted SiPcSx compounds.

Experimental implementation:

To test hypothesis of A05, the reaction was carried out again with a 30 % oleum concentration at 50 °C. For this purpose, 1 ml of 30 % oleum was filled in a 10 ml flask and was placed in an oil bath which was heated up to 50 °C. At intervals of 1, 1.5, 2, 2.5 hours samples were taken and worked up according to reaction A02. These samples were then controlled by RP-TLC.

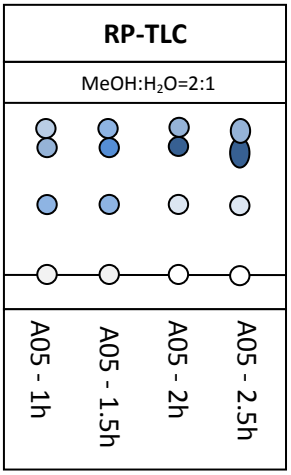

TLC-15a

In this RP-TLC experiment (TLC 15a) it can be seen clearly that already after 1 hour the almost entire SM had stopped reacting. Moreover, it was noticeable that the yield of spot No. 2 is already very intensive, but the spot No. 1 was not observable.

At longer reaction times at this temperature a trend was observed that the concentration of the low-substituted complex was reduced and a larger concentration of the higher substituted products was formed at higher Rf values. After 2.5 hours the reaction was stopped and worked up according to the instructions of reaction A02.

Conclusions of the reaction A05:

- Higher reaction temperatures of 50 °C speed up the reaction.
- After a reaction time of 1 hour the entire SM has already been used up and the optimum for the production of low-substituted products has already been exceeded.
- At longer reaction times the yield of low-substituted reaction products started to decrease.

D.2.1.6 Reaction A06

Hypothesis on reaction A06:

- The yield from the mono-substituted product would even be bigger if the reaction is carried out at an increased temperature but at a lower oleum concentration.

Experimental implementation:

For this synthetic experiment 1ml 30 % oleum was filled in a 10 ml flask. Then 107 µl H_2O was added with a pipette whereby a 5 % oleum concentration was produced. After that the

solution was heated up to 50 °C using an oil bath and then 3.75 mg (= 5 mg of 75 % SiPc 6.52 * 10^{-6} mol) SiPc was added to the oleum in the flask. After 15, 30, 45 minutes and after 1, 1.5, 2, 4 and 7 hours, samples were drawn and worked up according to the instructions of reaction A02. These samples were then tested in RP-TLC experiments.

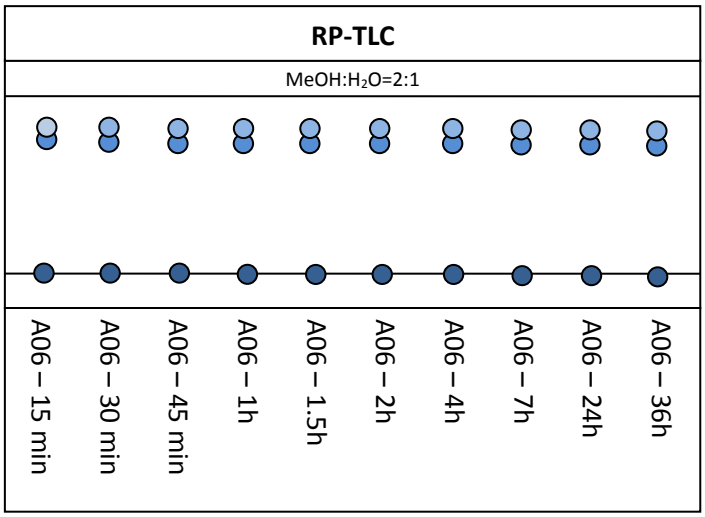

TLC-16a

In this RP-TLC experiment it could be seen that relatively large amounts of highly substituted SiPcSx (x= 2-4) complexes were formed at the very beginning of the reaction. This ratio hardly changed over the whole period of 1.5 days.

Even after workup of the reaction there was hardly any product found and because of that the experimental solution was discarded.

Conclusions of reaction A06:

- In this synthetic experiment using increased temperature and a 5 % oleum concentration no or a very small formation of low-substituted compounds has been occored.

D.2.1.7 Reaction A07

Hypotheses on reaction A07:

- In reaction A05 it was shown that already after one hour relatively large amounts of low substituted SiPcSx complexes were formed at a temperature of 50 °C. In this experiment, the effect of even higher reaction temperatures and shorter reaction times

should be examined. Perhaps this condition has a positive impact on the yield of low-substituted SiPcSx complexes.

- The aim was to find a better TLC separation method, in which the separation of SiPcS1 and SiPcS2 can be achieved more easily. The new method should enable also a separation of a big scale reaction with column chromatography.

Experimental implementation:

For this synthesis 1 ml of oleum was first filled in a 10 ml flask and heated up to 70 °C in an oil bath. Then 3.75 mg (= 5 mg of 75 % SiPc 6.52 * 10^{-6} mol) SiPc was added to the oleum and was stirred. During this experiment samples were taken after 15 and 30 minutes and after 1 and 1.5 hours, worked up with the instructions of reaction A02 and then were examined with RP-TLC.

Result:

TLC 17a shows that already after the reaction time of 15 minutes, almost all of the starting material was consumed. In addition, there were hardly any low substituted SiPcSx complexes formed. Furthermore the yield of low substituted SiPcSx complexes continued to decrease over time.

For this reason, the reaction was terminated and worked up after 1.5 hours. Since there was almost no product left no TLC separation could have been performed with that reaction mixture.

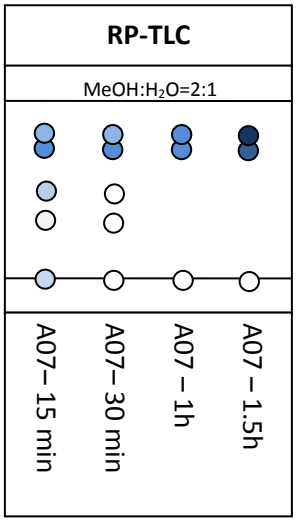

TLC-17a

Conclusion of reaction A07:

- The hypothesis that a synthesis at a temperatures of 70 °C would lead to bigger yields of low substituted SiPcSx complexes was disproved. The opposite effect was achieved because the products mostly formed in that reaction were high substituted SiPcSx (x= 2-4) complexes.

D.2.1.8 The search for better TLC separation method

To find a good way to separate the reaction mixture many TLC separation experiments were performed. Many different solvents (MeOH, H_2O, toluene, pyridine, THF, diethyl ether, DMF,

$HCCl_3$, hexane, acetone, ethyl acetate) were mixed in different ratios and were applied for both RP and NP-TLC plates. Since none of the TLC-experiments lead to a promising result also different literature of similar complexes was searched through for possible recommendations for separation methods. Finally a paper was found [29] in which a AlPcSx (X = 1-4) mixture could be separated with NP-TLC using a solvent mixture of EA:EtOH:NH_3 (= 7:4:4). Because this AlPc- complex was synthesized in a very similar way, this separation method was tried out.

Comparison of RP-TLC and NP-TLC with the new solvent mixture showed some interesting results.

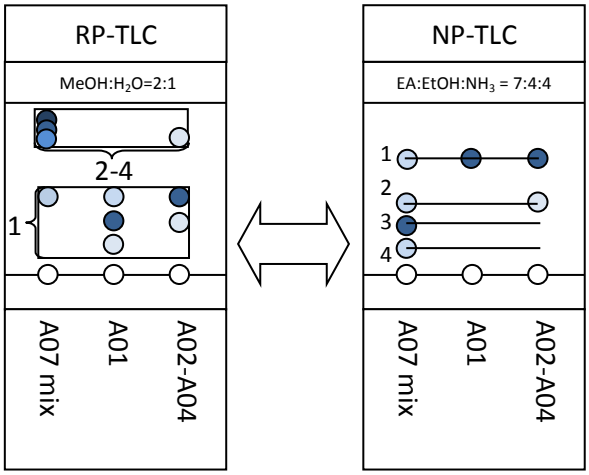

TLC-18a TLC-19a

Conclusions from the TLC experiments 18a & 19a:

- It seemed that although the product A01 showed three spots in RP-TLC, all these spots were the same product according to the new NP-TLC separation.
- The product mixture of A02-A04 seemed to include just small impurities of SiPcS2. The rest was almost exclusively the product SiPcS1.
- The separation with RP-TLC was not accurate enough to obtain the pure mono-substituted complex.
- With the new solvent mixture also a large scale column chromatography should be possible.
- The fact that the solvent mixture contained a fair amount of NH_3, suggested that this solvents could cause a decomposition of the complex due to the strong basicity.

D.2.1.9 TLC experiments

New Objective:

- With the knowledge of the retention behavior for NP-TLC of the different substituted complexes SiPcS1-4 and the fact that there was also a pure fraction of SiPcS1, more TLC experiments should be conducted to find out whether a separation of SiPcS1 from the higher-substituted SiPcSx complexes is also possible with another solvent mixture that did not contain NH_3.
- In addition it should be tried to clarify if the three spots of the reaction A01 (see TLC-8a) in RP-TLC were really all the same product. (There was already the indication by the ESI-MS measurements (Appendix E.1.1) and by the absorption spectra (Chapter D.2.1.3, Figure 32) of the experiment A03.

Hypothesis on the TLC experiments:

- Through consultation with Professor Ishii the idea was born that the different spots in the RP-TLC could be all the same product but different forms of agglomerates. If these agglomerates were in equilibrium with each other, this theory could be confirmed with a 2D RP-TLC experiment.

Experimental implementation:

For this experiment, a 5x5 cm square RP-TLC plate was prepared. Then a relatively concentrated sample of the purified reaction solution of reaction A01 was applied in the bottom right corner of the TLC plate. After that the TLC plate was put into a TLC chamber (MeOH:H_2O = 2:1) and was separated in the first dimension. This time even 5 five instead of three spots were separated due to the higher concentration of the sample. After that the TLC plate was thoroughly dried with a blow dryer and then the TLC plate was rotated by 90° and again placed in the same TLC chamber. This time the separated spots from the first separation step were separated again in a second dimension. For a better illustration and understanding of the 2D TLC experiment a normal 1D TLC with the same concentrated sample was added to the first dimension of development to be able to interpret the 2D TLC more easily.

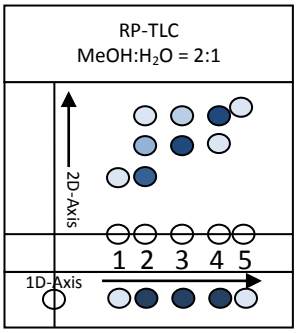

TLC-20a

Conclusions of 2 D TLC experiment:

- Due to the high concentration of the sample on the TLC plate small impurities (spot No. 1 and No. 5 of TLC 20a) were observable after the TLC separations in both dimensions.
- Especially the spots No. 2-4 showed an interesting pattern after the development in the 2nd dimension, which will be explained in the next sub-paragraph.

Proposed explanation of the splitting patterns in the 2D TLC experiment:

From the separation pattern of the NP-TLC and the RP-TLC (TLC-18a & TLC-19a) of the purified reaction A01 was concluded that the three spots of the RP-TLC were all the same product. In the 2D TLC (TLC-20a) it can be seen that the three spots (No. 2, 3, 4) were able to transform within each other. A possible explanation for this behavior could be the formation of different sized agglomerates which are in equilibrium with each other. This can easily be supported by analyzing the spot pattern of spot No. 2-4. For example the spot No. 2 supposed to be one separated substance with one specific Rf value after the TLC separation in the second dimension. After the TLC separation in the second dimension it can be seen that again three spots were obtained. Furthermore, the spot No. 3 and spot No. 4 also split up for the separation in the second dimension into two separate spots. One illustration of a possible explanation is proposed in Figure 33.

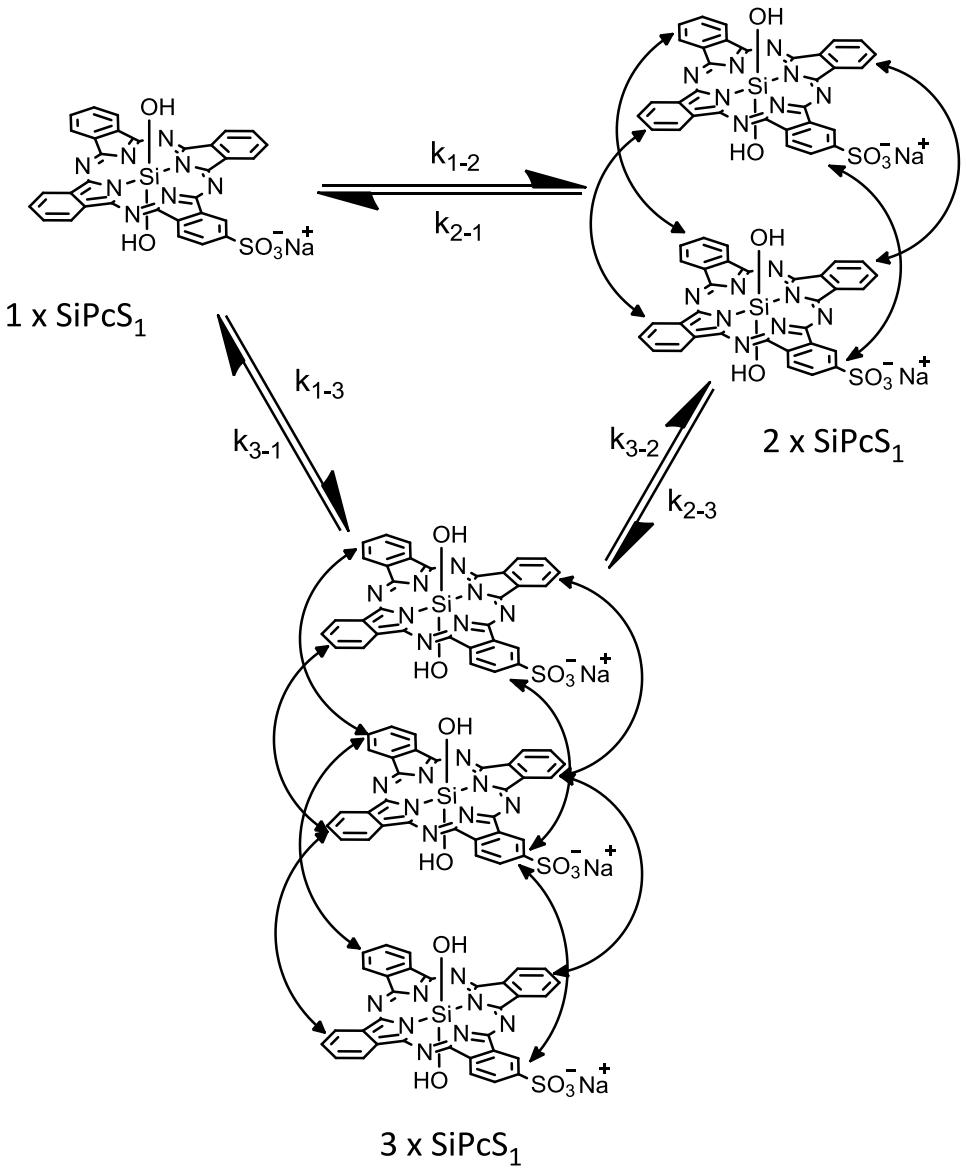

Figure 31: Aggregation equilibrium between different forms of SiPcS1 agglomerates

It seemed reasonable to suppose that each of these different TLC spots were agglomerates of the same complex but different sized in numbers. In Figure 33 it is assumed that the three different agglomeration spots were the single (1 x SiPcS1), two times (2 x SiPcS1) and three times (3 x SiPcS1) SiPcS1 agglomeration of the complex. This could be explained because of a π -π stalking effect (shown by the arrows in the picture) of the aromatic rings of the complexes or because of interaction between the axial hydroxy groups. Due to the TLC scheme it was also believed that the spot No. 2 belongs to the 3 x SiPcS1, spot No. 3 to the 2 x SiPcS1 and spot No. 4 to the 1 x SiPcS1. According to the color intensities of the separated spots in the second dimension, the equilibrium constants between the individual complex agglomerates could be estimated. For spot No. 2 (3 x SiPcS1) it is easy to see that this

agglomerate relatively easy disintegrates to the 2 x SiPcS1 agglomerate but disintegration to the 1 x SiPcS1 is not that fast (It possibly goes the normal disintegration pathway first to 2 x SiPcS1 agglomerate and then disintegrates further to 1 x SiPcS1).

The spot No. 3 (2 x SiPcS1) also tends to disintegrate to the 1 x SiPcS1 complex. However, in the observed time frame during the separation it was not capable to form the triple agglomerate. Spot No. 4 (1 x SiPcS1) was relatively stable compared to the two other forms of agglomerates. However, it can be seen that also a small amounts of 2 x SiPcS1 agglomerates were formed. This was also a proof of concept that these two agglomerated forms were in equilibrium. There is reason to believe that depending on the solvent of the TLC, the solid phase, the temperature and the concentration of the solution applied on the TLC, this equilibrium ratios could be affected for the individual agglomerate types.

TLC separation experiments:

Since it was discovered that the separation with RP-TLC was restricted and that the up-scaling would also cause problems on an RP column chromatography, attempts for a new separation method with NP-TLC were made. The new method should be without the use of NH_3 and it should at least separate the desired product (SiPcS1 and their agglomerates) from the other byproducts.

Numerous TLC experiments were carried out and the results of the TLC experiments were compared with the result of RP-TLC (MeOH:H_2O = 2:1) and the so far best separation method with NP-TLC (EA:NH_3:EtOH = 7:4:4). Specifically, the mobile phase of MeOH with $HCCl_3$ showed promising results.

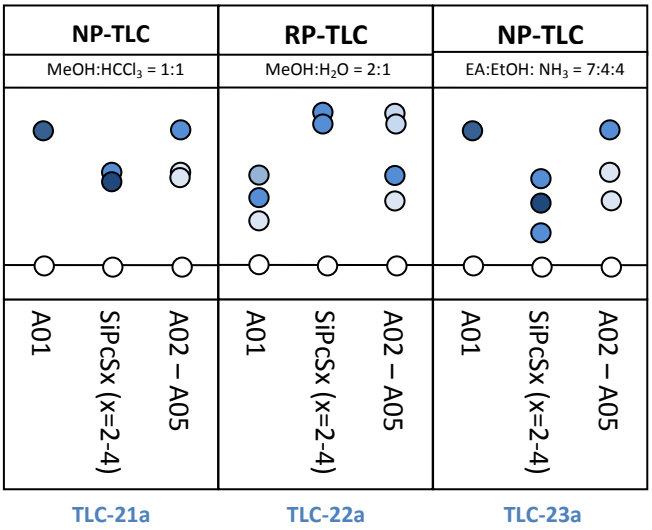

As it can be seen in TLC 21a – 23a some TLC experiments with the solvent mixture (MeOH:$HCCl_3$) showed that already a 1:1 mixture of the solvents resulted a separation of SiPcS1 and all other higher substituted compounds in two separated spots. The only downside of this solvent mixture was that this mixture was not able to separate the different higher substituted SiPcSx (x = 2-4) as it was possible with the EA:NH_3:EtOH solvent mixture. Therefore with this new separation technique it would not be possible to estimate the yield ratios of the different higher substituted complexes.

Two big advantage of this new mobile phase for the separation was on the one hand that it could be scaled up quite easily to separate also a large scale reaction by using column chromatography and on the other hand that it no longer included the ammonia. Nevertheless, the desired product SiPcS1 could be separated from the remaining byproducts with the same purity as with the solvent mixture of EA:NH_3:EtOH.

Conclusions on TLC experiments:

- The solvent mixture MeOH:$HCCl_3$ = 1:1 on NP-TLC could successfully separate the product SiPcS1 from the higher substituted SiPcSx (x = 2-4) with the same efficiency as the mixture of EA: EtOH: NH_3 = 7:4:4.
- This separation method opens up the possibility to separate the product via column chromatography and to scale up the separation method.
- NP-TLC with a solvent mixture of EA:EtOH:NH_3 = 7:4:4 as a mobile phase and RP-TLC with a solvent mixture MeOH:H_2O = 2:1 as a mobile phase are two good separation methods that can be used to monitor the yields of the products visually.
- With the 2D RP-TLC experiment the mystery of the three spots in RP-TLC could be solved and conclusions on the different agglomerates were drawn.

D.2.1.10 Reaction A08

Hypotheses on reaction A08:

- From all the synthetic experiments carried out up to that point, the reaction A05 showed the best results according to the formation of mono-substituted SiPcS1 complex. The reaction conditions of this reaction were set with a reaction time of one hour, at a reaction temperature of 50 °C and with an oleum concentration of 30 %. Since for these reaction conditions no samples were taken before one hour, the reaction yield for shorter reaction times than one hour should be examined in this next experiment. The optimum time could be probably found at even shorter reaction times than one hour.

Experimental implementation:

For this experiment, 1 ml of 30 % oleum was filled into a 10 ml flask. To prevent a local temperature increase when the starting material was added the oleum was first cooled down to 0 °C with ice water. Afterwards 3.75 mg (= 5 mg of 75 % SiPc, 6.52 * 10^{-6} mol) SiPc was added to the oleum, the ice water cooling bath was replaced with an oil bath and the reaction solution was heated up to a temperature of 50 °C. In time intervals of 15 minutes samples were drawn, worked up according to the instructions of reaction A02 and were analyzed on their composition with the TLC control experiments.

TLC tests explanation:

Based on both the results of the RP-TLC and NP-TLCs it could be seen that already after 15 minutes a relatively large amount of the mono-substituted SiPcS1 complex has been formed. After 15 minutes it could be seen that the SM was not fully consumed. Over time the amount of starting material decreased and after 45 minutes it was already used up and not visible anymore on the TLC plate. Although the majority of the products were formed in the first few minutes, the product spots continuously gained intensity up to a reaction time of one hour. Also the amount and the number of byproducts increased over time.

The reaction was stopped after one hour because the experiment A05 has already shown that under the same reaction conditions the yield for SiPcS1 (according to TLC spot intensity) continuously decreased when the reaction time was exceeding one hour.

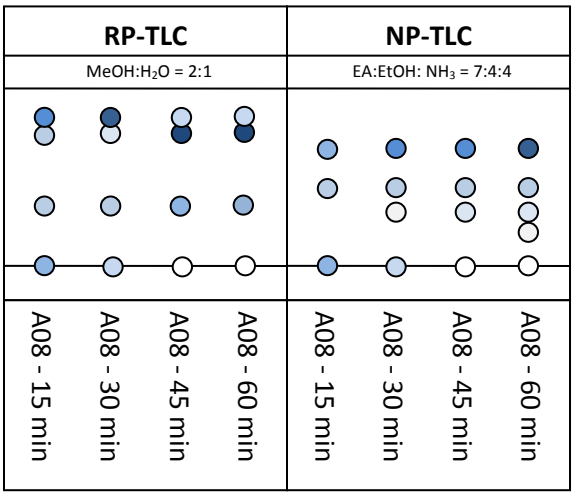

The reaction was processed according to work up instructions of reaction A02 and then the product was separated with NP-TLC and MeOH:$HCCl_3$ (1:2) as mobile phase. After scraping down the product spots from the TLC plates, extraction with MeOH and subsequent filtration, the solvent was again removed on the evaporator, dried under high vacuum for several hours and finally the product was weighed on a balance. The weight of the product obtained on the balance was 7.8mg which corresponded to a yield of 176.8 %.

This result was discussed with Professor Ishii. According to him this result could be due to a strong hygroscopic behavior of the complex. The adsorbed water distorted the true weight. For this reason, a second method was proposed in order to determine the yield of the reaction. This method could calculate the yield by using the absorption spectrum. By measuring the maximum intensity of the Q-band, a calculation with the Beer-Lambert Law (see Appendix G.1.3) results the concentration and therefore also the amount of the synthesized product. The value for the molar extinction coefficient (ε) for that calculation used was 250,000*.

The product was dissolved in methanol and diluted so that the concentration of the solution did not exceed the intensity level of the absorption spectrometer. Then the intensity of the Q-band was measured from three prepared samples and using the Beer-Lambert law the yield was calculated to be on average 1.19 mg. This corresponded to 27 % of the maximum possible yield.

Conclusions of the reaction A08:

- The conclusion of the experiment A05 and A07 revealed that the optimum reaction conditions for synthesizing the compound SiPcS1 were by using 30 % oleum at a reaction temperature of 50 °C with a reaction time of 1 hour.
- Furthermore, this experiment showed that the measured value of the balance should not be used because the synthesized complex was very hygroscopic and therefore showed a much higher value.
- This fact also explained, why the reaction yield in the reaction A01 was so high. This was only achieved because of the misleading water content in the product sample.

D.2.1.11 Reaction A09

Hypotheses on reaction A09:

- In this experiment, the reaction A08 should be scaled up using four times bigger amount of the starting material. However, the same reaction conditions as in reaction A08 should be applied. The separation of the various reaction products should be carried out by using column chromatography (NP – MeOH:$HCCl_3$).

* This value is already published in the literature for the extinction coefficient of $SitBPc(OH)_2$ (the first generation of this compound). Since this compound is relatively similar to the newly synthesized $SiPc(OH)_2S1$ this value is now used for calculating the yield.

Experimental implementation:

In this synthesis 4 ml 30 % oleum was filled in a 30 ml flask. The oleum was first cooled down with ice water to 0 °C. Afterwards 15 mg (= 20 mg of 75 % SiPc, 2.61 * 10^{-5} mol) SiPc was added to the oleum. Then the ice water bath was replaced by an oil bath and the reaction was heated up to a temperature of 50 °C. After one hour reaction time, the oil bath was again replaced for ice water to prevent an overheating during the addition from water to stop the reaction.

Workup of reaction A09:

The product worked up was according to the instructions of reaction A02. The only difference was that for the solid-liquid extraction with MeOH, the flask was put into an ultrasonic bath in order to improve the dissolving process of the products which were incorporated in the solidified salt. After filtration the solvent was removed on the evaporator and then it was again dissolved in a few milliliters of MeOH:$HCCl_3$ = 3:1.

Column chromatography for small scale reaction:

A 50 cm long and chromatography column was prepared. First in the stopcock was plugged with cotton wool. Then 100ml NP-SiO_2 was filled into a 300ml beaker and was slurried with a solvent mixture of MeOH: $HCCl_3$ = 1:7. Then, the silica-solvent slurry was transferred into the column and rinsed several times with the same solvent, which caused a solidification of the silica particles in the column. The solvent was then drained to the phase boundary and the previously resolved product mixture was applied onto the silica column using a long pasteur pipette. It was then initially rinsed with pure $HCCl_3$ and the eluting solvent was recycled by distillation in a rotary evaporator and was then reused several times for rinsing. Over time, the MeOH concentration of the mobile phase was slowly increased which lead to a separation of the different complexes in the column. Thus, a gradient chromatography was performed with 100 % $HCCl_3$ at the beginning and finally with 100 % MeOH in the end. The pure MeOH was used in the end to also elute and collect all the byproducts. The transition to very high concentrations of MeOH was changed after the product SiPcS1 was successfully collected. In this separation (as well as for the following once) it is noticeable that at the very beginning a very dilute byproduct was separated. This compound, however was easy to separate from the product compound. After the individual fractions were collected, the

purity was controlled with TLC experiments, the matching product fractions were combined and the solvent was removed in the rotary evaporator. As a next step, the product was re-dissolved with MeOH and an appropriate dilution for the absorbance measurement was prepared in order to calculate the yield of the reaction A09. The yield of the product was 3.2 mg according to the calculation which was 18.2 % of the maximum yield possible.

Purification of reaction A01-A08:

The same column chromatography separation method was then carried out with all not yet separated fractions of the previous experiments. After extensive drying under high vacuum 7.8 mg SiPcS1 were weighed according to the balance and the calculation with the absorption spectrum resulted 1.32 mg which seemed more reliable.

Conclusions of the reaction A09:

- The column chromatography separation method worked very well and the yield of desired product SiPcS1 is also relatively good.
- One workup step, in which some product was possibly lost, was the extraction of the salt with MeOH. Despite of the use of the ultrasonic bath which ought to lead to an overall better yield, there were often relatively large pieces of salt left, in which the product was still trapped inside. This subsequently could not be dissolved with MeOH and thus might have reduced the yield of the reaction. For future big scale reactions, the salt should be triturated with a mortar to fine powder and after that the extraction could be carried out with MeOH much better.
- Since the reaction procedure of the first step reaction was solved at that point, the second reaction step could now be carried out in a small scale reaction. Additionally further optimization of the workup procedure of the reaction A should be investigated.

D.2.1.12 Reaction A10

A further upscaling step was carried out that enough of the product could be obtained for reaction B.

Experimental implementation:

25 ml of 30 % oleum was filled into a 100 ml flask. To avoid the potential impact of a local overheating during the addition of SM, the oleum was cooled down by ice water to 0 °C. Thereafter, 100 mg (= 136 mg of 75 % SiPc, 1.74 * 10^{-4} mol) SiPc was added to the oleum, the ice water bath was replaced by an oil bath and heated up to a temperature of 50 °C. After the reaction time of one hour, the reaction was stopped. The oil bath was again replaced by an ice water bath. Then alternately water and Na_2CO_3 was added to the reaction. This process released a lot of CO_2. Very much foam was formed (see Figure 34)

Figure 32: Foam formation during the neutralization process with Na_2CO_3

When the heat generation of the neutralization process was gone, the reaction solution was poured into a 2 liter beaker to continue the neutralization process. The total amount of water used for that process was approximately 500 ml. After the pH value of the solution was higher than 7 and no more foaming was observed, the solvent was removed in multiple smaller steps on a rotary evaporator (see Figure 35).

Figure 33: Process of removing the solvent after the neutralization reaction of reaction A by using a rotary evaporator

During this evaporation process also much foam and bubbles were formed and boiling retardation was often observed. The resulting solid salt-product mixture was then scraped with a spatula from the wall of the flask and was then triturated with a mortar to a fine powder (see Figure 36)

Figure 34: Salt-SiPcS1 mixture triturated with a mortar to a fine powder

When the salt was too firmly adhered to the glass wall of the flask, that it could not be removed with a spatula, the salt-product mixture was again dissolved with water and the drying process was repeated over again. The resulting powder after grinding with the mortar and was then extracted several times with MeOH. The solid salt particles were then filtered off from the product which was dissolved in MeOH via vacuum filtration with membrane filters (see Figure 37).

Figure 35: Equipment setup of the filtration process

The deep blue solution was reduced to a minimum of solvent on the rotary evaporator. In the meantime, a chromatography column was prepared for the separation of the product mixture. Since this big scale reaction was by several orders of magnitude bigger than the previous once, a column with larger diameter (7cm) was used for that separation. Cotton wool was again used to plug the stopcock opening. The amount of SiO_2 which was used for this separation was 400 ml. The SiO_2 powder was slurried in a solvent mixture MeOH:$HCCl_3$ = 1:9. The slurry was transferred into the column and was rinsed several times with the same solvent, which caused a solidification of the silica particles in the column. The solvent was then drained to the phase boundary and the pre-dissolved product-solution mixture was applied onto the column using a long pasteur pipette (see Figure 38).

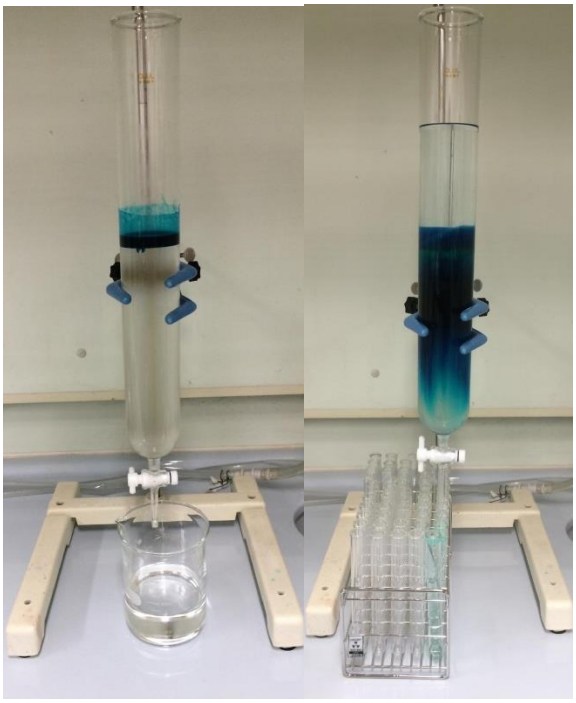

Figure 36: Separation of the different products of reaction A by using column chromatography

After that the column was rinsed with pure $HCCl_3$ to remove MeOH. This was done to achieve a slow and efficient separation. The eluting solvent was collected and again recycled by distillation in a rotary evaporator and could therefore be reused several times.

Over time the MeOH concentration was slowly but continuously increased. Thereby the different substituted complexes separated along the column. Thus, a gradient chromatography was performed which started with 100 % $HCCl_3$ and ended with 100 % MeOH to finally elute also the byproducts. After the individual product fractions were controlled by TLC according to their purity, the product fractions containing the pure compound SiPcS1 were combined and the solvent was removed in the rotary evaporator. Then the collected product was re-dissolved in MeOH and a diluted solution for the absorption measurement was prepared. Then the yield was calculated using the Beer-Lambert law. The yield of the product according to the calculations of the absorption intensity was 18.5 mg which was an 18.5 % yield of the maximum possible amount. (The result, according to the balance was 40.2 mg.)

This instruction was the most optimized implementation description and it has been used another 5 times for the production of the first reaction product.

A11: 20.2 mg 20.2 %
A12: 17.4 mg 17.4 %
A13: 9.35 mg 9.35 %
A14: 16.6 mg 16.6 %
A15: 22.6 mg 22.6 %

D.2.2 Second reaction step

After the first reaction step was optimized and a fair amount of pure SiPcS1 was synthesized and purified the second reaction step for synthesizing the fluorescent vitamin C detecting complex was performed in small scale reactions.

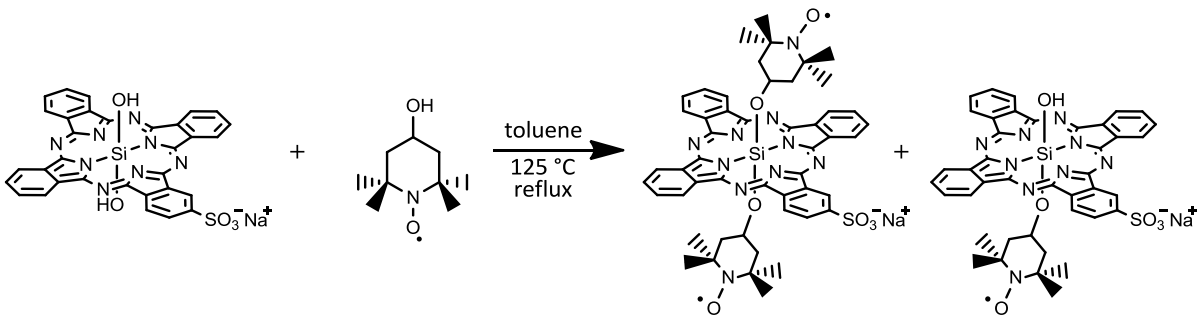

SiPcS1
MW: 676.67 g/mol

TEMPOL
MW: 172.24 g/mol

R2cS1
MW: 985.13 g/mol

R1cS1
MW: 829.89 g/mol

Figure 37: Second reaction step for the synthesis of the final product R2cS1

D.2.2.1 Reaction B01

Hypothesis of the reaction B01:

- This reaction should test whether the reaction product of the first step reaction SiPcS1 could react in the same way with 4-hydroxy-TEMPO as in the synthesis of R2c which was already successfully accomplished. [30]

Experimental implementation:

The product from the first reaction step was dissolved in MeOH and by means of absorption spectroscopy, the concentration was determined and an equivalent of 0.12 mg (1 eq, 1.77 * 10^{-7} mol) SiPcS1 was transferred into a 50 ml flask. The solvent was removed in the rotary evaporator and was dried under high vacuum. It was tried to solve the residue in 20 ml of toluene but because of the poor solubility of SiPcS1 in toluene this was not working properly. To accelerate the solving process the flask was put in an ultrasonic bath for 20 minutes. After the substance was dissolved 3.2 mg (100 eq = 1.77 * 10^{-7} mol) TEMPOL was weighed and added to the reaction solution. Then the flask was connected with a nitrogen flooded condenser and the reaction flask was then heated under reflux with an oil bath to 125 °C. After 48 h the reaction was stopped and the solvent was reduced to a minimum on the

evaporator. Afterwards some TLC experiments were carried out to examine about the yield of the product.

Previous knowledge about the separation compounds with free radicals:

In previous ESR measurements that have been carried out with the first generation of the vitamin C detecting R2c complex, it was discovered that NP silica could not be used for the separation of substances with free radicals. The reason for this was that the radical sites of the complex would come into geometrical proximity with the OH-groups of the silica particles during the separation. This proximity would cause an exchange of the protons of the free OH-groups of the silica particles with the nitroxid-groups of the complex and would therefore destroy the free radical (see Figure 40). However, since free radicals are essential for the quenching effect in the fluorescent complex, NP-TLC or NP-silica particles cannot be used for the separation of these substances.

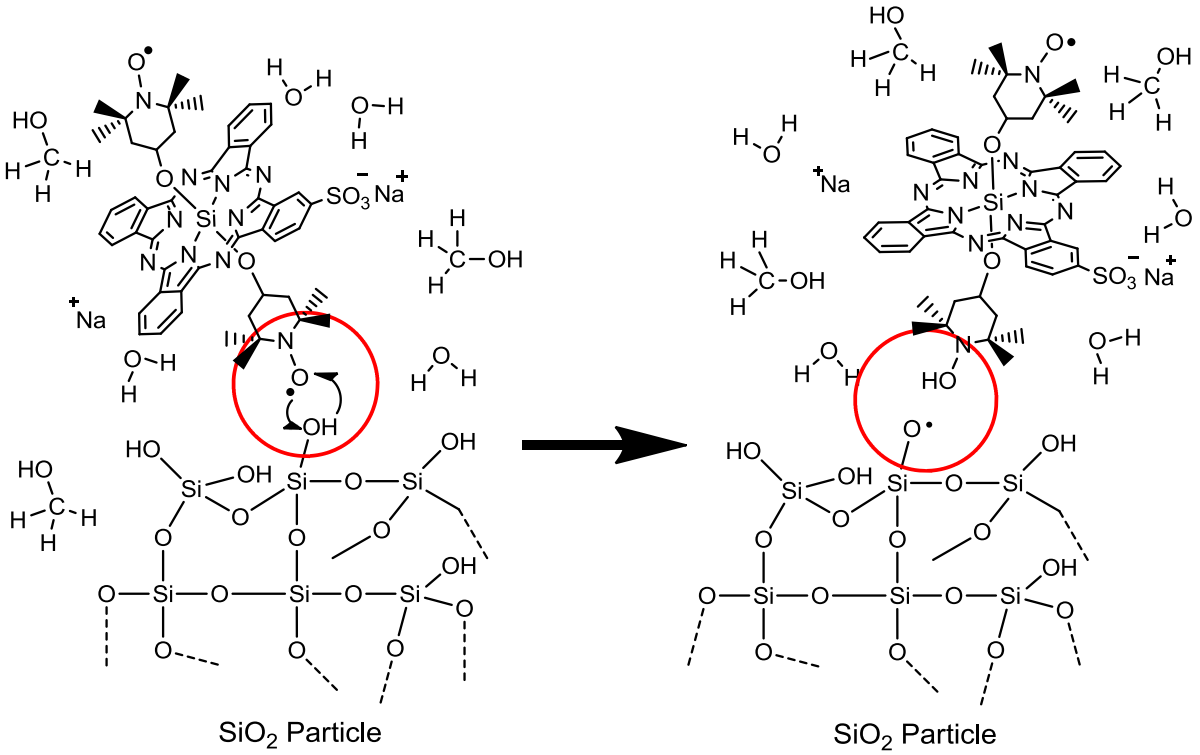

Figure 38: The process of exchanging a proton for a radical

According to the recommendation of Professor Ishii also the solvent MeOH should be avoided for a separation process.

TLC separation experiments of R2cS1:

Numerous experiments have been carried out with AlO_3-TLC and RP-TLC to achieve a good separation of the two different products formed in reaction B. One possible separation method was found with RP-TLC using the mobile phase MeOH:H_2O = 4:1.

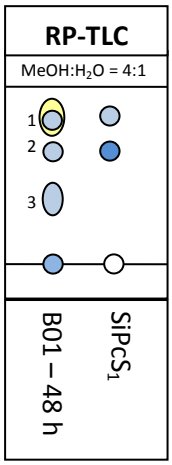

TLC-1b

In TLC-1b it can be seen that in reaction B01 there was still some SM left (SiPcS1 on spots No. 1 and No. 2). For this TLC separation there was also another new spot discovered (spot No. 3). This new spot might be either the product R2cS1, the byproduct R1cS1 or a mixture of both of them. Another aspect that is worth mentioning was that behind spot No. 1 there was also a yellow glow observable. This was attributed to the excess of 4-hydroxy-TEMPO. Another fact that should be mentioned was that, during this reaction, a second new byproduct was formed, which was not moving during the TLC separation. This second product could be the again decomposed starting material of the first step reaction (SiPc) or just another product which was formed in this reaction.

In order to examine, whether the spot No. 3 was the right product or not, a RP-TLC separation was carried out.

Because of that, the same separation procedure as in reactions A was conducted with big RP-TLC plates (TLC-2b). The individual separated spots were then scraped from the TLC plate, extracted with MeOH, filtered and then a solution for an ESI-MS measurement was prepared. Since the concentration on the TLC plate for the separation was a lot higher than that of the small TLC experiment even five spots were separated and collected and were finally measured by the ESI-MS.

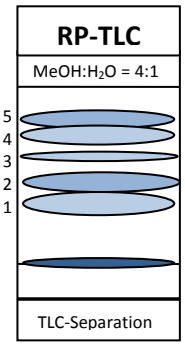

TLC-2b

ESI-MS measurement of reaction B:

The ESI-MS measurement tried to answer the question which spot belonged to which substance. For spot No. 1 just the fragments were found and for spot No. 2 no identifiable fragments were detectable. Only in spot No. 3 a substance at m/z 961 was detected. This fragment from the negative spectrum belonged to the desired product R2cS1. Furthermore there was also the peak at m/z 807 detectable with a low intensity. This was the peak of the byproduct R1cS1. However, this could also be due to the fragmentation of the R2cS1

complex or because of an incomplete separation process of the substances from the TLC plates. Spot No. 4 also showed a relatively intense R1cS1 signal and a signal of the starting material SiPcS1 (m/z = 653). These two substances were also detected in spot No. 5. (Some of the relevant ESI-MS spectra are included in the Appendix G.1.2)

Conclusion of reaction B01:

- The reaction was successful because the right product R2cS1 was formed in that reaction.
- The ESI-MS measurement was just limited helpful because it was not possible to make any accurate classification of the two products according to the collected TLC spots.
- A better separation method had to be found.
- The use of RP silica particles hides the risk that not all OH-groups of the silica particles are saturated with organic carbon chains. This could cause the same destruction of the radical sites of the axial TEMPO ligands of the complex like the normal silica particles do that (see Figure 40).

D.2.2.2 Reaction B02

Hypothesis of the reaction B02:

- In this reaction it should be tested whether a reaction time of 3 days results in a better yield of the R2cS1 product (at least according to the TLC tests)

Experimental implementation:

This time the reaction was carried out the same way as in reaction B01. The only difference was that the reaction time was extended to 72 hours. After stopping the reaction the solvent was reduced and RP-TLC experiments were carried out under the same conditions as for reaction B01. The results indicated that longer reaction times lead to a poorer yield of R2cS1 (see TLC-3b). The new spot No. 3 at a low Rf-value showed a lower intensity than in the reaction after 48 hours. The solvent of the reaction solution was removed

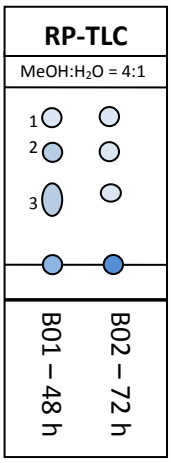

TLC-3b

with rotary evaporator and the product mixture was stored under light shutter.

Conclusion:

- Longer reaction times have bad effects on the yield of the desired product R2cS1.

D.2.2.3 Reaction B02

Hypothesis of the reaction B02:

- Because the very low concentration of SiPcS1 in the reaction solution, the TLC tests were sometimes difficult to interpret. Therefore in this reaction the reaction should be scaled up using more starting material.
- Furthermore some samples for shorter reaction times should be taken and tested if these conditions would be better for the reaction yield.

Experimental implementation:

The implementation is again the same as for reaction B01. This time however, instead of 0.12 mg starting material, 0.4 mg (1 eq, 5.9 * 10^{-7} mol) of SiPcS1 and 25.9 mg (100 eq, 5.9 * 10^{-5} mol) of 4-hydroxy-TEMPO was used. Also the amount of toluene solvent was increased from 25 ml to 30 ml.

During this reaction samples were drawn after 6, 16, 24, 39, 45 and 50 hours and were analyzed by RP-TLC test. In TLC-4b the trend can be seen, that the product spots No. 3 and 4 increased over time but also the starting spot was getting more intense. Also for these TLC experiments it has to be mentioned that the TLC spots were still relatively low concentrated which made it quite difficult to compare the results. The reason for this uncertainty was because depending on the amount that had been applied as a reaction spots on the TLC the color intensity on the separated TLC substances would be also strongly affected.

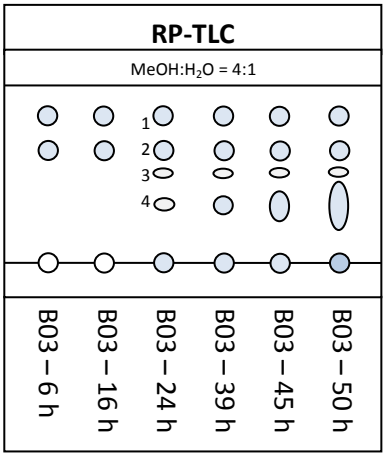

TLC-4b

Since the previous experiment has shown that reaction times longer than 48 hours lead to a decrease of the product spots No. 4 (which was believed to be the desired product R2cS1),

the reaction was stopped after 50 hours. Then the solvent was removed on a rotary evaporator and then another TLC assay was performed with bigger TLC-spot concentration (see TLC-5b). In this TLC-test it could be clearly observed that two new products were formed.

Since spot No. 4 was believed to be the R2cS1, the decision was made to do a TLC separation and collect that spot to perform an ESR measurement. This measurement should indicate the existence of two TEMPO radicals on the product.

Before the measurement was carried out, another RP-TLC-assay was done to confirm the purity of the separation (TLC-6b). The results were striking.

This result showed that apparently during the TLC separation with RP-TLC the already purified product breaks up again re-forming starting material (SiPcS1) and mono-substituted complex R1cS1.

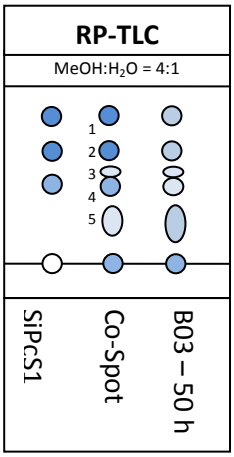

TLC-5b

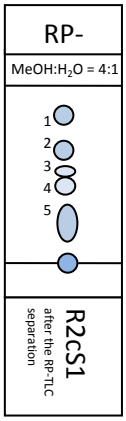

TLC-6b

Conclusion:

- RP-TLCs should not be used for the separation of R2cS1 and R1cS because a separation with that TLC destroys the product and form again the starting material and mono-substituent.

D.2.2.4 Reaction B04 and B05

Hypothesis of the reaction B04 and B05:

- Now that the optimum reaction conditions have been confirmed to be 48 hours a reaction up-scaling should be examined
- In the meantime, a new separation method with AlO_3-TLC should also be found.

Experimental implementation of B04:

For this synthesis an equivalent of 1.5 mg (1eq, 2.22 * 10^{-6} mol) of the complex SiPcS1 was transferred into a 300 ml flask (using Beer-Lambert law and absorption spectrum). Attempts were then made to solve the complex in 100 ml toluene. Since the solubility of SiPcS1 was not very good in this solvent, the flask was placed in an ultrasonic bath for 1 h. after the

complex was solved, 34.6 mg (100 eq, 2.22 * 10^{-4} mol) of 4-hydroxy-TEMPO was added, connected to a nitrogen purged condenser and was heated with an oil bath up to 125 °. After 48 hours, the reaction was cooled down and the solvent was reduced on an evaporator. The TLC experiment showed the same result as in the experiment B03 after 50 hours (TLC-4b).

Experimental implementation of B05:

This experiment was a bigger up-scaling the previous synthesis. In this experiment 40.2 mg (1eq, 5.94 * 10^{-5} mol) SiPcS1 was dissolved in MeOH, transferred to a 500 ml flask and the solvent was subsequently removed. Then it was tried to solve SiPcS1 in 300 ml toluene. Since the concentration of SiPcS1 was much bigger in this experiment a normal ultrasonic bath was not enough to dissolve the entire substance. For this reason 5g of glass beads were added into the flask which should support the dissolving process by physical friction of the glass beads. That should speed up the dissolution process. Since the glass beads covered only a small portion of the flask´s surface the angle of the flask in the ultrasonic bath was changed every 10 minutes. For those parts of the flask where the glass beads didn´t come in contact with the flask wall the flask was connected to an evaporator. The angle of the spinning flask was set to an appropriate position to clean also those areas of the flask with the beads that were not accessible with the ultrasonic bath. In this procedure no longer of ultrasound of the ultrasonic bath caused the attrition of the SM from the flask but the friction of the beads with the glass wall of the flask by the rotation of the flask on the evaporator caused the friction. Additionally, the water bath of the evaporator was heated up to 50 °C to improve and accelerate the dissolving process.

After the starting material was successfully removed from the flask wall, 0.927 g (100eq, 5.94 * 10^{-3} mol) 4-hydroxy-TEMPO was added to the reaction. Then the flask was connected to a nitrogen purged condenser and was heated with an oil bath at 125 °C to reflux. After 48 hours, the reaction was cooled and the solvent was reduced on the rotary evaporator. The TLC experiment showed the same result as in the previous experiment after 50 hours (TLC-4b).

After that the remaining solution was removed on a rotary evaporator and the product was stored in a vial in dark environment until a suitable separation method for the reaction mixture would be found.

Since this was most optimized method for the synthesis of the second reaction step the exact same procedure (but similar but different scales) was carried out another four times to further collect the final product R2cS1.

B06: 40 mg (SM - SiPcS1), 926 mg TEMPOL, 300 ml toluene;
B07: 20.6 mg (SM - SiPcS1), 460 mg TEMPOL, 150 ml toluene;
B08: 17 mg (SM - SiPcS1), 400 mg TEMPOL, 150 ml toluene;
B09: 22.6 mg (SM - SiPcS1), 532 mg TEMPOL, 150 ml toluene;

Because the product mixtures were separated later after a good separation process was found no yield for the single reaction can be calculated because the products were separated all together (see Chapter …)

Second ESI-MS measurement of reaction B:

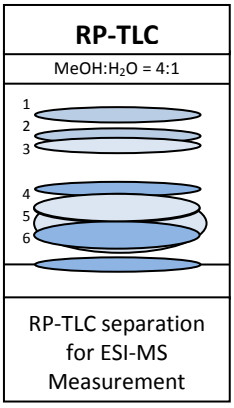

TLC-7b

Since the first ESI-MS measurement didn´t produce reliable information about the different spots of the TLC separation, the same measurement was repeated a second on one of the big scale reactions. In this RP-TLC separation even six spots could be identified, isolated and were prepared for the ESI-MS measurement (See TLC 7b).
This time the ESI-MS measurement was more successful and also more meaningful. For the spot No. 1 and No. 2 the negative-spectrum showed a small spot at 653 m/z. This was the signal peak from the starting material SiPcS1. The spot No. 3 showed m/z of 807 which was a signal peak for R1cS1 and the TLC-spots 4-6 all showed a signal at 962 m/z which was the desired product R2cS1. (Some of the relevant ESI-MS spectra are included in the Appendix G.1.2)

Conclusions:

- With this second ESI-MS measurement it was confirmed that the spots No. 1 and No. 2 on TLC-7b were SM, spot No. 3 was R1cS1 and spots No. 4-6 were the desired product R2cS1.
- Unfortunately, this measurement didn´t change the fact that RP-TLC couldn´t be used for the separation as it had been shown in reaction B03. (The RP-TLC separation was

possible, but the product was not stable thus forming again a mixture of SM, R1cS1 and R2cS1.)

- In this reaction it was also confirmed that the reaction time of 48 hours forms an optimum yield of the reaction B which is also correct in a big scale reaction (due to the intense spots on the TLC).
- The ESI-MS measurement also revealed that R2cS1 forms agglomerates on RP-TLC like for the first step reaction. This was the reason why several product spots were observed on the TLC assay.

Conclusion of reaction A and B:

- Since reaction A and reaction B, has been optimized for all possible parameter, the last challenge was to find a suitable separation method for the reaction mixture (R2cS1, R1cS1 and SiPcS1).
- In the end, the desired product should be synthesized in an amount of total 10 mg. This amount should be enough to perform the measurements (elemental analysis, extinction coefficient measurement, fluorescence measurement).

D.2.2.5 TLC experiments

Summary of knowledge:

According to the RP-TLC the synthesis of the desired complex R2cS1 could be achieved with an already quite good yield. As a next step a method had to be found to be able to separate the starting material from the mono-substituted R1cS1 complex and from the complex R2cS1. NP-TLC could not be used for the separation because it would destroy the radical sites on TEMPOL ligand. RP-TLC also couldn´t be used because of the instability of the product in this separation. Therefore AlO_3-TLCs have to be used to find an appropriate separation method. In addition, a suitable solvent mixture and solvent ratio would have to be explored to achieve a good separation of all three substances.

Experimental implementation:

In order to achieve a proper separation about 300 AlO_3-TLC arrays were performed. The solvents used for these experiments were EtOH, MeOH, iPrOH, THF, DMF, DCM, $HCCl_3$,

hexane, pyridine, H_2O, acetone, acetic acid, toluene, acetonitrile, ethylacetate, NH_3 and pentanol. Many of these solvents were mixed together in various ratios and were tested for their separation capabilities.

From all these 300 tests two of them seemed to produce promising separation results.

First promising TLC array:

When AlO_3-TLC was used with the solvent mixture-ratio of EtOH:$HCCl_3$:H_2O = 5:5:1, a good separation seemed to be achieved as it can be seen in TLC-8b. Due to this TLC experiment, a separation with a large TLC plate was performed. The two spots were separated, collected (scaped from the TLC, extracted and filtered) and then the products were measured by ESI-MS. The ESI-MS measurement however had shown that both of the spots had been the product R2cS1. By comparison the spot of the starting material on the left side of the TLC with the spots on the right side, it can be seen that the starting material had the same Rf value as the TLC-spot No. 2 of the compound mixture. This meant that this method could not be used for the separation of the SM and the product.

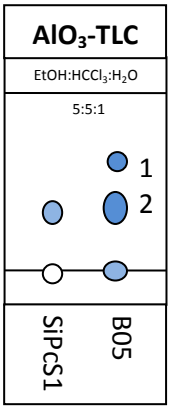

TLC-8b

Second promising TLC experiment:

The solvent mixture EtOH:H_2O in different mixing ratios seemed to be a promising mobile phase for the separation of the three substances SM, R2cS1 and R1cS1 (see TLC-9a). This was especially of interest, since this solvent mixture could be easily used for the performance of a column chromatography. Therefore, a small scale column chromatographic experiment was performed with a Pasteur pipette as column. The pipette was stuffed with cotton wool at the thin opening and was then filled with AlO_3 powder slurried in $HCCl_3$. Thereafter, a small amount of the substance mixture of the reaction B05 was applied to the mini-column. The column was first washed with $HCCl_3$ to remove the solvent of the applied product mixture (toluene). After that, the solvent composition was changed to $HCCl_3$:EtOH:H_2O (30:8:2). As soon as the more polar solvent came in contact with the complex mixture in the column, the blue spot began to move slowly down the column. After

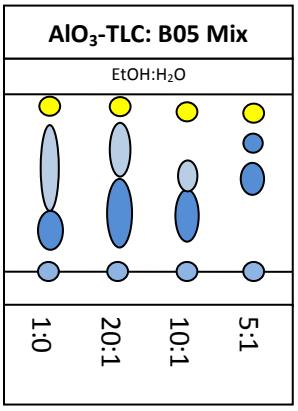

TLC-9b

some time, the ratio of the solvents was changed to 30:16:4 and was finally changed to 10:2:1. During that separation four fractions were collected and then analyzed by RP-TLC. Although in the first fraction an excess of TEMPOL could be separated, but the other three fractions didn´t show any differences in the mixture composition. All of them contained starting material and the products R1cS1 and R2cS1.

Third promising TLC experiment:

On an internet forum it was advised to use a mixture of different polar solvent to succeed in a separation of substances with very similar and strong polarity. Since the three substances that had to be separated for this synthesis all had very similar polarity because of the sulfate group that they had in common it was tried to use mixtures of 3 or 4 different polar solvents with many different solvent ratios.

The solvent mixture which finally showed relatively good results was a mixture of ethyl acetate:EtOH:acetic acid:H_2O with a solvent ratio of 8:2:0.5:1. As it can be seen in TLC-10b the separation of the two spots was not very good which implied that column chromatography couldn´t be used for that separation method.

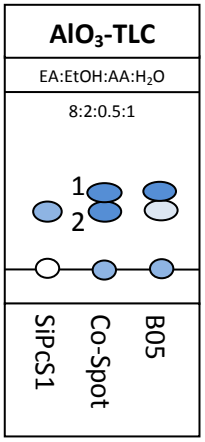

TLC-10b

As it can be seen in the TLC (10b), a separation of SM and R2cS1 was possible to achieve with that solvent mixture. Since the amount of R1cS1 in the reaction was very low (as seen in TLC-6b) and since it could also have the same retention behavior as the starting material, it was decided to use this separation method to separate a part of the reaction mixture and to analyze the fractions further.

AlO_3-TLC separation:

The relatively strong dilute toluene solution of B06 was applied for the TLC separation of the two spots on a larger scale. Therefore the solution was put on a big AlO_3-TLC plate and was then separated in a TLC chamber filled with ethyl acetate:EtOH:acetic acid:H_2O (8:2:0.5:1). To achieve a good separation the mobile phase was able to move up to the very top of the TLC plate that the two product spots were just below in the middle of the TLC plate.

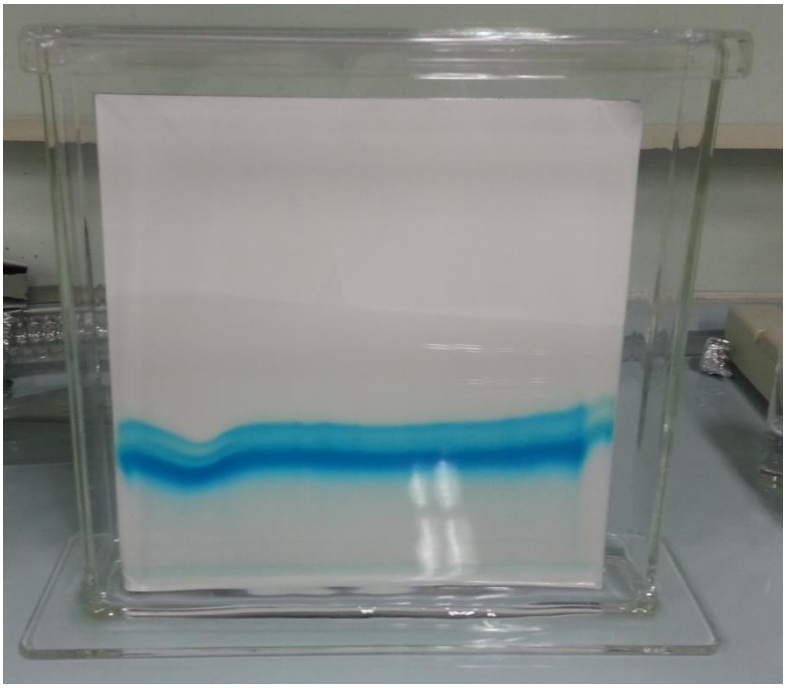

Figure 39: TLC separation on a AlO_3-TLC plate with ethyl acetate:EtOH:acetic acid:H_2O (8:2:0.5:1) as a mobile phase

After some of the reaction mixture was separated with the TLC plates, the product spot was scraped from the TLC plate and was extracted with a solvent mixture H_2O:EtOH = 1:1. The particles were then removed by vacuum filtration. To make sure that the collected product was not contaminated with SM this separation procedure was repeated a second time with the already purified sample. After the second separation, the sample was dissolved in toluene and an ESR measurement is performed.

First ESR Measurement:

This was the first measurement, where the successful synthesis and existence of R2cS1 with two intact TEMPOL radicals as axial ligands was confirmed. As already described in the general part, the smaller peaks which can be seen in addition to the large main peak are indications for the presence of two radicals which were coupling with each other. Therefore they provide this additional smaller signal peaks. The only drawback of this measurement was (as a consultation with the professor Ishii revealed) that the measured sample was probably still strongly contaminated with 4-hydroxy-TEMPO. This assumption was plausible because TEMPOL was used in this reaction in a large excess (100 times the amount of the complex). These impurities would also explain the unnaturally intensive three main peaks.

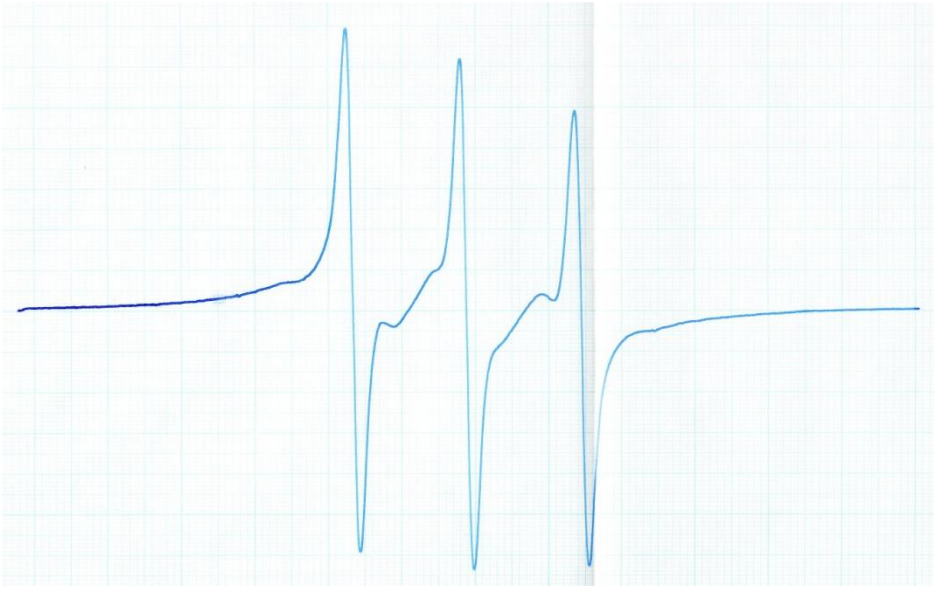

Figure 40: First ESR measurement with the additional smaller peaks as indication for a successful synthesis of R2cS1

Conclusion for the next ESR measurement:

- Since TEMPOL is used in the second step reaction in the 100-fold concentration compared to SiPcS1, it is especially important that the workup steps in future experiments include an additional procedure such as column chromatography in which TEMPOL should be thoroughly flushed with a solvent that could move the TEMPOL but not the complex (i.e. $HCCl_3$).

Second ESR measurement:

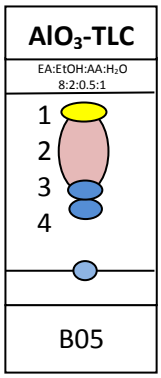

TLC-11b

Before the next ESR measurement was prepared another TLC-test was carried out to check if the theory of the contamination with TEMPOL was true. After the separation the TLC plate was dried and then it was placed into a UV-chamber. In the chamber it was possible to see that the major part of the TEMPOL was concentrated at a very high Rf value but under the UV light it was also possible to observe that also at very low Rf values there were still residues of that compound visible in a reddish color (see TLC-11b). Therefore it was decided that for the next purification an additional column chromatography step should be carried out in which the compound mixture should be flushed with $HCCl_3$ to remove the TEMPOL. This washing step should be prior to the TLC separation.

Experimental implementation:

For the separation procedure of TEMPOL a small chromatography column was prepared. First cotton wool was used to plug the stopcock opening. Then the column was filled with 50 ml AlO_3-particel slurried in $HCCl_3$. The column was flushed with $HCCl_3$ until the particles have been solidified. Then the remaining solvent was drained to the phase boundary the compound mixture which was dissolved in EtOH:H_2O (5: 1) was applied on the column with a Pasteur pipette.

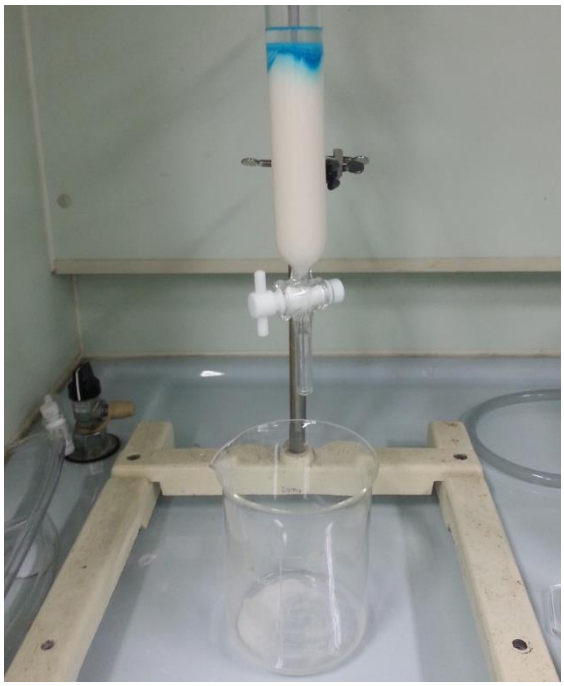

Figure 41: Removing TEMPOL from the reaction solution by flushing the product mixture with $HCCl_3$ in AlO_3 gel

Afterwards, the column was rinsed with several liters $HCCl_3$, wherein the collected solvent was recycled with the evaporator and was reused. After that, the solvent composition was changed again to EtOH:H_2O (5:1), whereby the blue compounds could be eluted again from the column. After removing the solvent on the evaporator, the product was re-dissolved in a small amount of EtOH and a TLC separation was carried out in the same way as described before. After that the purified product was again measured with ESR.

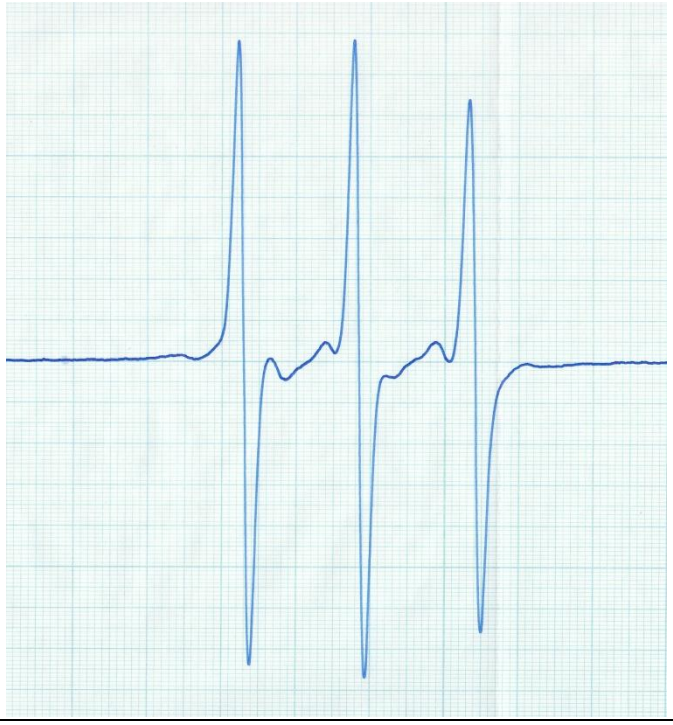

Figure 42: Second successful measurement of R2cS1 with ESR with still quite strong impurities of TEMPOL

In this measurement, the main peaks were still a lot more intensive than the secondary peaks, but small improvements could already be detected in this measurement.

Conclusion for the next measurement:

The previous experiments have shown that the synthesis for the compound R2cS1 was working very well and also the purification procedure was working. The only thing that was not fully understood was how to remove the large excess of TEMPOL completely from the reaction mixture. Obviously the previous experiment was not enough for completely purifying the product.

D.2.2.6 Purification of the product mixture B05-B09

From all performed second step reactions B the aim was to obtain 10 mg of the product R2cS1. Since all of the starting material was used up in the five reactions B05-B09 the reaction mixtures were now separated as follows.

The combined mixture product was applied onto a small chromatographic column filled with AlO_3 gel (prepared in the same way as in the previous purification experiment). This column was extensively flushed with $HCCl_3$ for 5 hours. After that time, the solvent composition was changed again to EtOH:H_2O (5:1), whereby the blue compounds eluted from the column. After removing the solvent on the evaporator, the product was re-dissolved in a small

amount of EtOH and a TLC separation using AlO_3-TLC plates and ethyl acetate:EtOH:acetic acid:H_2O (8:2:0.5:1) as a mobile phase. After the separation the product spot on the TLC plate was scaped down with a spatula, was extracted with EtOH, was filtered and the solvent was finally removed on the evaporator. This separation step was repeated five times for the entire product compound. From all the second step big scale reactions that have been carried out to obtain the complex R2cS1, 9.8 mg of purified final product could be obtained. With this synthesized and purified final product some further measurements were carried out

D.2.3 Measurements of the complex R2cS1

D.2.3.1 ESR measurement

After this intensive purification procedure the compound R2cS1 was purified sufficiently to measure a good ESR spectrum. In the spectrum that can be seen in Figure 45 the main peaks and the smaller side peaks have a good intensity. This spectrum proves that the synthesized compound R2cS1 has two functioning radical sites.

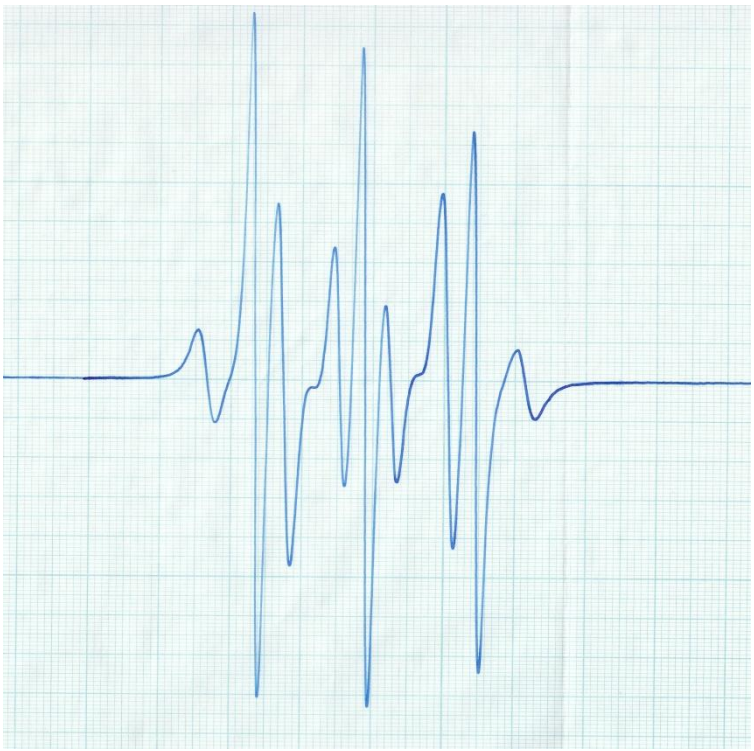

Figure 43: ESR spectrum from the newly synthesized complex R2cS1 showing a peak pattern that indicates two intact radical sites on the silicon TEMPOL ligands

D.2.3.2 MCD and absorbance measurement

As it was already noticed in the measurement of the absorption spectrum, there was a clearly defined split in the Q-band of the spectrum. A MCD measurement was measured to clear whether these two bands were caused by impurities or due to a splitting of the orbital energies because of the asymmetry of the complex caused by the sulfate group. The result of this measurement can be seen in Figure 46.

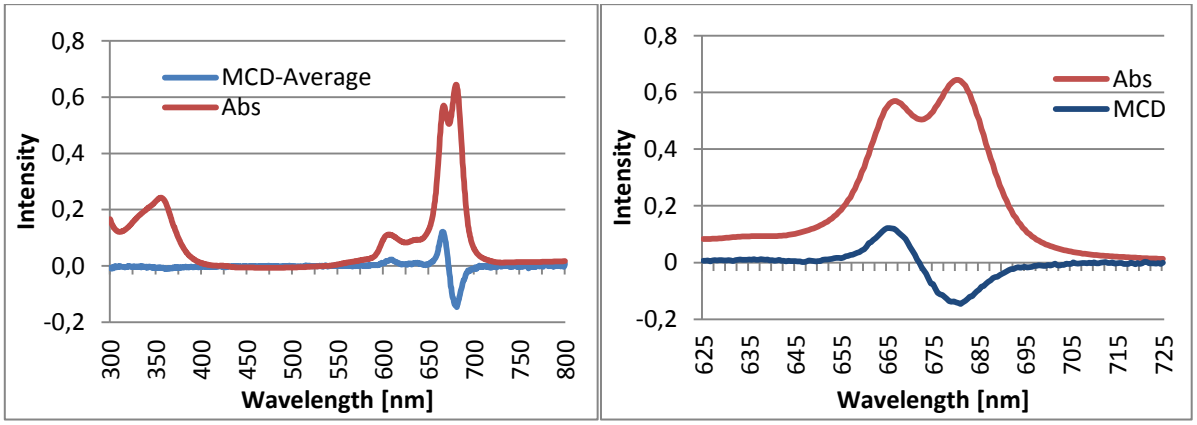

Figure 44: MCD measurement overlapping with an absorption spectra indicating that the Q-band splitting is caused by an orbital energy split because of the asymmetry of the complex

It can be clearly seen in the two spectra (MCD and absorption spectrum) that the displacements of the peak maxima were found for both the absorption and for the MCD spectrum at the same wavelength. This suggested that the two peaks were caused by the same substance and not as previously thought due to contamination. This indicated that the strong polarity of the sulfate group in the SiPcS1 complex as well as in R2cS1 split the energy levels of the orbitals, causing a splitting of the Q-band in these spectra. In Figure 46 the two spectra are displayed with different resolution ranges. The peak maxima are located at a wavelength of 666.5 nm (peak 1) and 680.5 nm (peak 2).*

D.2.3.3 DFT calculation

In order to further confirm that the two peaks from the absorption measurement have been from one and the same substance, a DFT calculation was performed with the starting material SiPc and the final product R2cS1. In this calculation oscillator strength and the excitation energies form the HOMO and LUMO energy levels of the two compounds was theoretically calculated. First the complexes were drawn in the computer program ChemDraw. With the program Hyperchem the geometric structure was optimized and then

* It has to be mentioned that depending on the used solvent the intensity of the first peak was varying quite strongly. Sometimes the peak was very obvious and easy to see but sometimes just a shoulder of the Q-band was measurable.

DFT calculation was performed with the program Gaussian. To speed up the calculation time the structure of the complex R2cS1 was simplified by replacing the two axial TEMPO ligands by chloride atoms. This could be done because the axial ligands have no major impact on the symmetry considerations for the calculated compounds. With the program Gaussian also the HOMO, HOMO +1, LUMO and LUMO-1 energies of the molecular orbitals were calculated for 1 each R2c and R2cS1 which can be seen in the Appendix E.3.3 in Figure 62-66.
The calculations of the excitation states of the Q-bands for the two compounds additionally confirmed the previously performed MCD measurement. Gaussian calculated two separate Q-bands for the complex R2cS1. The calculation of R2c resulted only one peak for the Q-band. For the calculation of the complex R2cS1 it can clearly be seen that the first peak at lower wavelengths had smaller oscillator strength than the second peak of the Q-band. This fact is also in accordance with the observations in the absorption measurement. The exact calculation results can be found in Appendix G.3.2.

D.2.3.4 Fluorescence measurement

In this experiment the actual sensitivity towards vitamin C of the newly synthesized complex R2cS1 should be compared with the sensitivity of the old first generation of the complex R2c. Samples of the same concentration were prepared (as described below) and the fluorescence signals were measured over time after the addition of vitamin C.

Experimental implementation:

21 mg lipids were weighed into a 10ml vial and were then dissolved in 3.6 ml $HCCl_3$. At the same time the sample R2cS1 (or R2c) was dissolved in toluene and with the absorption spectrum the quantity was determined by calculation with the Beer-Lambert law. Then the required quantity of 156 mg ($1.58 * 10^{-7}$ mol) of R2cS1 complex or 174.9 mg ($1.58 * 10^{-7}$ mol) of R2c complex was pipetted into a 10 ml flask and the solvent was removed on the evaporator. Then the complex was re-dissolved in 180 µl THF. Thereafter, the 3.6 ml of $HCCl_3$ lipid solution was added to the dissolved complex, the solvent was again fully removed and the mixture was thoroughly dried in vacuum. After that 2 ml of a 10 times diluted PBS solution was pipetted into the flask and 0.5 g of small glass beads were also added. The flask was then sealed with a glass stopper which was additionally sealed with parafilm. Since the

dried complex-lipid mixture was solidified on the glass wall it couldn´t easily be solved by the PBS solution, the flask with the glass beads was vortexed until no more substance could be observed on the flask wall. After that the sealed flask was placed in a 50 °C heated water of the ultrasonic bath. The correct spatial positioning of the flask in the ultrasonic bath was set to a spot in the water bath, where the glass beads began to move by the resonance the glass wall with the ultrasound. After one hour in the ultrasonic bath, the flask was removed and the condensed water formed on the inner wall of the glass was collected by rotating the flask and the remaining solvent in the glass in a proper position. Then the solution was transferred to a centrifuge tube and together with a second water-filled centrifuge tube as a counterbalance the sample was placed in the centrifuge and was centrifuged for 10 minutes at 3500 rpm. The clear bluish colored liquid was carefully separated from the residue of the lipids and collected in a vial.

This procedure was both performed with the R2cS1 complex as well as with the first generation of Vitamin C detected complex R2c in order to compare their fluorescence capabilities.

In order to determine the total amount of the complex substance in the solution an absorptiometry was carried out with 100 µl of the dissolved complex sample in PBD and 1900 µl DMF. The DMF causes a disintegration of the formed micelles and liposomes and therefore freeing the encapsulated complex molecules into the solution again. According to the absorbance measurement the fluorescence vial was prepared in a way that the concentration of the complex reached an absorption peak maximum intensity of one. Therefore 100 µl of the dissolved R2cS1 complex sample was mixed with 1.7 ml PBS solution and 250 µl of the dissolved R2c complex was mixed with 1.55 ml PBS solution (because the intensity of the R2c complex was much lower in the previous absorption measurement). For the measurement 200 µl of the different vitamin C solutions were added to the vial. The preparation of these vitamin C solutions is explained below.

Preparation of the vitamin C solution:

Since the fluorescence measurement is strongly influenced by dissolved oxygen in the vitamin C solution the preparation of these solutions was carried out in a nitrogen flooded glovebox. The preparation of the standard solution of vitamin C was performed also in this glovebag. Before the solid vitamin C was dissolved in the PBS solution, the solvent was

bulled with nitrogen for two hours. The prepared standard solution was then used to prepare all the different concentrated vitamin C samples: 10 mM, 5 mM, 1 mM, 500 µm, 100 µm, 50 µm. The concentration of the sample solution was set in a way that the mentioned amount of vitamin C would be added in the fluorescence experiment by adding an aliquot of 200 µl of the prepared vitamin C samples.

The prepared vials with the according vitamin C concentrations were then tightly closed and sealed with parafilm and stored in a refrigerator until the fluorescence measurement was carried out.

The results of the fluorescence measurement:

The fluorescence was measured at a wavelength of 690 nm and the intensity was recorded over time. Figures 47 and 48 the intensity behavior over time is plotted on this diagram for both complexes R2cS1 and R2c. It can be clearly seen that the intensity for the complex R2cS1 is increasing much faster than the intensity of R2c. This indicates that the sensitivity of R2cS1 towards fluorescence development after vitamin C addition is as expected much better than the fluorescence development of R2c. This results also in a much lower detection limit for R2cS1. The second generation of the complex is capable of detecting even vitamin C amount of 50 µM in 2 milliliter solution whereas the complex R2c already struggles with amounts of 500 µM. This means the second generation is about 10 times more sensitive towards vitamin C than the first generation of the complex.

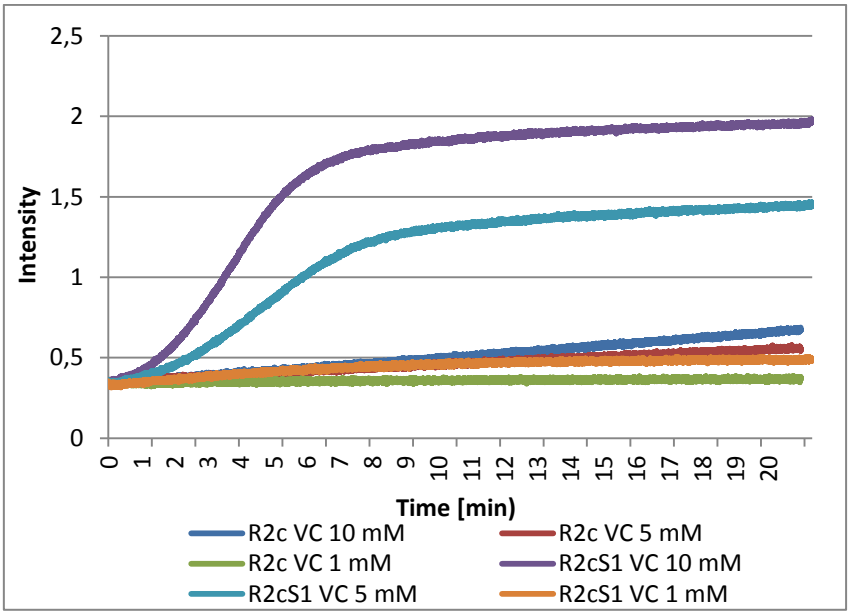

Figure 45: Fluorescence measurement after adding different amounts of vitamin C to the complex solutions of R2cS1 and R2c (high concentrations)

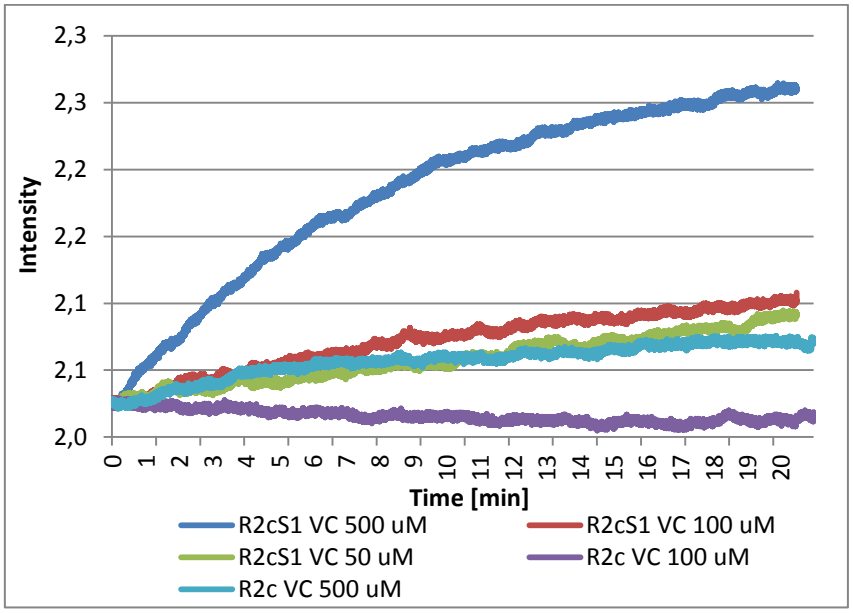

Figure 46: Fluorescence measurement after adding different amounts of vitamin C to the complex solutions of R2cS1 and R2c (low concentrations)

Also the fluorescence measurement for different wavelengths for R2cS1 and R2c (Figures 49 and 50) show that the new complex is much better than the old one. For this measurement 10 mM vitamin C were added and after 20 minutes the spectrum was measured. Especially the intensity increase at a wavelength of 690 nm is very impressive and explains also the big differences in the first fluorescence measurement where the signal development for that wavelength over time was recorded.

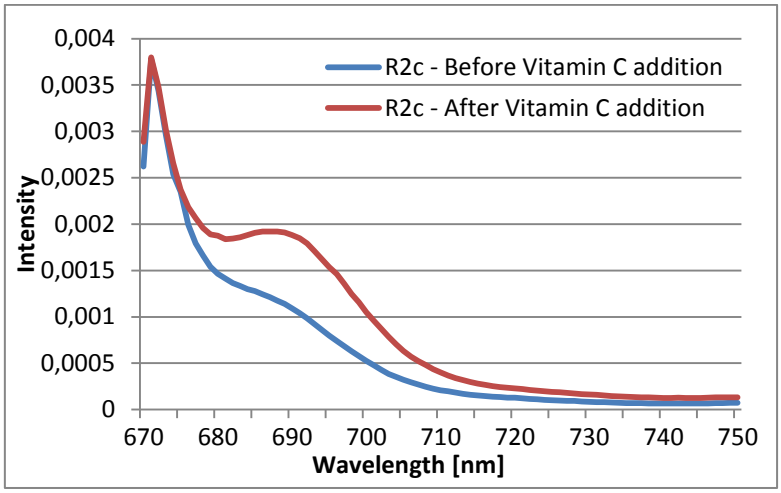

Figure 47: Fluorescence measurement of R2c after vitamin C addition for different wavelengths

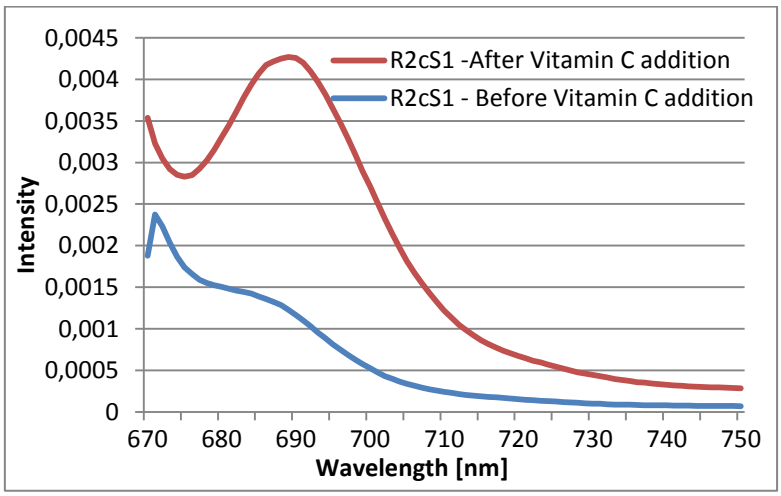

Figure 48: Fluorescence measurement of R2cS1 after vitamin C addition for different wavelengths

D.2.3.5 Elemental analysis

For this measurement the product R2cS1 was dried in high vacuum overnight. The next day 1 mg of the sample was scratched with a clean spatula and transferred into a small aluminum cup which was then measured by the elemental analysis. Four times around 1 mg of a standard compound was also prepared as a standard sample and then all samples were measured by the elemental analysis.

This measurement was carried out four times but unfortunately the exact ration of carbon nitrogen and hydrogen could not be detected. Perhaps the sample was still a little bit contaminated with some salt or another inorganic material.

D.3 Summary and conclusion

In this research project a new vitamin C detecting fluorescent complex was synthesized. This was achieved in a two-step reaction. In the first reaction step the core structure of SiPc was modified in a reaction with oleum by attaching a polar sulfate group on the complex. After that the product mixture was successfully separated by using a column chromatography. In the second reaction step two TEMPOL molecules were attached as axial ligands to the silicon central atom. By using column chromatography with AlO_3 gel for separating the excess of TEMPOL and by using AlO_3-TLC plates the starting material was successfully removed from the reaction mixture. This TLC separation was repeated several times to obtain a pure product.

With that produce a successful ESR measurement was performed confirming the presence of two radical sites on the TEMPOL ligands.

The measurement of MCD, absorbance and the DFT calculation explained that because of the asymmetry of the new complex caused by the sulfate group, the energy of the orbitals responsible for the Q-band get shifted which results in a Q-band splitting in the absorption measurement.

The final fluorescence measurement after vitamin C addition revealed that the new complex R2cS1 has a 10 times higher sensitivity for vitamin C detection compared to the first generation of vitamin C detecting complex R2c.

The elemental analysis was unfortunately not successful. This could be caused by some inorganic contamination. Because of that, the experiment for determining the extinction coefficient was not performed in this research project.

E) Appendix

E.1 ESI-MS spectra

E.1.1 Reaction A

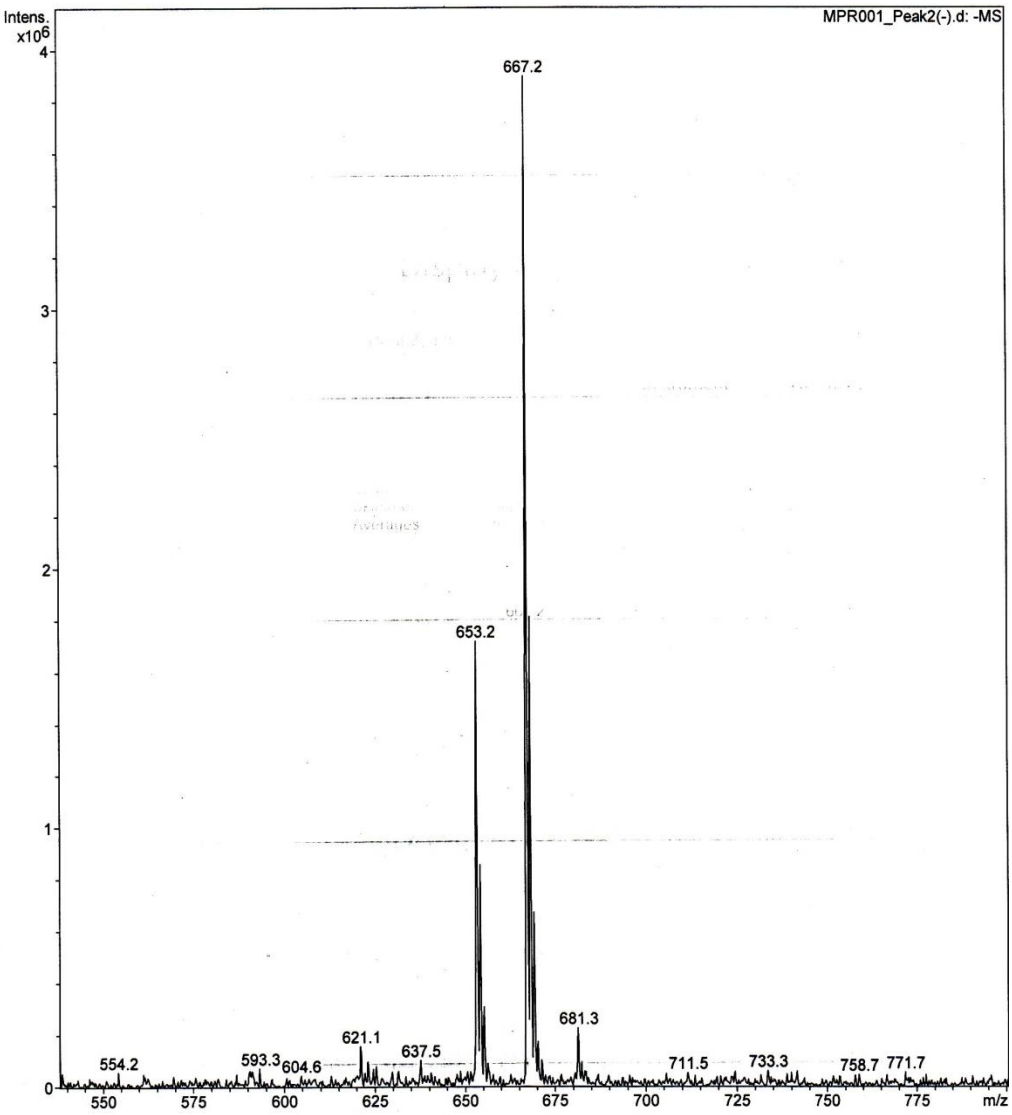

Figure 49: ESI-MS spectrum of the first separated SiPcS1 compound of reaction A01, showing the product peak at m/z 653 in the negative spectrum

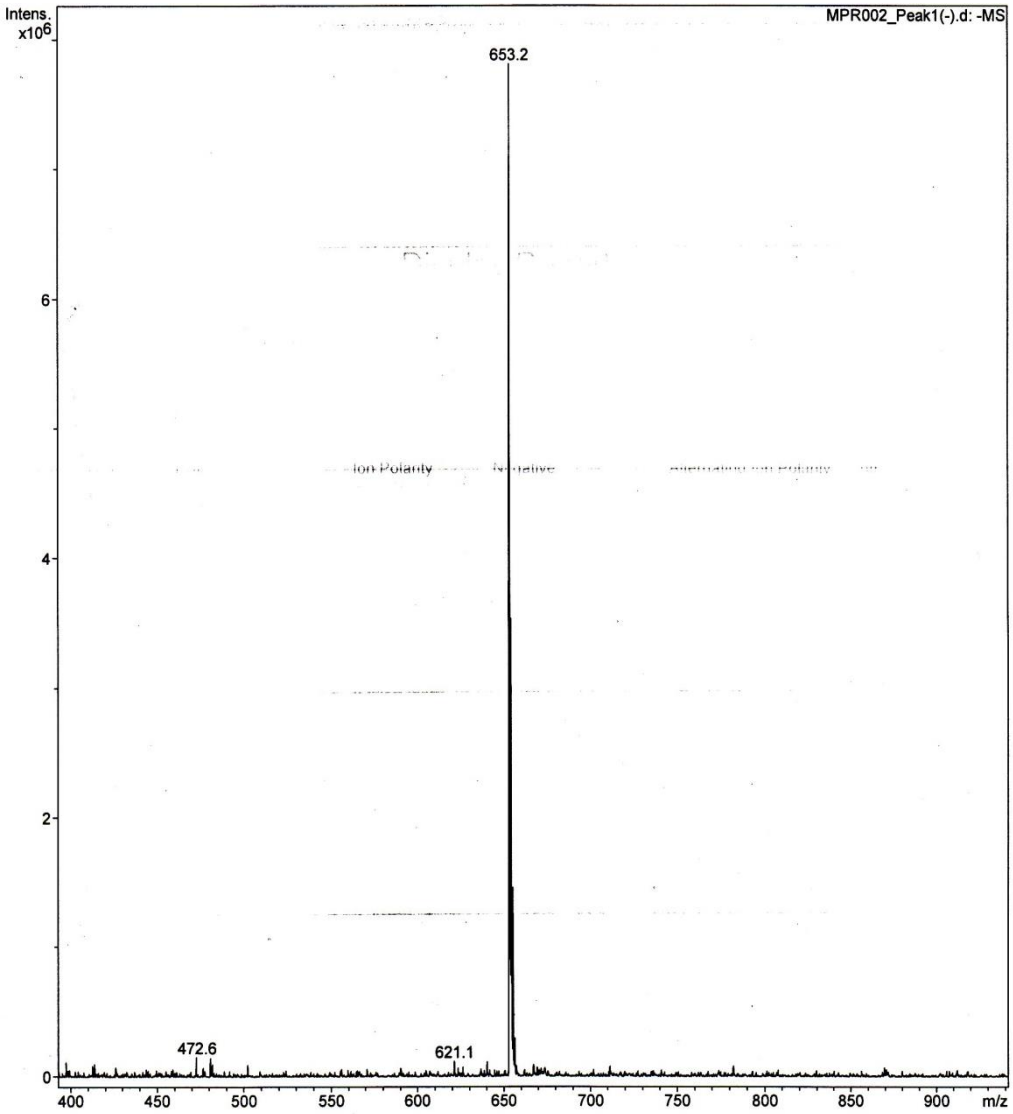

Figure 50: ESI-MS spectrum of reaction A03 of the first separated TLC- spot showing the SiPcS1 complex at m/z 653 in the negative spectrum

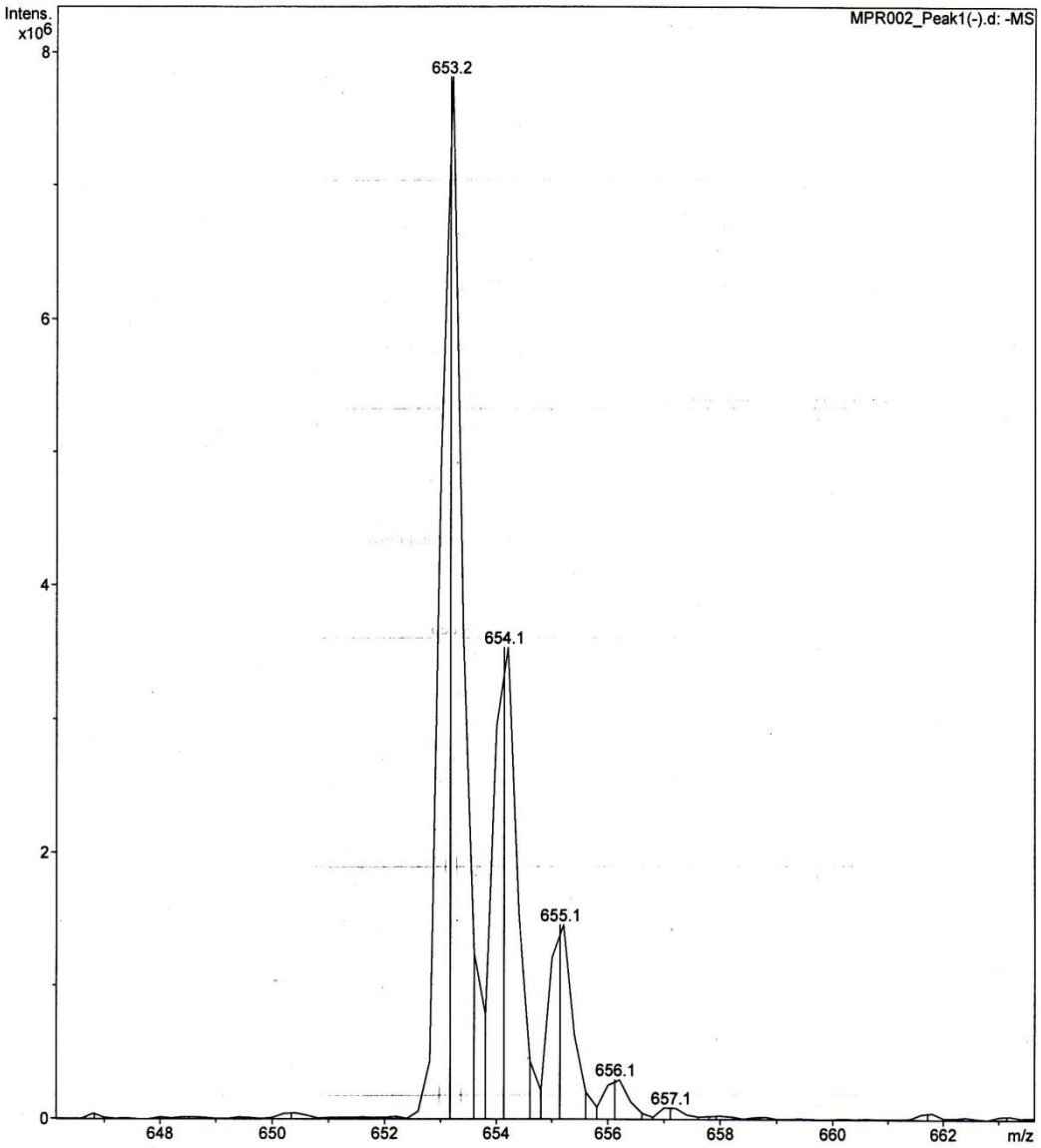

Figure 51: ESI-MS spectrum of reaction A03 of the first separated TLC- spot showing the SiPcS1 complex at m/z 653 in the negative spectrum with the according isotope pattern

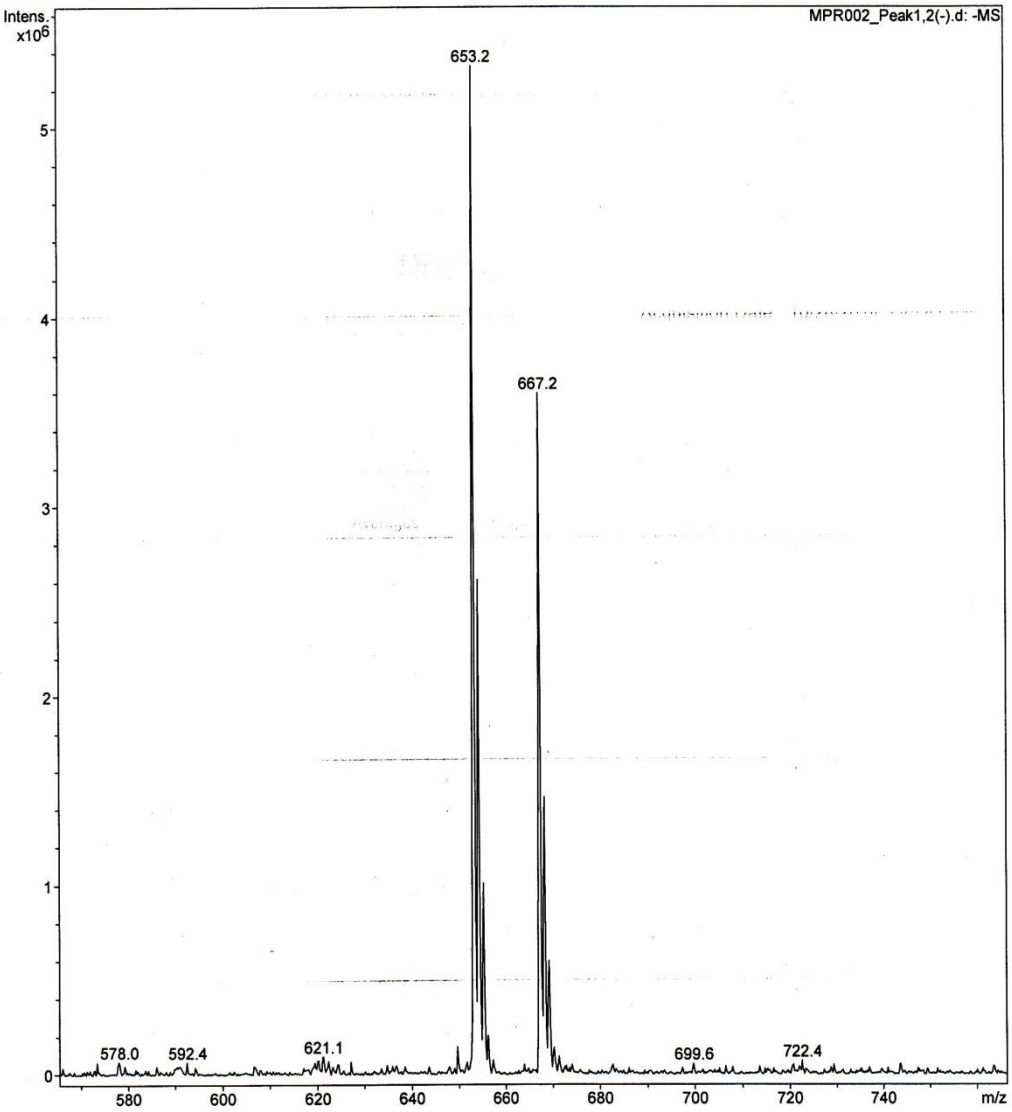

Figure 52: ESI-MS spectrum of reaction A03 of the second separated TLC- spot showing the SiPcS1 complex at m/z 653 in the negative spectrum

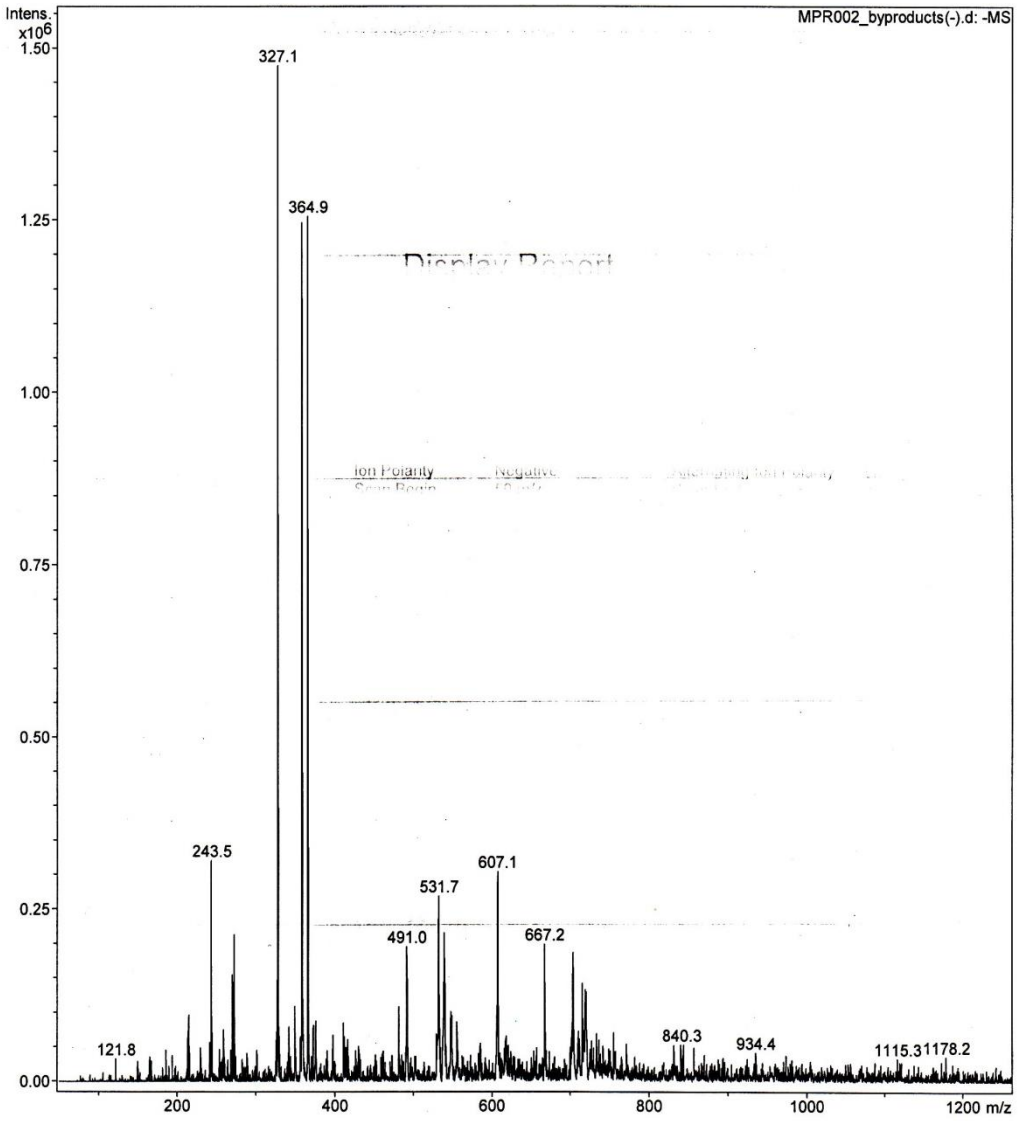

Figure 53: ESI-MS spectrum of reaction A03 showing the byproduct mixture with a lot of fragment peaks in the positive spectrum

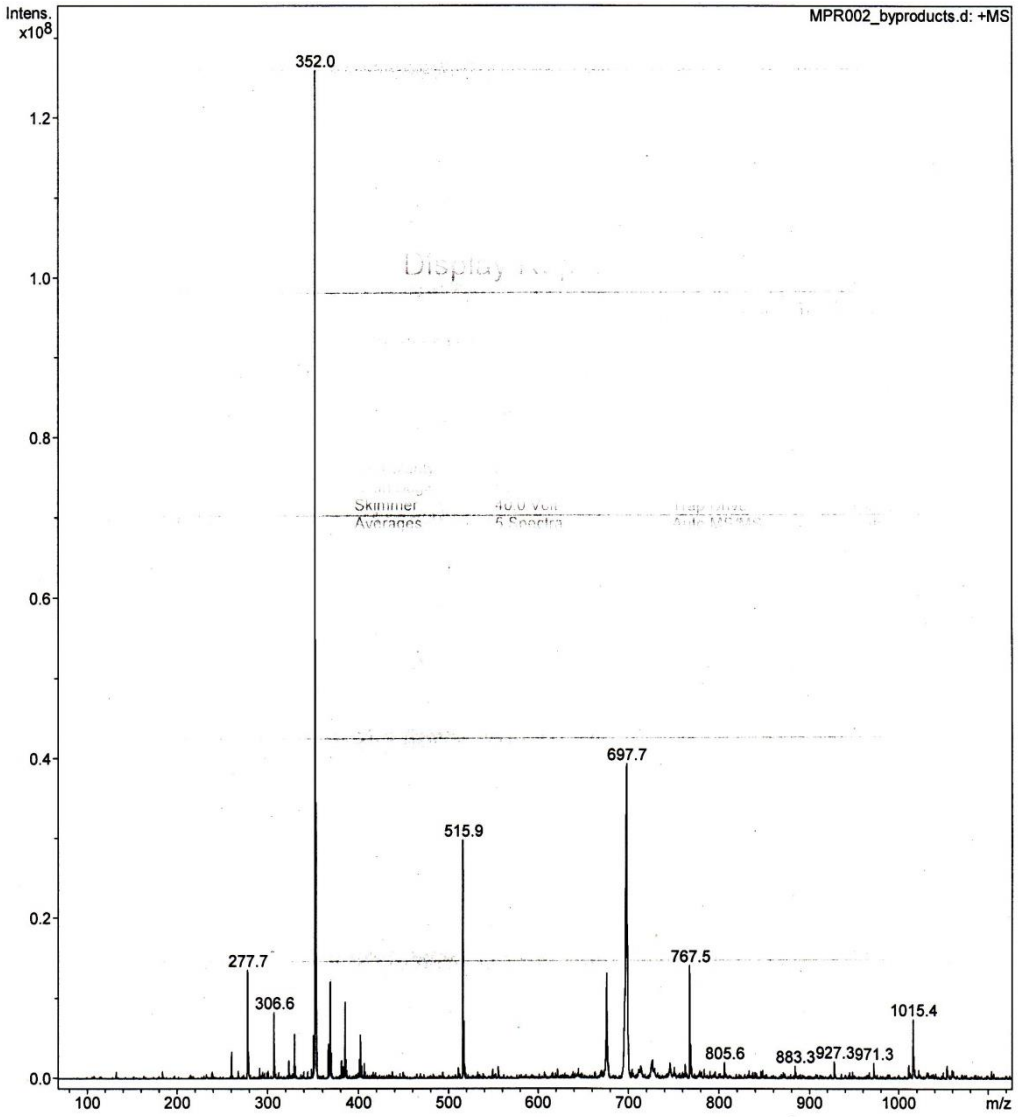

Figure 54: ESI-MS spectrum of reaction A03 showing the byproduct mixture with a lot of fragment peaks in the negative spectrum

E.1.2 Reaction B

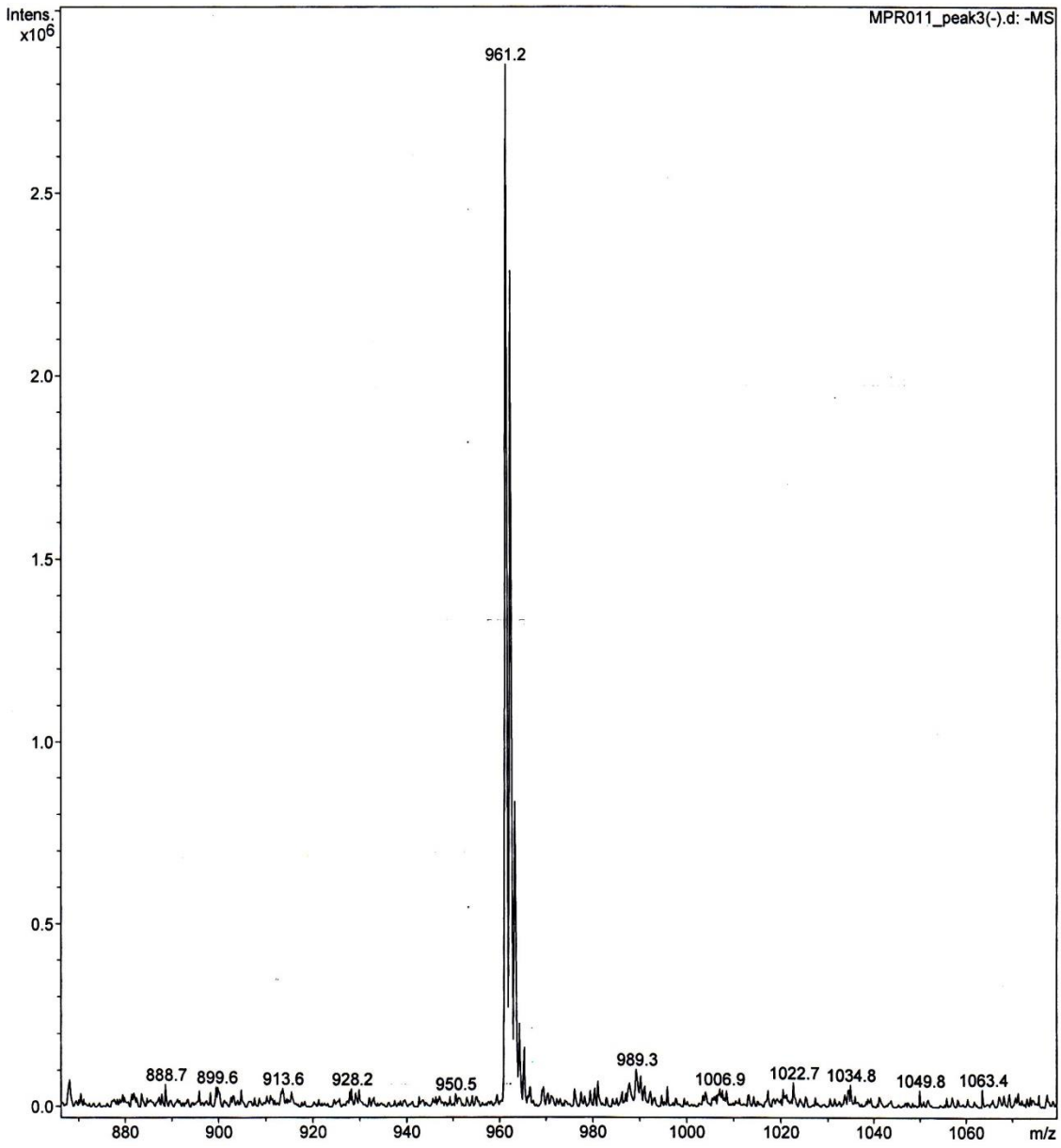

Figure 55: ESI-MS spectrum of reaction B01 of the separated spot No. 3 showing the R2cS1 complex at m/z 961 in the negative spectrum

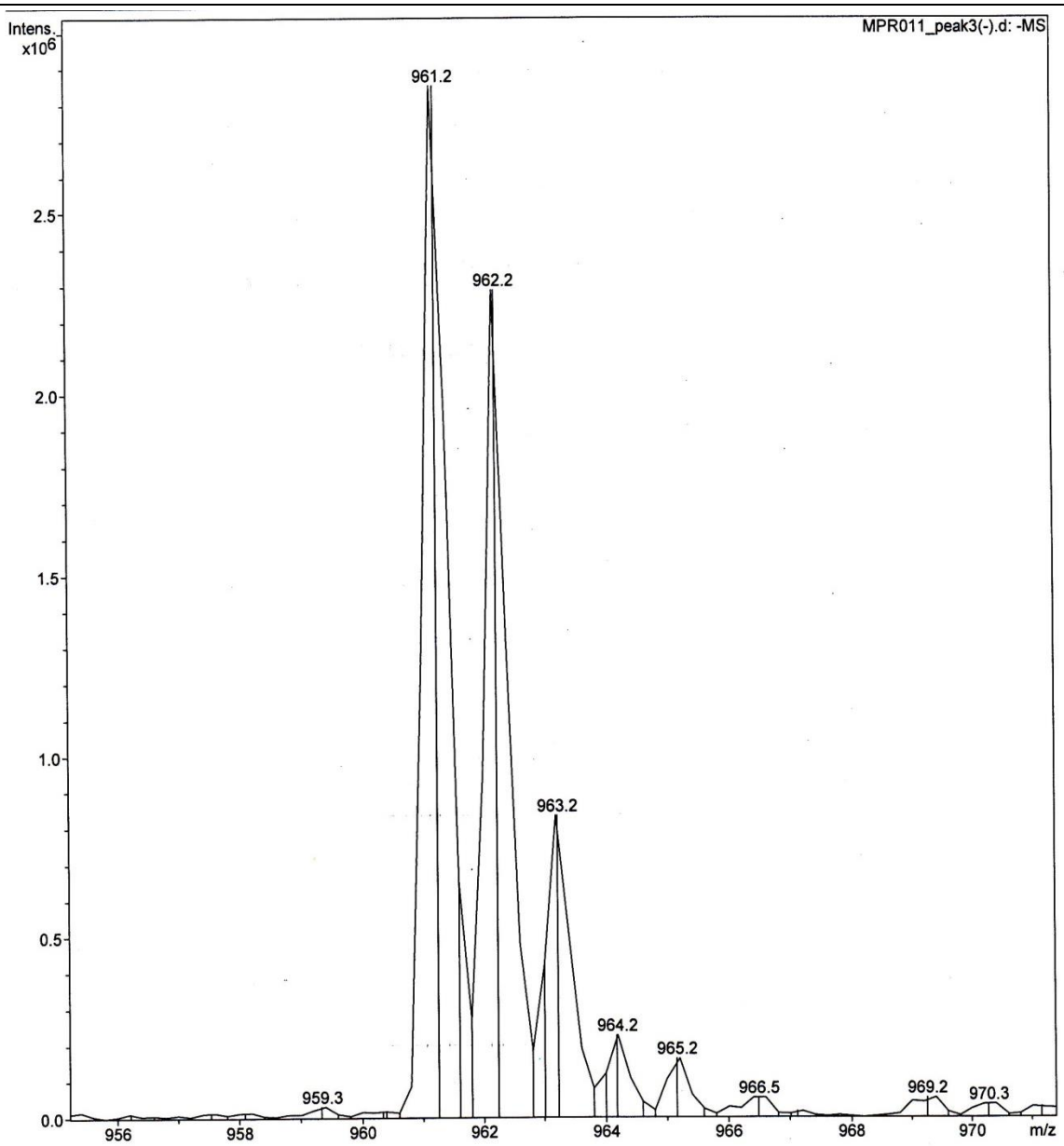

Figure 56: ESI-MS spectrum of reaction B01 of the separated TLC-spot No. 3 showing the R2cS1 complex at m/z 961 in the negative spectrum with the according isotope pattern

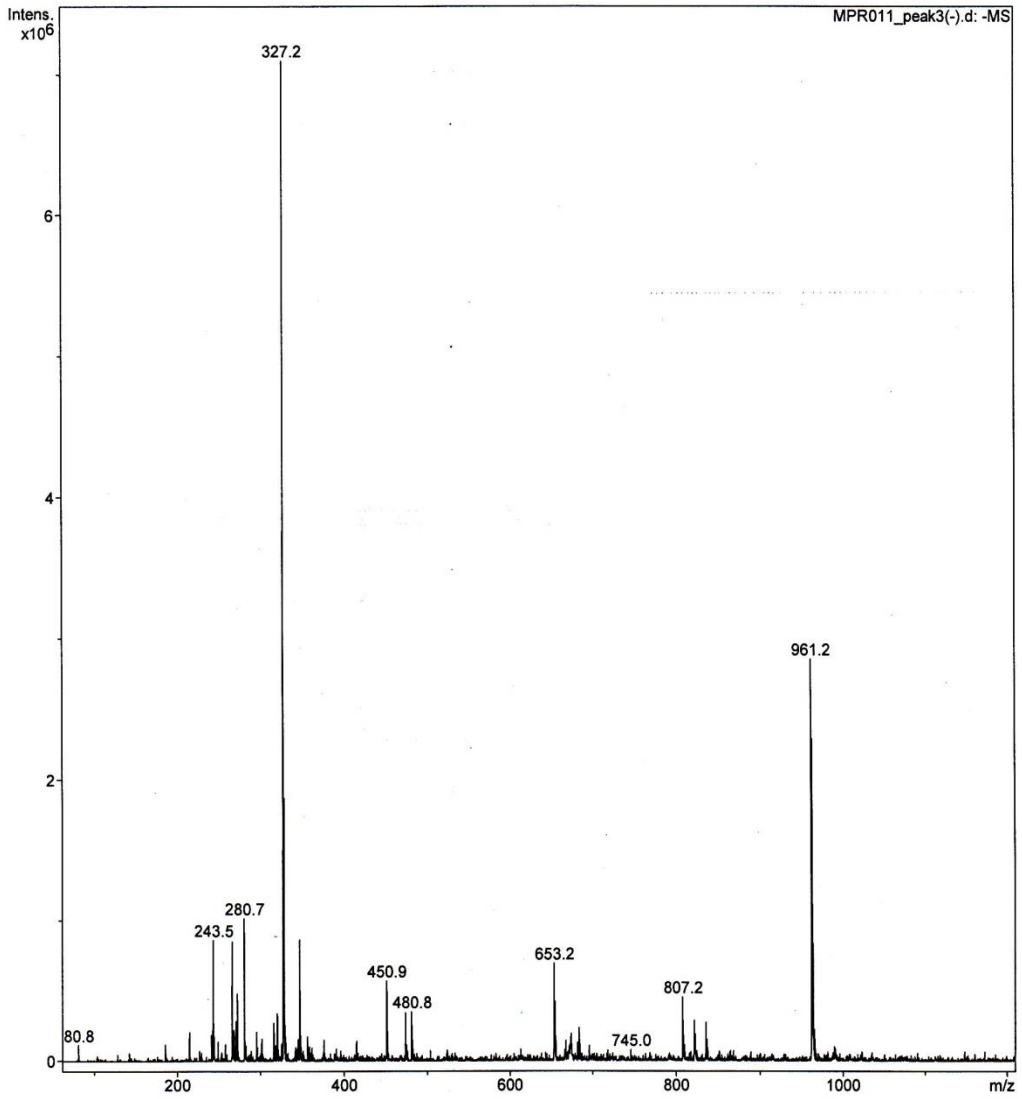

Figure 57: ESI-MS spectrum of reaction B01 of the separated TLC-spot No. 3 showing the R2cS1 complex at m/z 961 and a low intensity m/z 807 signal for the byproduct R1cS1 in the negative spectrum

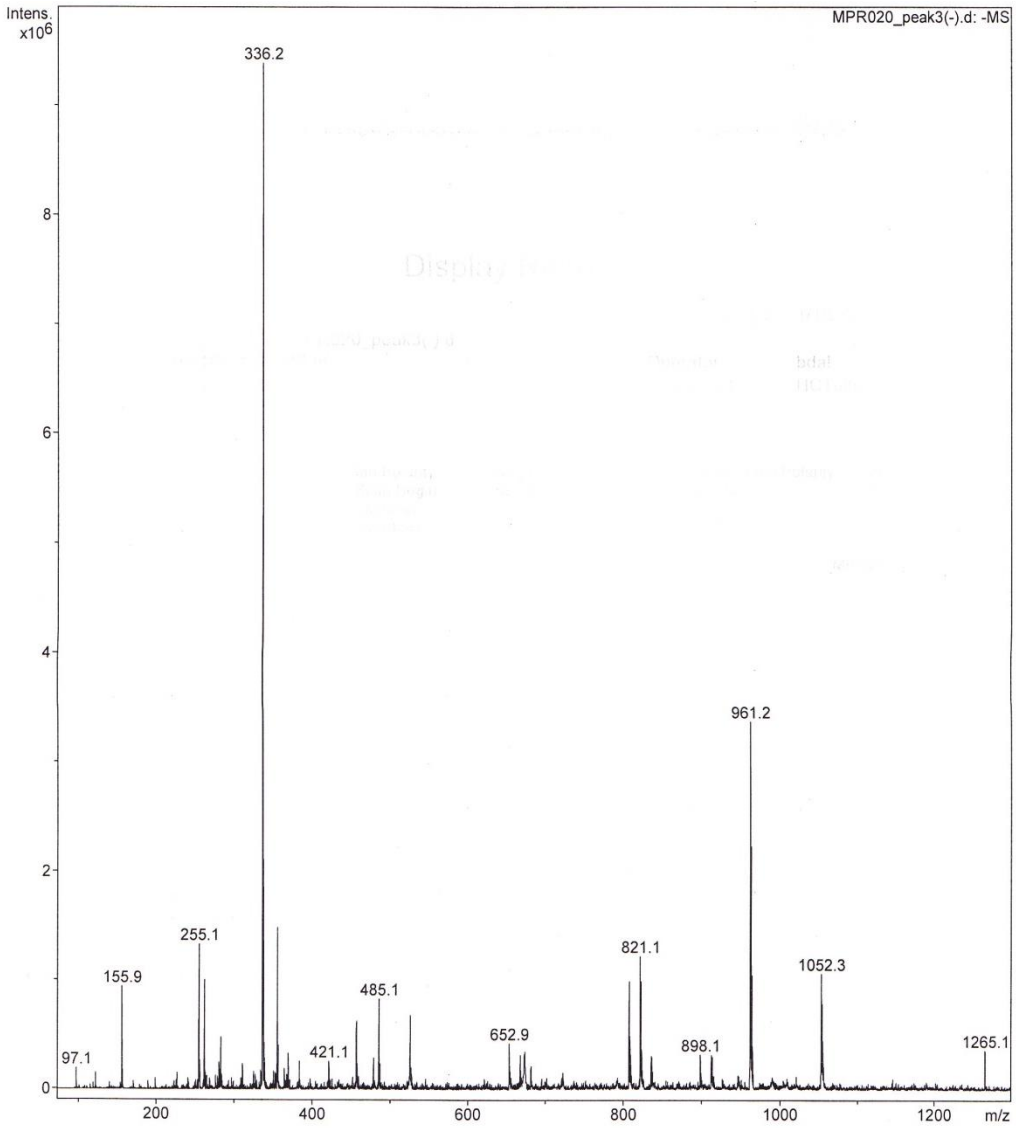

Figure 58: ESI-MS spectrum of reaction B of the separated TLC-7b-spots No. 4-6 showing all the R2cS1 complex at m/z 961 and a low intensity m/z 653 signal for the starting material SiPcS1 in the negative spectrum

E.2 Preparation procedure for changing oleum concentration

Based on the "Cornerstone Chemical Company" brochure [31] in which all the information on various oleum concentrations is provided the 5 % oleum concentration was calculated as follows.

30 % Oleum = 30 % SO_3 dissolved in H_2SO_4

This corresponds to a H_2SO_4 concentration of 106.8 %.

If in 100g - 30 % Oleum, 6.8 g H_2O would be added the mass would increase um 30g

$\frac{6.8g}{18\frac{g}{mol}[MW_{H_2O}]}$ = 0,37 mol

$MW_{[SO3]}$: 80 g/mol => $0.37mol * 80\frac{g}{mol} = 30\ g$ (Definition of oleum concentration)

To reduce the oleum concentration from 30 % to 5 % water has to be added that the a total H_2SO_4 concentration is 101.3 % [31]

This means 6.8g – 1.3g =5.5g water has to be added to 100g 30 % oleum.

In the experiment for this thesis 1 ml H_2SO_4 / 30 % Oleum was used which has following density at room temperature δ = 1.952 [31]

30 %	1.00 g	0.068 g	H_2O added
	1.95 g	0.133 g	to get 100 % H_2SO_4
5 %	1.00 g	0.013 g	H_2O added
	1.95 g	0.026 g	to get 100 % H_2SO_4

0.133 g H_2O are approximately equal to 133 µl and 0.026g are also approximately equal 26 µl. Therefor the amount of water to add to 1 ml 30 % oleum to get 5 % oleum is 133 µl – 26 µl = 107 µl of H_2O.

E.3 The Beer-Lambert law & preparation of sample for yield calculation

The Beer-Lambert law states that the absorbance of a solution is directly proportional to the concentration of the absorbing species in the solution and the path length. Thus, for a fixed path length, UV/Vis spectroscopy can be used to determine the concentration of the absorber in a solution using following formula.

$$lg\left(\frac{I_0}{I}\right) = \varepsilon_\lambda * c * d \qquad (6)$$

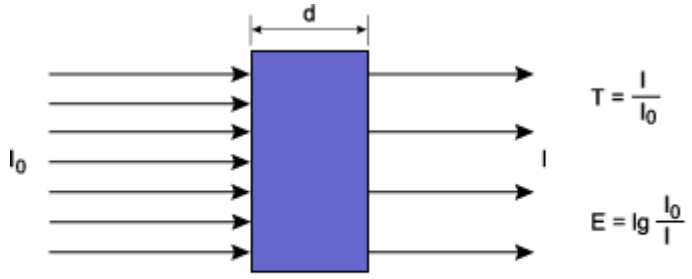

Figure 59: Dependence of the light attenuation of layer thickness d and concentration c (T = transmission) [32]

In this formula d is the path length; c is the concentration, ε_λ is the molar extinction coefficient and I_0 and I are the intensity of light of the light before and after passing through the sample. [32]

For the concentration determination of the purified reaction solution the solvent was completely removed. Afterwards the dried complex was again dissolved in a few milliliter of solvent (mostly in MeOH for the reaction A and toluene for reaction B). Because this solution was much too concentrated for an absorption measurement an aliquot part of the solution it was further diluted. This process was repeated until a suitable concentration was reached which could be measured with UV/VIS absorption measurement. [32]

E.4 DFT calculation

E.4.1 DFT calculation R2cS1-orbitals:

Excitation energies and oscillator strengths:

Excited State 1: Singlet-A 1.9460 eV 637.13 nm f=0.3644
156 ->162 0.11355
159 ->162 0.26910
160 ->161 0.58337
This state for optimization and/or second-order correction.
Copying the excited state density for this state as the 1-particle RhoCI density.
Excited State 2: Singlet-A 1.9936 eV 621.91 nm f=0.2963
158 ->161 -0.11496
159 ->161 -0.30190
160 ->162 0.57620
Excited State 3: Singlet-A 2.6271 eV 471.95 nm f=0.1569
156 ->161 -0.15153

159 ->161 0.60103
160 ->162 0.17824
Excited State 4: Singlet-A 2.6693 eV 464.48 nm f=0.1571
158 ->162 -0.14740
159 ->162 0.61598
160 ->161 -0.14542
Excited State 5: Singlet-A 3.0432 eV 407.42 nm f=0.0000
157 ->161 0.70409

E.4.2 DFT calculation SiPc-orbitals

Excitation energies and oscillator strengths:

Excited State 1: Singlet-A 1.9774 eV 627.00 nm f=0.3186
136 ->142 0.15021
139 ->142 0.28253
140 ->141 0.58041
This state for optimization and/or second-order correction.
Copying the excited state density for this state as the 1-particle RhoCI density.
Excited State 2: Singlet-A 1.9776 eV 626.93 nm f=0.3184
136 ->141 -0.15033
139 ->141 -0.28269
140 ->142 0.58039
Excited State 3: Singlet-A 2.6672 eV 464.85 nm f=0.1479
136 ->141 -0.16808
139 ->141 0.61100
140 ->142 0.15800
Excited State 4: Singlet-A 2.6675 eV 464.80 nm f=0.1478
136 ->142 -0.16822
139 ->142 0.61108
140 ->141 -0.15785
Excited State 5: Singlet-A 3.1034 eV 399.51 nm f=0.0000
137 ->141 0.61361
138 ->141 0.34514

E.4.3 HOMO and LUMO energy calculation of R2c and R2cS1

LUMO+1(162) -0.11536eV
LUMO (161) -0.11829eV
HOMO (160) -0.19455eV
HOMO-1(159) -0.23330eV

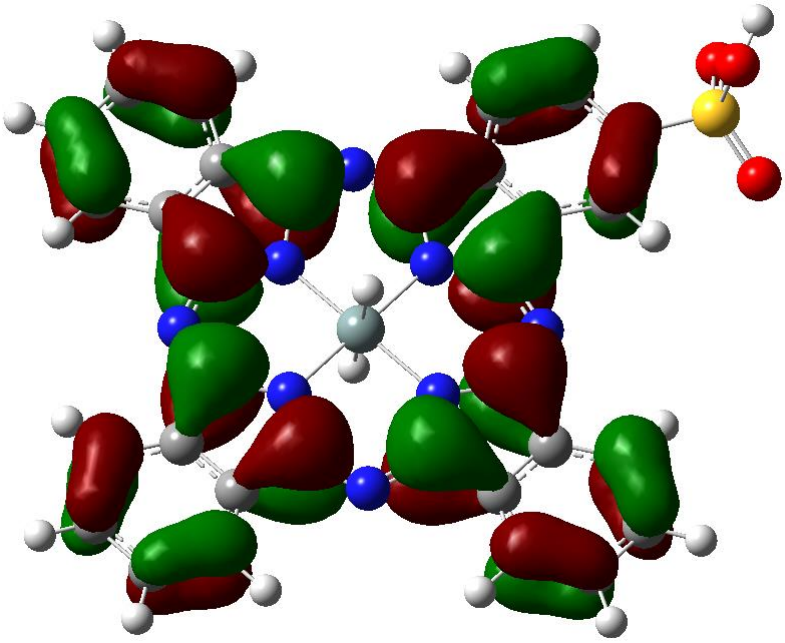

Figure 60: DFT calculation of HOMO molecule orbitals of R2cS1

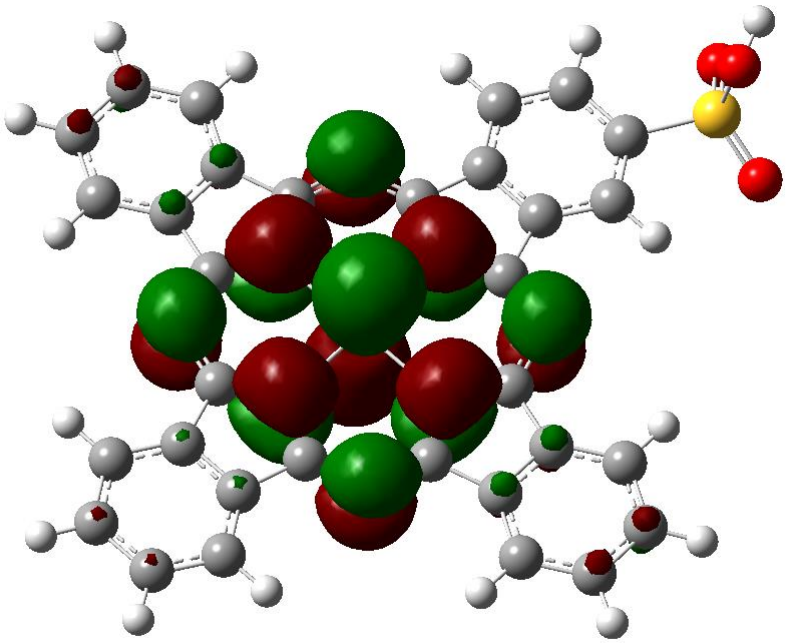

Figure 61: DFT calculation of HOMO-1 molecule orbitals of R2cS1

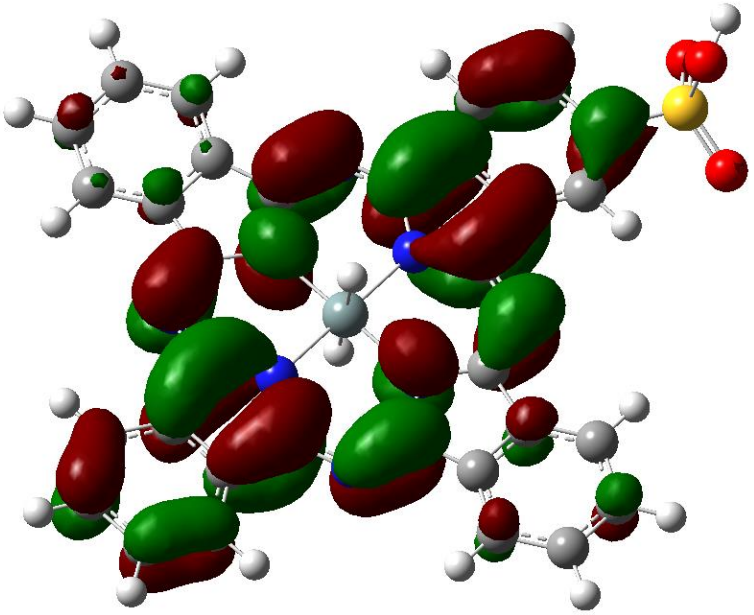

Figure 62: DFT calculation of LUMO molecule orbitals of R2cS1

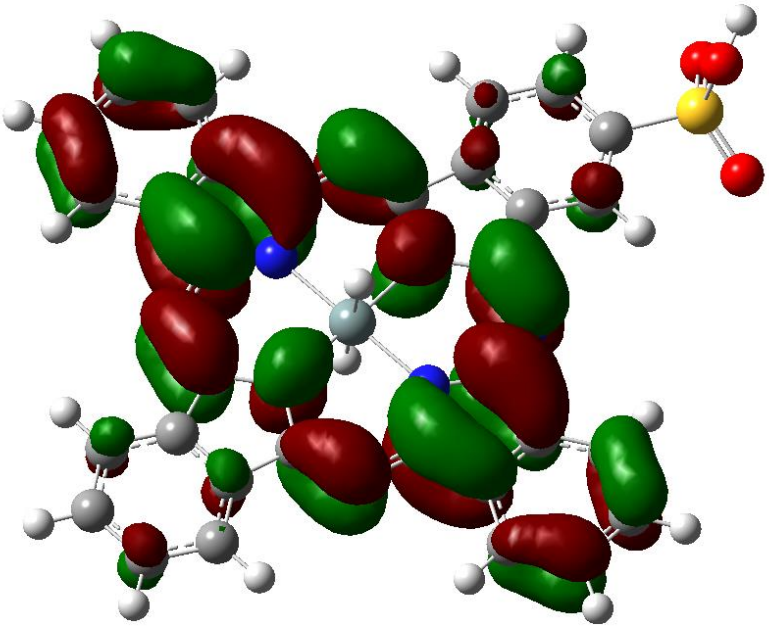

Figure 63: DFT calculation of LUMO+1 molecule orbitals of R2cS1

E.5 TLC arrays

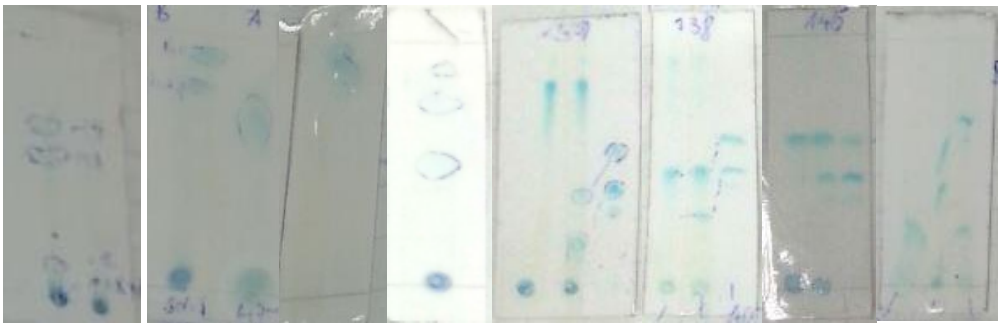

TLC-2a TLC-3a TLC-4a TLC-5a TLC-7a TLC-9a TLC-10a TLC-11a

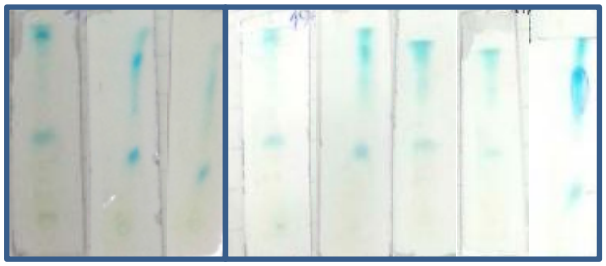

TLC-14a TLC-15a

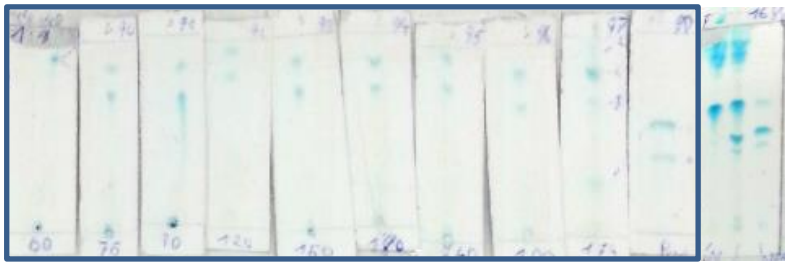

TLC-16a TLC-18a

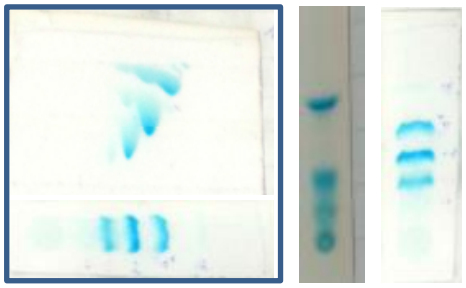

TLC-20a TLC-19a TLC-22a

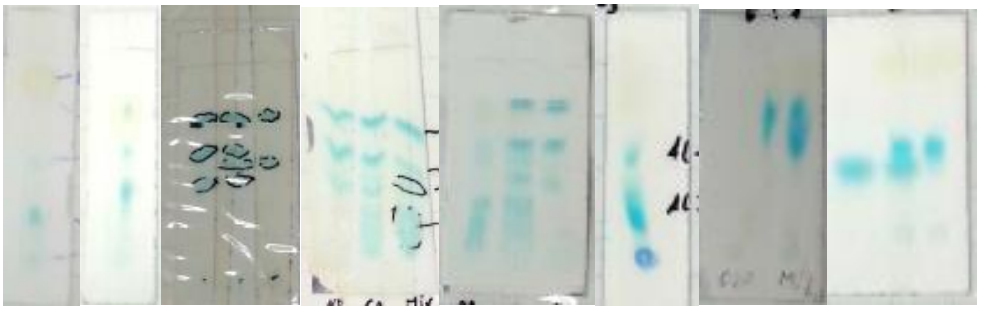

TLC-1b TLC-4b TLC-5b TLC-7b TLC-8b TLC-9b TLC-10b

F) Table of Illustrations

Table of Illustrations

Figure 1: First and second generation of the vitamin C detecting complex .....**Fehler! Textmarke nicht definiert.**
Figure 2: Positioning of the complex R2cS1 in the liposome .....**Fehler! Textmarke nicht definiert.**
Figure 3: First and second generation of ascorbate detecting complexes .....**Fehler! Textmarke nicht definiert.**
Figure 4: Positioning of the complex R2cS1 in the liposome .....**Fehler! Textmarke nicht definiert.**
Figure 5: Formel schema of the first step reaction - the synthesis of SiPcS1....**Fehler! Textmarke nicht definiert.**
Figure 6: Formel schema of the second step reaction for the synthesis of R2cS1 .....**Fehler! Textmarke nicht definiert.**
Figure 7: Increaced fluorescence after the reaction of R2cS1 with ascorbic acid .....**Fehler! Textmarke nicht definiert.**
Figure 8: Basic structure of (a) metal-phthalocyanaine and (b) metal-porphyrin complex.....**Fehler! Textmarke nicht definiert.**
Figure 9: Metals that have been used to make metal phthalocynanines [Y] .....**Fehler! Textmarke nicht definiert.**
Figure 10: Molecular structure of Pc.....**Fehler! Textmarke nicht definiert.**
Figure 11: Electron transitions and associated wavelength of Pc [7] **Fehler! Textmarke nicht definiert.**
Figure 12: Electronic absorption (black), fluorescence (red), phosphorescence (red), and T-T absorption (blue) spectra of Si(IV)t-BuPc$(OH)_2$ in toluene [W].....**Fehler! Textmarke nicht definiert.**
Figure 13: Excited-state energy diagram and decay kinetics of Pc with closed-shell atoms [U] ...**Fehler! Textmarke nicht definiert.**
Figure 14: Electronic absorption spectra of Zn(II)tBuPc (black line) and Zn(II)PEP (red line)[2]....**Fehler! Textmarke nicht definiert.**
Figure 15: Molecular orbitals of Zn(II)PC and Zn(II)Por [2] .....**Fehler! Textmarke nicht definiert.**
Figure 16: Absorption behaviour of the different substances in biological tissue [S] **Fehler! Textmarke nicht definiert.**
Figure 17: Reaction of vitamin C with the nitroxids of the SitBuPc-complex.....**Fehler! Textmarke nicht definiert.**
Figure 18: Excited-state diagrams of Pcs linked to one (middle) and two (lower) nitroxide-radicals with that of normal Pc (upper).....**Fehler! Textmarke nicht definiert.**
Figure 19: Steady-state EPR and TREPR spectra of SiPc$(TEMPO)_2$ and decay dynamics from the excited multiplet states.....**Fehler! Textmarke nicht definiert.**
Figure 20: Energy diagrams of SiPc, SiPc-TEMPO and SiPc-$(TEMPO)_2$. The D_3 state of SiPc-TEMPO and the S_3 and T_3 states of SiPc-$(TEMPO)_2$ are constituted by the excited singlet SiPc and doublet TEMPO radicals. The D_1 and Q_1 states of SiPc-TEMPO and the S_1, T_1 and Q_1 states of SiPc-$(TEMPO)_2$ are constituted by the excited triplet SiPc and doublet TEMPO radicals. .....**Fehler! Textmarke nicht definiert.**
Figure 21: Steady state EPR spectra of SiPc-TEMPO (a) and SiPc-$(TEMPO)_2$ (b). A simulation spectrum (c) was calculated as a spin-correlated radical pair .....**Fehler! Textmarke nicht definiert.**
Figure 22: First (left) and second (right) generation of the vitamin C detecting complex.....**Fehler! Textmarke nicht definiert.**

Figure 23: Reaction A: First step of the synthesis of the complex R2cS1.....**Fehler! Textmarke nicht definiert.**
Figure 24: Reaction B: Second reaction step for the synthesis of the complex R2cS1**Fehler! Textmarke nicht definiert.**
Figure 25: Reduction reaction of the complex R2cS1 with vitamin C which causes a stronger fluorescence signal.....**Fehler! Textmarke nicht definiert.**
Figure 26: The new synthesized complex will be encapsulate in liposomes and micelles which should protect the radical sites to react with reactive species in a biological environment...**Fehler! Textmarke nicht definiert.**
Figure 27: Experimental setup for measuring the time dependent fluorescence development after adding vitamin C to the in PBS dissolved complex solution.....**Fehler! Textmarke nicht definiert.**
Figure 28: First reaction step: Synthesis of SiPcS1.....**Fehler! Textmarke nicht definiert.**
Figure 29: Retention behavior of the first-step reaction product mixture for reversed phased TLC (left) and normal phased TLC (right).....**Fehler! Textmarke nicht definiert.**
Figure 30: Illustration of the filtration of the first synthesis.....**Fehler! Textmarke nicht definiert.**
Figure 31: Illustration of a liquid-liquid extraction for the first synthesis.....**Fehler! Textmarke nicht definiert.**
Figure 32: Absorption spectra of the different peaks after separation with RP-TLC..**Fehler! Textmarke nicht definiert.**
Figure 33: Aggregation equilibrium between different forms of SiPcS1 agglomerates.....**Fehler! Textmarke nicht definiert.**
Figure 34: Foam formation during the neutralization process with Na_2CO_3 65
Figure 35: Process of removing the solvent after the neutralization reaction of reaction A by using a rotary evaporator 66
Figure 36: Salt-SiPcS1 mixture triturated with a mortar to a fine powder 66
Figure 37: Equipment setup of the filtration process 67
Figure 38: Separation of the different products of reaction A by using column chromatography..... 68
Figure 39: Second reaction step for the synthesis of the final product R2cS1 69
Figure 40: The process of exchanging a proton for a radical 70
Figure 41: TLC separation on a AlO_3-TLC plate with ethyl acetate:EtOH:acetic acid:H_2O (8:2:0.5:1) as a mobile phase 80
Figure 42: First ESR measurement with the additional smaller peaks as indication for a successful synthesis of R2cS1 81
Figure 43: Removing TEMPOL from the reaction solution by flushing the product mixture with $HCCl_3$ in AlO_3 gel 82
Figure 44: Second successful measurement of R2cS1 with ESR with still quite strong impurities of TEMPOL 83
Figure 45: ESR spectrum from the newly synthesized complex R2cS1 showing a peak pattern that indicates two intact radical sites on the silicon TEMPOL ligands..... 84
Figure 46: MCD measurement overlapping with an absorption spectra indicating that the Q-band splitting is caused by an orbital energy split because of the asymmetry of the complex .. 85
Figure 47: Fluorescence measurement after adding different amounts of vitamin C to the complex solutions of R2cS1 and R2c (high concentrations) 89
Figure 48: Fluorescence measurement after adding different amounts of vitamin C to the complex solutions of R2cS1 and R2c (low concentrations) 89

Figure 49: Fluorescence measurement of R2c after vitamin C addition for different wavelengths..... 90
Figure 50: Fluorescence measurement of R2cS1 after vitamin C addition for different wavelengths. 90
Figure 51: ESI-MS spectrum of the first separated SiPcS1 compound of reaction A01, showing the product peak at m/z 653 in the negative spectrum ..... - 93 -
Figure 52: ESI-MS spectrum of reaction A03 of the first separated TLC- spot showing the SiPcS1 complex at m/z 653 in the negative spectrum..... - 94 -
Figure 53: ESI-MS spectrum of reaction A03 of the first separated TLC- spot showing the SiPcS1 complex at m/z 653 in the negative spectrum with the according isotope pattern..... - 95 -
Figure 54: ESI-MS spectrum of reaction A03 of the second separated TLC- spot showing the SiPcS1 complex at m/z 653 in the negative spectrum..... - 96 -
Figure 55: ESI-MS spectrum of reaction A03 showing the byproduct mixture with a lot of fragment peaks in the positive spectrum ..... - 97 -
Figure 56: ESI-MS spectrum of reaction A03 showing the byproduct mixture with a lot of fragment peaks in the negative spectrum ..... - 98 -
Figure 57: ESI-MS spectrum of reaction B01 of the separated spot No. 3 showing the R2cS1 complex at m/z 961 in the negative spectrum ..... - 99 -
Figure 58: ESI-MS spectrum of reaction B01 of the separated TLC-spot No. 3 showing the R2cS1 complex at m/z 961 in the negative spectrum with the according isotope pattern..... - 100 -
Figure 59: ESI-MS spectrum of reaction B01 of the separated TLC-spot No. 3 showing the R2cS1 complex at m/z 961 and a low intensity m/z 807 signal for the byproduct R1cS1 in the negative spectrum..... - 101 -
Figure 60: ESI-MS spectrum of reaction B of the separated TLC-7b-spots No. 4-6 showing all the R2cS1 complex at m/z 961 and a low intensity m/z 653 signal for the starting material SiPcS1 in the negative spectrum ..... - 102 -
Figure 61: Dependence of the light attenuation of layer thickness d and concentration c (T = transmission) [XX]..... - 104 -
Figure 62: DFT calculation of HOMO molecule orbitals of R2cS1 ..... - 106 -
Figure 63: DFT calculation of HOMO-1 molecule orbitals of R2cS1 ..... - 106 -
Figure 64: DFT calculation of LUMO molecule orbitals of R2cS1 ..... - 107 -
Figure 65: DFT calculation of LUMO+1 molecule orbitals of R2cS1 ..... - 107 -

G) References

References

[1] K. Ishii, *Chem. Commun*., **2011**, 47, 4932-4934 (and citations therein);

[2] Kadish, K.; Smith, K.; Guilard, R.; (Eds.) *The Porphyrin Handbook*; Academic: New York, **2003**; Vol. 15-20.;

[3] Cram101 Textbook Reviews -e-Study Guide for: Organic Chemistry ;

[4] W. M. R. S. Costa: Coodrination chemistry of Re(I) carbonyl complexes as pharmaceutically important compounds and synthesis, characterization and metalation of novel phthaloxyanine analogs, Diss., University of Akron, **2011**, p 75;

[5] W. M. Hikal: Self-assembled novel multi-porphyrin micro-crystals as a photocatalyst for 2,4,6-trinitrotoluene degradation, Diss., University of Oklahoma, **2008**, p 2;

[6] P. Vollhardt, N. E. Schore. *Organic Chemistry: Structure and Function*. 5th ed. New York: W. H. Freeman & Company, **2007**

[7] Kadish, K.; Smith, R. M.; Guilard, R.; Eds.; *World Scientific*: Singapore, **2010**; 32, pp. 173-270. (and citations therein);

[8] Thomas L. und M. Ian Phillips, Phthalocyanine Research and Applications, **1990;**

[9] A. Braun, J. Tcherniac: "Über die Produkte der Einwirkung von Acetanhydrid auf Phthalamid", in: Berichte der Deutschen Chemischen Gesellschaft, **1907**, 40 (2), pp. 2709–2714;

[10] H. de Diesbach, E. von der Weid: "Quelques sels complexes des o-dinitriles avec le cuivre et la pyridine", in: Helvetica Chimica Acta, **1927**, 10 (1), pp. 886–888;

[11] Robertson, J.M., An X-ray study of the structure of the phthalocyanines. Part 1. Journal of the Chemical Society, **1935**, 615-21.

[12] (a) P. Linstead, J. Chem. Soc., **1934**, 1016; (b). M. Robertson, J. Chem. Soc, **1934**, 615;

[13] , Werner J., Lianos, Panagiotis, Schubert, Ulrich (Eds.), Molecular Materials and Functional Polymers, **2001,** p. 4

[14] Ishii, K.; Kitagawa, Y. In Handbook of Porphyrin Science, Kadish, K.; Smith, R. M.; Guilard, R.; Eds.; World Scientific: Singapore, **2010**; Vol. 32, pp. 173-270 (and citations therein);

[15] O. Bremen: Darstellung, Charakterisierung und Eigenschaften von Phthalocyanin-Molekularsiekompositen in der photokatalysierten Oxidation von natriumsulfid, Diss., University of Bremen, **2003**, pp. 49-54 (and citations therein)

[16] G. Schnurpfeil, A.K. Sobbi, W. Spiller, H.Kliesch, D. Wöhrle, J. of Porphyrins and Phthalocyanines 1, **1997**, 159.

[17] K. Kubo: Phtalocyanine-based fluorescence probes for detecting vitamin C, Masterthesis, University of Tokyo, 2010, p. 3

[18] J.R. Gispert, *Coordination Chemistry Wiley-VCH*., **2008** p. 483.

[19] K. Ishii, *Coordination Chemistry Reviews 256*, **2012** 1556–1568 (and citations therein);

[20] K. Ishii, N. Kobayashi, in: K.M. Kadish, K.M. Smith, R. Guilard (Eds.), *The Porphyrin Handbook*, vol. 16, Academic Press, San Diego, **2003**, p. 1.

[21] K. Ishii, N. Kobayashi, K. M. Kadesh, K.M. Smith, R. Guiland, (Eds), Phthalocyanines*: Spectroscopic and electrochemical Characterization*, **2003**, Vol. 16

[22] IUPAC, Compendium of Chemical Terminology, 2nd ed. (the "Gold Book"), **1997**, Online corrected version: (21.10.2015) http://goldbook.iupac.org/B00618.html

[23] K. Ishii; K. Kubo; T. Sakurada; K. Komori; Y. Sakai, *Chem. Commun*. **2011**, 47, 4932

[24] K. Ishii; T. Ishizaki; N. Kobayashi, *J. Chem. Soc*., Dalton Trans., **2001**, 3227–3231 (and citations therein)

[25] K. Ishii; N. Kobayashi, *Coordination Chemistry Reviews* 198, **2000**, 231–250

[26] C.D. Buckley, D.A. Hunter, P.J. Hore, K.A. McLauchlan, *Chem. Phys*. Lett. 135, **1987**, 307.

[27] E. Lozinsky et al., *J. Biochem. Biophys*. Methods 38, **1999,** 29–42 (and citations therein).

[28] Picture of Liposome: (16.9.2015) https://de.wikipedia.org/wiki/Liposom#/media/File:Phospholipide_in_Wasser.svg

[29] K. Palewska et al. / *Journal of Photochemistry and Photobiology A: Chemistry* 197, **2008** 1–12.

[30] K. Ishii, *J. Am. Chem. Soc*. **1998**, 120, 10551-10552

[31] Cornerstone Chemical Company Sulfuric Acid brochure, **2010**

[32] Cammann, K., Hrsg., *Instrumentelle Analytische Chemie, Spektrum Akademischer Verlag*: Heidelberg, **2001**; p. 5-4, 5-6, 5-8.